UNIVERSITÀ DEGLI STUDI DI NAPOLI "FEDERICO II"

POLO DELLE SCIENZE E DELLE TECNOLOGIE

FACOLTÀ DI INGEGNERIA

DIEL

DIPARTIMENTO DI INGEGNERIA ELETTRICA

Grid Services For Measurements on Digital Wireless Communications Systems

Aniello Napolitano

TESI DI DOTTORATO DI RICERCA IN INGEGNERIA ELETTRICA

XXII CICLO

(coordinatore: prof. Guido Carpinelli)

TUTOR

PROF. MASSIMO D'APUZZO

(UNIV."FEDERICO II", NAPOLI - DIEL)

CO-TUTOR

PROF. LEOPOLDO ANGRISANI

(UNIV. "FEDERICO II", NAPOLI - DIS)

DIPARTIMENTO DI INGEGNERIA ELETTRICA - VIA CLAUDIO 21 – 80125 NAPOLI

Abstract

The research activity accounted for in this Ph.D thesis belongs to the general field of electrical and electronic measurement. The attention is focused on the implementation of GRID services for performance assessing of digital wireless communication systems. The original contribution consists in the development of two original measurement methods, the former allows measuring the modulation quality of systems compliant with IEEE 802.16d-2004 standard by means of any hardware characterized by a enough sample rate and input band width, and the latter carries out reliability and efficiently the in-service measurements also in presence of in-channel interferences.

The high computational burden experienced during the wide experimental phase by proposed methods has encouraged their implementation according to GRID Service paradigm. Respect to the classic Web Service, GRID Service provides the possibility of both sharing the proposed methods among researches and technicians who work on the same topics, and processing some proposed methods stages in parallel way on several calculus nodes, thus reducing the whole processing time. Differently from the normal GRID Service, the developed GRID Services involve the measurement instrumentation, such digital acquisition systems and waveform generator, other than the calculus nodes. Suitable strategies for discovering, accessing, setting the measurement instruments have to be provided for. To this aim, new GRID architecture has been proposed, which virtualizes the measurement instruments into new components, namely instrumentation devices, and makes use of classic mechanisms already presented in GRID architecture, such as PBS scheduler, for dealing with the instruments discovery issue.

To take advantage from the proposed GRID Services, a proper web portal is also implemented. An intense experimental phase is executed for assessing the methods and GRID Services performance by applying emulated and real communication signals. Measurement results are analyzed and compared to those achievable through the application of existing methods and/or instrument available on the market. Particular attention is also made to the processing time measurement of GRID Service with respect to a sequential implementation, in order to evidence the gains provided by a parallel implementation.

Acknowledgments

At the end of a long time period, many are the persons I would like to thank for their supports and constant help.

Prof. Leopoldo Angrisani and Prof. Massimo D'Apuzzo, to which I express my personal gratitude and whose continuous inspiration and scientific support have been driving factors to accomplish this goal. Specially, Prof. Angrisani that in all these years has never done fail his support to me, giving me the possibility to grow professionally in many fields.

A sincere thanks goes to Prof. Guido Carpinelli, who has coordinated the Ph.D course with competence, devotion and always with a bit of fun.

The luck to work in the unique workgroup of Electrical and Electronic Measurements of University of Naples "Federico II", has allowed to know special colleagues with whom a strong relationships of friendship rather than working have been establishing.

A special thanks to Rosario and Michele, colleagues and great friends of room 1.06, with whom have had the occasion of exchanging ideas and cooperating, but most important, I have experienced enjoyment and unforgettable moments, such as Seattle, Gaeta, and so on.

To the only woman in the workgroup, Annalisa plus "one", I extend a sincere thanks for her availability and cooperation and I would like to wish her great happiness in work, but especially for what will grow.

Nicola e Mauro, colleague and friends of "sunset boulevard", to which I say a warm thanks for the advices and suggestions, and whose suggest to escape from that place, because nothing is lost yet !!!

I would like to direct a very special thanks to Prof. Aldo Baccigalupi for his human support and helpful hints, whose enthusiasm and interest put into work will be a guide for the future.

I am also personally grateful to Prof. Nello Polese for his motivation and his kindness, and Prof. Felice Cennamo, for his precious encouragement.

It is also my sincere desire to acknowledge Antonio Grillo, Umberto Cesaro and Alessandro Teotino for their help and available.

I cannot forget the FS srl, with all its man, with which for two years I have consolidated a wonderful human and professional relationship, that I hope will continue for as long as possible.

A huge embrace goes to my family, led by my brothers, Francesco and Enrica, who have always supported me through my entire life and that I hope to have made them happy.

Last but not least, a warm thanks is for my beloved Alessia, sweetness of my life, which makes every day of my life an unique and special day, and without her I would never know the happiness.

Contents

Introduction

Wireless communications systems are nowadays a ubiquitous presence in any activity field: financial, productive, social, and scientific. This is encouraged by the incessant technical improvements of mobile phones and cellular networks, which are making them overcome more and more their original purpose (voice connection among people) to become multifunctional and mobile working desktop, capable of granting useful job support for business applications or continuous amusement for traditional customers.

Moreover, the development and diffusion of several wireless communications standards (IEEE 802.11a/b/g, IEEE 802.15, and IEEE 802.15.4), due to the availability of license-free frequency bands and liberalization of new portions of the radio spectrum, are making wireless systems and networks widespread in localized areas (millions of homes, factories and university campuses), thus providing wideband and nomadic access to the available services, often critical such as video surveillance and remote healthcare. A direct consequence of such a sustained development is that R&D (Research and Development) engineers and manufactories have been, and still are, involved in designing and developing components and systems characterized by higher and higher performance in terms of achievable transmission data rate and spectral effectiveness with a consequently increase of systems complexity. WiMAX systems associated with IEEE 802.16d-2004 standard and/or high speed Wi-Fi networks based on IEEE 802.11n standard are only some example. Periodic measurements on these systems have to be executed in order to assure high performance for long time. At the same time requirements imposed by both national and international standard and regulations have to be met. To

this aim, proper metrics both in modulation domain, such as EVM (Error Vector Magnitude), RCE (Relative Constellation Error), and I/Q impairment, and frequency domain, as spectrum mask, channel power, carrier frequency, and channel bandwidth, have to be measured and compared with systems nominal values both before the system installation and after in-service.

Reliable measurements of considered metrics are not a simple task to be accomplished. In fact, the like-noise nature and high crest factor (ratio of peak power to average power) of wideband signals exploiting in wireless communications systems cause manifold drawbacks in frequency domain metrics estimation, while the complexity adopted in actual modulation techniques for reaching higher transmission rate, influence the accuracy of modulation domain metrics measurements. Proper digital processing algorithms, suitably tailored on a specific wireless digital communication systems, have to be developed for obtaining reliable and repeatable outcomes.

Additional issues must be faced when the in-service performance assessment of wireless digital communication systems. In this operating condition only the radio signal is available (useful signal), which could interact with many interfering signals in the time domain or frequency domain or both. A long list of potential offenders may, in fact, be active, capable of generating and transmitting signals that accidentally or intentionally interfere with the useful one. For these reasons, the measurements of cited metrics in both domains could conduct to unfeasible results, because the useful signal is in presence of in-channel interferences, which makes difficult to properly extract the information and to measure the power spectrum of the radiated useful signal; fundamental step for gaining the values of relevant frequency domain metrics. This is particularly true for modern telecommunication systems that do not use an own licensed band, but rather share an unlicensed band with other systems, such in the case of those based on the standard IEEE 802.11x (WiFi), IEEE 802.15.4 (ZigBee) or IEEE 802.15 (Bluetooth). The classic methods for power spectrum estimation, already proposed in literature and based on parametric or non parametric approaches, have not succeeded when they are applied in these critical scenarios.

The research activity accounted for in this Ph.D thesis has focused on the development of new measurement methods, based on digital signal processing, capable of assessing the performance of wireless communication systems. In particular, two original measurement methods has been developed. The first one allows to assess the modulation quality for systems compliant with IEEE 802.16d-2004 standard (WiMAX fixed) by means of any hardware characterized by a enough sample rate and input band width, the second one overcomes the limitations of in-service measurements in order to allow reliable and effectiveness measurements. All the proposed methods have been extensively tested by applying them to simulated, emulated and real communication signals. Measurement results have been analyzed and compared to those achievable through the application of existing methods and/or

instrumentation available on the market. Particular attention has been also paid in measurement of algorithms computational burden, in terms of elaboration times. The high results obtained during the experiment phase have encouraged, according to the scientific trend, the development of the above methods on a GRID computing infrastructure. Moreover, in order to let the methods sharing among researchers and technicians, working on similar topics, the proposed methods have been implemented according to GRID Service paradigm. GRID service, in fact, is a new hardware/software approach that is capable of merging the higher processing performance of parallel GRID computing with key mechanisms and standard Web services.

Differently from classic GRID infrastructure, in which only hardware resources, as personal computer and workstations, are typically exploited, the proposed GRID has investigated on the possibility of integrating the measurement instruments, as data acquisition systems and waveform generator used in the measurement procedures, with computational nodes; an attractive solution, has been presented hereinafter. Finally, a Web Portal has been implemented to provide a simple interface to exploit the proposed methods.

The Ph.D. thesis is organized as follows. In Chapter I, the scheme of modern digital wireless communication systems is introduced along with the description of main metrics for assessing their performance. Chapter II provides the fundamental stages of proposed measurement procedures, and the results achieved through a wide comparative experimental activity intended to assess their performance are provided. Chapter III gives an overview on classic GRID infrastructure and architecture along with the current software platforms exploited for implementing GRID Services. Moreover, the proposed solution for integrating the measurement instruments in the GRID computing is given. In Chapter IV the implementation of proposed methods as GRID Services is described, highlighting the tasks of the methods that have been distributed in parallel way and the instruments involved in the measurements. Results of a comparative analysis executed on processing times elapsed to fulfill the method between the sequential and parallel implementation are also given. As expected, GIRD Service implementation provides reliable performance with lower processing times. The last part of Chapter IV describes the web portal and its functionalities. Finally, conclusions are drawn in Chapter V.

Chapter I

Digital Wireless Communication Systems and Testing

I.1 Communication systems

Electrical communication systems are designed to send messages or information from a source that generates the messages to one or more destinations. In general, a communication system can be represented by the functional block diagram shown in Fig. I.1. The information generated by the source may be of the form of voice (speech source), a picture (image source), or plain text in some particular language. An essential feature of any source that generates information is that its output is described in probabilistic terms; i.e., the output of a source is not deterministic. Otherwise,. there would be no need to transmit the message. A transducer is usually required to convert the output of a source into an electrical signal that is suitable for transmission. At the destination, a similar transducer is required to convert the electrical signals that are received into a form that is suitable for the user.

The heart of the communication system consists of three basic parts, namely, the *transmitter,* the *channel,* and the *receiver*.

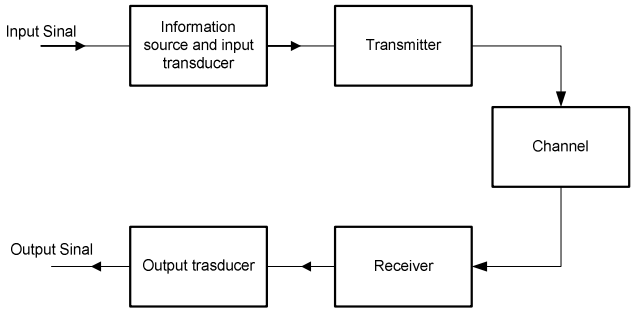

Fig. I.1 Main blocks of communication system

The transmitter converts the electrical signal into a form that is suitable for transmission through the physical channel or transmission medium. For example, in radio and TV broadcast, the Federal Communications Commission (FCC) specifies the frequency range for each transmitting station. Hence, the transmitter must translate the information signal to be transmitted into the appropriate frequency range that matches the frequency allocation assigned to the transmitter. Thus, signals transmitted by multiple radio stations do not interfere with one another. Similar functions are performed in telephone communication systems where the electrical speech signals from many users are transmitted over the same wire. In general, the transmitter performs the matching of the message signal to the channel by a process called *modulation.* Usually, modulation involves the use of the information signal to systematically vary either the amplitude, frequency, or phase of a sinusoidal carrier. For example, in AM radio broadcast, the information signal that is transmitted is contained in the amplitude variations of the sinusoidal carrier, which is the center frequency in the frequency band allocated to the radio transmitting station. This is an example of *amplitude modulation.* In FM radio broadcast, the information signal that is transmitted is contained in the frequency variations of the sinusoidal carrier. This is an example *of frequency modulation. Phase modulation (PM)* is yet a third method for impressing the information signal on a sinusoidal carrier. transmitter, as indicated above, to convert the information signal to a form that matches the characteristics of the channel. Thus, through the process of modulation, the information signal is translated in frequency to match the allocation of the channel. The choice of the type of modulation is based on several factors, such as the amount of bandwidth allocated, the types of noise and interference that the signal encounters in transmission over the channel, and the electronic devices that are available for signal amplification prior to transmission. In any case, the modulation process makes it possible to accommodate the transmission of multiple messages from many users over the same physical channel. In addition to modulation, other functions that are usually performed at the transmitter are filtering of the information-bearing signal and amplification of the modulated signal.

The communications channel is the physical medium that is used to send the signal from the transmitter to the receiver. Whatever is the physical medium for signal transmission, the essential

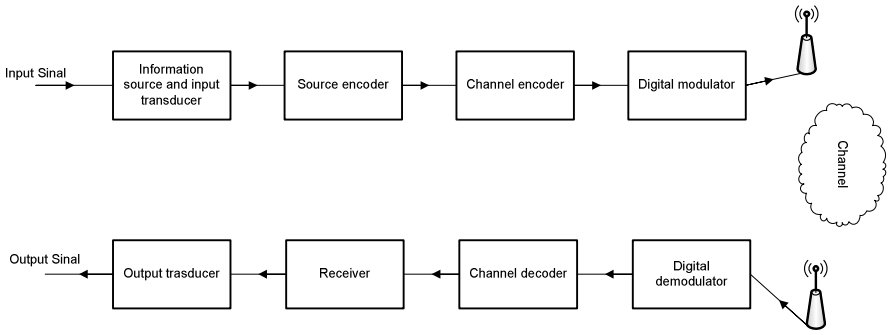

Fig. I.2 Main blocks of digital wireless communication system

feature is that the transmitted signal is corrupted in a random manner by a variety of possible mechanisms. The most common form of signal degradation comes in the form of additive noise, which is generated at the front end of the receiver, where signal amplification is performed. This noise is often called *thermal noise*. These phenomena are usually characterized as random phenomena and described in statistical terms. The effect of these signal distortions must be taken into account on the design of the communication system. In the design of a communication system, the system designer works with mathematical models that statistically characterize the signal distortion encountered on physical channels. Often, the statistical description that is used in a mathematical model is a result of actual empirical measurements obtained from experiments involving signal transmission over such channels. In such cases, there is a physical justification for the mathematical model used in the design of communication systems. On the other hand, in some communication system designs, the statistical characteristics of the channel may vary significantly with time. In such cases, the system designer may design a communication system that is robust to the variety of signal distortions. This can be accomplished by having the system adapt some of its parameters to the channel distortion encountered.

The function of the receiver is to recover the message signal contained in the received signal. If the message signal is transmitted by carrier modulation, the receiver performs *carrier demodulation* in order to extract the message from the sinusoidal carrier. Since the signal demodulation is performed in the presence of additive noise and possibly other signal distortion, the demodulated message signal is generally degraded to some extent by the presence of these distortions in the received signal.

I.2 Digital wireless communication system

Up to this point we have described an electrical communication system in rather broad terms based on the implicit assumption that the message signal is a continuous time varying waveform. We refer to such continuous-time signal waveforms as *analog signals* and to the corresponding information sources that produce such signals as *analog sources*. Analog signals can be transmitted directly via carrier modulation over the communication channel and demodulated accordingly at the receiver. We call such

a communication system an *analog communication system.* Alternatively, an analog source output may be converted into a digital form and the message can be transmitted via digital modulation and demodulated as a digital signal at the receiver. In the last case a *digital communication systems* is realized.

There are some potential advantages to transmitting an analog signal by means of digital modulation. The most important reason is that signal fidelity is better controlled through digital transmission than analog transmission. In particular, digital transmission allows us to regenerate the digital signal in long-distance transmission, thus eliminating effects of noise at each regeneration point. In contrast, the noise added in analog transmission is amplified along with the signal when amplifiers are used periodically to boost the signal level in long-distance transmission. Another reason for choosing digital transmission over analog is that the analog message signal may be highly redundant. With digital processing, redundancy may be removed prior to modulation, thus conserving channel bandwidth. Yet a third reason may be that digital communication systems are often cheaper to implement.

In some applications, the information to be transmitted is inherently digital. In such cases, the information source that generates the-data is called a *discrete (digital) source.* In a digital communication system, the functional operations performed at the transmitter and receiver must be expanded to include message signal discretization at the transmitter and message signal synthesis or interpolation at the receiver. Additional functions include redundancy removal, and channel coding and decoding. Figure 1.2 illustrates the functional diagram and the basic elements of a digital communication system. The source output may be either analog signal, such as audio or video signal, or a digital signal, such as the output of a computer which is discrete in time and has a finite number of output characters. In a digital communication system, the messages produced by the source are usually converted into a sequence of binary digits. Ideally, we would like to represent the source output (message) by as few binary digits as possible. In other words, we seek an efficient representation of the source output that results in little or no redundancy. The process of efficiently converting the output of either an analog or a digital source into a sequence of binary digits is called *source encoding* or *data compression* The sequence of binary digits from the source encoder, which we call the *information sequence* is passed to the *channel encoder.* The purpose of the channel encoder is to introduce, in a controlled manner, some redundancy in the binary information sequence which can be used at the receiver to overcome the effects of noise and interference encountered in the transmission of the signal through the channel. The binary sequence at the *output* of the channel encoder is passed to the *digital modulator,* which serves as the interface to the communications channel. If the communication channel is wireless the signals is routed to an antenna, which produce the radiated field. We shell call these system, *digital wireless communication system.* In wireless transmission, as expected, the channel is usually the atmosphere (free space), that introduces many drawbacks, as man-made noise and atmospheric noise picked up by a receiving

antenna. Interference from other users of the channel is another form of additive noise that often arises in wireless communication systems. In some radio communication channels, such as the ionosphere channel that is used for long range, short-wave radio transmission, another form of signal degradation is multipath propagation. Such signal distortion is characterized as a non additive signal disturbance which manifests itself as time variations in the signal amplitude, usually called fading.

I.3 Wireless communications systems testing

Several measurements have to be carried out for assessing the performance of digital communication systems. They can be performed by means of signal acquisition either at transmitter antenna port or directly on wireless channel, through the use of an ideal receiver. The former are usually executed before of the systems installation, while the latter are carried out after the installation stage and allow to validate the in-service systems performance. In both case, the aim is to verify their conformance of some metrics to requirements and specifications.

Measurements on the wireless digital communication systems are carried out in different domains: frequency domain and modulation domain.

The frequency domain analysis, which is carried out through DFT (Discrete Time Fourier)-based spectrum analyzers, allows to gain information on spectral occupancy, out-of band emissions, slight variation of carrier frequency, and singling out the presence of in-channel interfering signals.

Crucial information can be achieved in modulation domain by comparing the demodulated signal to an ideal reference; a number of possible impairments or non-idealities, which can effected the signals, are inferred by modulation domain measurements.

In the following, a brief description of most common measurement metrics, of both domain, are provided, according with the [I.1].

I.3.1 Frequency domain metrics

I.3.1.A Channel bandwidth

It is good practice, first, to perform a channel bandwidth measurement. In most cases of interest, depending on the baseband filter specifications, the 3 dB bandwidth approximates the symbol rate; its measurement can therefore reveal major errors in transmitter design.

I.3.1.B Carrier frequency

Carrier frequency measurements are of great importance. Not only can frequency errors result in possible interference, but they can also be responsible for possible problems in the carrier recovery process at receiver side.

I.3.1.C Channel power

Channel power is the average power of the signal in the channel. It is usually measured as the integral of power spectrum density over the frequency band of interest, although the measurement method depends on the particular communication standard [I.2-I.4].

I.3.1.D Occupied bandwidth

Occupied bandwidth (BW) is a measure of how much frequency spectrum is covered by the signal in question. The units are in Hz, and measurement of occupied BW generally implies a power percent age or ratio. Typically, a portion of the total power in a signal to be measured is specified. A common percentage used is 99%.

I.3.1.E Spurious

It can happen that spurious emissions, due to combination of signals in the transmitter, fall within the band of the communication system. Standards usually define power levels spurious that in-band emissions must not reach in order to avoid interference with other frequency channel of the system.

I.3.2 Modulation domain metrics

I.3.2.A EVM (Error Vector Megnitude)

Error vector magnitude (EV) is defined as the vector difference between the measured and ideal symbol position on the I/Q plane Its magnitude, EVM, is a key modulation quality metric in most modern communication systems [I.5], since most impairments and non-idealities of the transmitter affect its value. Fig. I.3 defines EVM and several related terms. As shown, EVM is the scalar distance between the two position, i.e., it is the magnitude of the difference vector. Expressed another way, it is

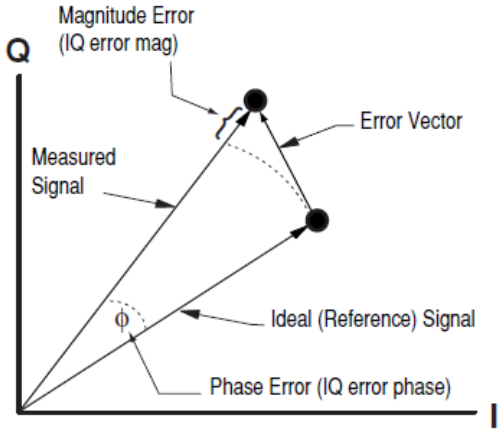

Fig. I.3 Example of EVM

the residual noise and distortion remaining after an ideal version of the signal has been stripped away.

I.3.2.B RCE (Relative Constellation Error)

Relative constellation error (RCE) [I.6] is a metrics very similar to the EVM. For an ideal transmitter, the signals would have all constellation points precisely at the ideal locations, however various imperfections in the implementation cause the actual constellation points to deviate from the ideal locations. The measure of the root mean square (RMS) between the actual and ideal points, averaged across a windows time in which fall a lot of constellations, defines the RCE value.

I.3.2.C I/Q impairments

I/Q impairments [I.7] can be caused by differences between the I and Q paths of the transmitter modulator. The most common are (i) gain imbalance, (ii) quadrature error, and (iii) voltage offsets. Difference between gains of the amplifiers on the I and Q branches can induce a distortion on the I/Q diagram, where gain on the Q branch is higher. The effect of gain imbalance is definitely more evident when IF section is implemented in an analog way. A phase shift between the two carriers modulated by signals on the I and Q paths not exactly equal to $\pi/2$ rad is responsible for a quadrature error. Finally, DC offsets possibly introduced in the I and Q braches, for instance added in the amplifier, determine a translation of the I/Q diagram.

I.4 Performance evaluation: some drawback

Measuring the aforementioned metrics is not a simple task to be fulfilled and several sources could affect the outcomes. In fact, the noise-like nature and high crest factor (ratio of peak to average power) of wideband signals involved in the analysis [I.8], makes unreliable the estimation of signal density power spectrum, from which the main metrics of frequency domain can be straightforwardly gained. Consequently, incorrect density power spectrum evaluation conducts to unreliable measurements of cited metrics.

Most efforts have been made to this purpose and many solutions, already proposed in literature, provide original methodologies, principally based on digital signal processing, to correct estimate the wideband signal power spectrum.

On contrary, the complexity increase associated with the modulation techniques [I.9] adopted by the actual transmitters for providing highest transmission rate with the same spectral occupation, makes difficult the development of "ideal" receiver; only thanks to that, the metrics in modulation domain can be properly estimated. To this aim, the major instrumentation company, such as Agilent Technology and Tektronix, provide attractive solutions for modulation quality assessment, that make use of existing and specialized measurement instrument, such as a real-time spectrum analyzer (RSA) or

a vector signal analyzer (VSA), with a proper digital signal processing software (analysis software). Their performance are strictly dependent on the adopted instrument; no functionality with a different measurement hardware is in principle assured. Moreover, their capabilities do not allow neither to pursue the continuous wireless communication system improvement nor to replace the adopted hardware with one that better match the signal features. An open-source, scalable and adaptable solutions would allow to overcome these limitations.

Further issues must be faced when the wireless digital communication system performance assessment is executed in-service. In this operating condition, only the signal radiated from the system under test (useful signal) is available. However, it may be affected from many interfering signals generated from non-intentional or intentional sources. Two wideband signals transmitted according to IEEE 802.11g standard on the same frequencies band, are an example of non-intentional interference. Otherwise, the presence of wideband interfering signal in a licensed band, generated from the non linearity of transmitter amplifier, is another example of non-intentional interference. As shown, a long list of potential offenders may, in fact, be active, capable of generating and transmitting signals that interfere with the useful one. In these conditions, measuring the power spectrum of the useful signal, which is the fundamental step for gaining the values of relevant frequency domain metrics might provide unfeasible results. In fact, the classic methods for power spectrum estimation, already proposed in literature and based on parametric [I.8, I.10] or non parametric approaches, have not succeeded when in-channel interference affects the useful signal. Same consideration can be drawn as regards the measurements of modulation domain metrics.

Two original measurement methods, one capable of achieving reliable and effectiveness results in modulation quality assessment for signals compliant with IEEE 802.16d-2004 standard and another able to overcome the aforementioned drawbacks for in-service measurements, will be presented in the next Chapter.

I.5 References

[I.1] "*Testing and troubleshooting digital RF communication transmitter designs,*" Application Note 1313, Agilent Technology Literature No. 5968-3578E, 2002.

[I.2] "*Understanding CDMA measurements for base stations and their components*," Application Note 1311, Agilent Technology Literature No. 5968-0953E, 2000.

[I.3] "*Understanding GSM/EDGE Transmitter and Receiver Measurements for Base Transceiver Stations and Their Components,*" Application Note 1312, Agilent Technology Literature No. 5968-2320E, 2002.

[I.4] "*Understanding PDC and NADC Transmitter Measurements for Base Transceiver Stations and Mobile Stations,*" Application Note 1324, Agilent Technology Literature No. 5968-5537E, 2000.

[I.5] "*Using Error Vector Magnitude Measurements to Analyze and Troubleshoot Vector-Modulate Signals,*" Product Note 89400-14, Agilent Technologies Literature No. 5965-2898E, 2000.

[I.6] IEEE 802.16TM-2004, Standard for local and metropolitan area networks – Part 16: Air interface for fixed broadband wireless access systems. (Revision of IEEE Std 802.16-2001) June 2004, ISBN 0-7381-4069-4 SH95246.

[I.7] L. Angrisani, A. Napolitano, M. Vadursi "*Measuring I/Q Impairments in WiMAX Transmitters*," IEEE Trans. Instrum. Measurements, Vol. 58, n.5, May. 2009, pp: 1299‐1306.

[I.8] L. Angrisani, M. D'Apuzzo, M. D'Arco, "*New digital signal-processing approach for transmitter measurement in third generation telecommunication systems*," IEEE Trans.on Instrum. And Measur., Vol. 53 no. 3, June 2004, pp. 622-629.

[I.9] "*Digital Modulation in Communications Systems: An Introduction*," Application Note 1298, Agilent Technologies Literature No. 5965-7160E, 2002.

[I.10] L. Angrisani, M. D'Apuzzo, M. D'Arco, "*A New Method for Power Measurements in Digital Wireless Communication Systems*," IEEE Trans. on Instrum. and Measur., vol.52, no.4, Aug. 2003, pp.1097-1106

Chapter II

Proposed Methods

II.1 Introduction

The chapter presents two original measurement methods. The first one allows to assess the modulation quality of signal compliant to IEEE 802.16d-2004 standard and the second one is capable of singling out the power spectrum of each signal involved into analysis, useful or interfering, in presence of in-channel interference, through which the metrics in frequency domain can be estimated. For each method, the state of the art is discussed, the proposed method is described, details about the experimental setup is given, and the experimental results are commented on in order to assess the method performance.

II.2 First measurement method: WIMAX signals modulation quality assessment

First measurement method is addressed to modulation quality assessment of signal compliant to IEEE 802.16d-2004 standard, commonly indicated as WiMAX.

WiMAX is a standards-based technology enabling the delivery of last mile wireless broadband access as an alternative to cable and asymmetric digital subscriber line (ADSL) [II.1]-[II.4]. Its

development and diffusion is being encouraged by broadband communication companies through the organization and sponsorship of workshops, training courses, and forums worldwide. Its deployment represents a real challenge for wireless communication researchers, technicians, and operators; the development of reliable migration strategies from pre-WiMAX systems is still in progress, and relevant questions related to spectrum regulation has to be faced in many countries. A complete characterization of WiMAX systems involves a great number of tests, each of which is characterized by a different measurement principle, operative procedure, required accuracy, and involved instrumentation. With special regard to transmitters, significant measurements have to be carried out, concerning power level, occupied bandwidth, adjacent channel power ratio (ACPR) and, above all, modulation quality [II.7]-[II.9].

A number of test solutions specifically addressed to modulation quality measurement can be found on the market, offered by major instrumentation and measurement companies. They all complement an existing and specialized measurement instrument, such as a real-time spectrum analyzer (RSA) or a vector signal analyzer (VSA), with a proper digital signal processing software (analysis software). The adopted instrument generally executes the downconversion of the radiofrequency (RF) input signal, and its successive digitization and demodulation. The analysis software often runs on an external workstation, connected to the instrument either via IEEE-802.3 or IEEE-488 standard interface, and gains the desired measurement information by digitally processing the baseband components of the signal. Moreover, it's strictly dependent on the adopted instrument; no functionality with a different measurement hardware is in principle assured. Stemming from the preliminary ideas given in [II.10], an alternative measurement approach with respect to those available on the market is presented. It relies on an original and modular digital signal processing algorithm for the estimation of modulation quality parameters related both to downlink and uplink connection, such as channel response, relative constellation error (RCE), and error vector magnitude (EVM).

Differently from the other measurement solutions, the proposed approach provides for a direct digitization of the RF input signal, without any preliminary analog downconversion. It doesn't depend on a specific acquisition hardware. General purpose digital scopes or data acquisition systems, characterized by suitable analog bandwidth and maximum sample rate, can profitably be used, with a consequent improvement in flexibility and efficiency. Furthermore, it operates with success in both transmission modes allowed by the standard [II.7], Time Division Duplex (TDD) or Frequency Division Duplex (FDD), and above all, whatever the frame structure, bursty or continuous, thus overcoming a notable limit of competitive solutions.

After being digitized, the input signal is demodulated in order to gain its baseband components. The obtained components are then properly resampled and passed to the so-called synchronization stage,

which recognizes the transmission mode and frame structure, and, for each subframe, performs timing recovery, channel equalization, and extraction of transmitted OFDM symbols. At the end, the aforementioned modulation quality parameters are estimated.

II.2.1 WIMAX FUNDAMENTALS

II.2.1.A OFDM modulation

A simplified OFDM implementation diagram is sketched in Fig. II.1. The input serial bit sequence, b_i, is parallelized into k groups, to each of which a quadrature amplitude modulation (QAM) is applied. The k complex sequences of QAM points $C_0(n)$, $C_1(n)$,.., $C_{k-1}(n)$ modulate orthogonal subcarriers; n stands for the discrete-time variable. For a given n, $C_0(n)$, $C_1(n)$,.., $C_{k-1}(n)$ is the so-called frequency-domain OFDM symbol, and it can be regarded as the FFT (Fast Fourier Transform) coefficients of the time-sequence $c_0(n)$, $c_1(n)$,.., $c_{k-1}(n)$, which is also named time-domain OFDM symbol; n plays the role of OFDM symbol time. Real and imaginary parts of the complex sequence resulting from the serialization of the IFFT output are, respectively, the I and Q component feeding the I/Q modulator. Their expression, in complex form, is

$$I_m(n) + jQ_m(n) = \sum_{h=0}^{k-1} C_h(n) e^{j2\pi h \frac{m}{k}}, \quad m = 0, 1, \ldots, k\text{-}1 \qquad \text{(II-1)}$$

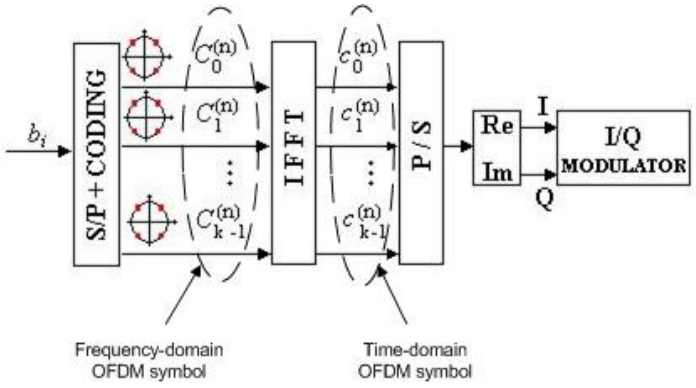

Fig. II.1 OFDM modulation scheme.

II.2.1.B Physical layer

Transmission modes. WiMAX physical layer supports both Frequency Division Duplex (FDD) and Time Division Duplex (TDD) transmission mode [II.6].

In the FDD mode, information data from the Base Station (BS) to Subscribe Station (SS), i.e. downlink data, and that from the SS to BS, i.e. uplink data, are conveyed through a dedicated channel

(different carrier frequencies are involved). For each channel, the frame structure can be either bursty or continuous. In the bursty case, it consists of a number of subframes separated by times gaps; in the continuous case, no time gap is present.

In the TDD mode a single carrier frequency is exploited. Downlink and uplink data are transmitted in different time windows, giving rise respectively to a downlink and uplink subframe in the same channel. Any frame, in particular, contains a downlink subframe followed by an uplink one, and it can have a bursty or continuous structure. In the bursty case, two suitable time gaps are used. More specifically, the transmit/receive transition gap (TTG) separates the downlink subframe from the uplink one, allowing the BS to switch from the transmitting state to receiving one and the SS from the receiving state to transmitting one, while the receive/transmit transition gap (RTG) separates the uplink subframe from the downlink one, allowing the BS to switch from the receiving state to transmitting one and the SS from the transmitting state to receiving one. During these gaps, both the BS and SS don't transmit. In the continuous case, the two subframes are sent back-to-back without gaps.

Frequency domain features. Frequency-domain OFDM symbols are transmitted through 256 uniformly spaced subcarriers. To grant guard bands, however, only 200 of them are active. Moreover, they are divided into two groups. The first group, consisting of 192 subcarriers (also referred to as active subcarriers), is exploited for data transmission, while the second smaller group, comprising 8 pilot subcarriers, is used for channel estimation. Subcarriers can be characterized by one of four different modulation schemes: binary phase shift keying (BPSK), quadrature phase shift keying (QPSK), 16-QAM and 64-QAM. Data length, in terms of number of bits in a single frequency-domain OFDM symbol, varies according to the adopted modulation scheme. Within each frequency-domain OFDM symbol, the same modulation scheme must be used; it can change from a frequency-domain OFDM symbol to another, with the exception of pilot subcarriers that are always BPSK modulated.

Time domain features. WiMAX signals are created through standard I/Q modulation techniques. The baseband I and Q components are first attained in digital form by applying an IFFT algorithm to a sequence made up of 256 complex values, which convey the points that modulate the subcarriers (see Fig. II.1). The sequence that results from the serialization of the IFFT output is prolonged through the so-called cyclic prefix technique [II.6][II.7]. In particular, the last g*256 values (cyclic prefix) of the aforementioned sequence are repeated at the beginning; g is often referred to as guard interval and can be equal to 1/4, 1/8, 1/16, or 1/32. The so-obtained new sequence is known as WiMAX time-domain OFDM symbol (in the following referred simply to as time-domain OFDM symbol), while the previous one as its useful part. The real and imaginary parts of the final sequence, which represent respectively the I and Q baseband component, are then extracted. The WiMAX signal can be created generating in analog

form the aforementioned components and giving them in input to an analog modulator. The generation frequency is fixed by the standard according to the requested bandwidth, which is in turn determined by the duration of the useful part of the symbol [II.7]. In particular, the reciprocal of this duration gives the subcarrier spacing. Adding the cyclic prefix to prolong the original time-domain OFDM symbol does not impact on the requested bandwidth, but improves multipath immunity and tolerance for symbol timing recovery.

The basic structure of a downlink subframe consists of a long preamble, a header, and several time-domain OFDM symbols. The long preamble contains two time-domain OFDM symbols: the first uses only 50 of 200 available subcarriers (every 4th subcarrier), the second all the even numbered, i.e. 100 subcarriers. All subcarriers associated with the first time-domain OFDM symbol of the long preamble are QPSK modulated. The time-domain OFDM symbols that complete the subframe contain both data and additional control messages.

An uplink subframe starts with a short preamble, which enlists a single time-domain OFDM symbol involving 100 QPSK modulated subcarriers. The short preamble allows the base station to synchronize on each individual subscriber and perform an initial channel estimation. After the short preamble, user data symbols are transmitted according to a suitable modulation scheme.

II.2.1.C Modulation quality assessment

For modulation quality assessment, the standard [6] defines the relative constellation error (RCE) as relevant figure of merit, which is very similar to the error vector magnitude (EVM) used in other digital communication systems [II.7]-[II.11]. For an ideal transmitter, the signals would have all constellation points precisely at the ideal locations, however various imperfections in the implementation cause the actual constellation points to deviate from the ideal locations. The measure of the root mean square (RMS) between the actual and ideal points, averaged across all frequency-domain OFDM symbols presented in the acquired signal, defines the RCE value [II.6]:

$$RCE = \frac{1}{N_f}\sum_{i=1}^{N_f}\frac{\sum_{j=1}^{L_P}\left[\sum_{\substack{k=-N_{used}/2\\k\neq 0}}^{N_{used}/2}\left\{\left(\mathrm{Re}(i,j,k)-\mathrm{Re}_0(i,j,k)\right)^2+\left(\mathrm{Im}(i,j,k)-\mathrm{Im}_0(i,j,k)\right)^2\right\}\right]}{\sum_{j=1}^{L_P}\left[\sum_{\substack{k=-N_{used}/2\\k\neq 0}}^{N_{used}/2}\left\{\mathrm{Re}_0(i,j,k)^2+\mathrm{Im}_0(i,j,k)^2\right\}\right]} \qquad \text{(II-2)}$$

where N_f is the number of detected subframes, L_p is the number of time-domain OFDM symbols within the i^{th} subframe, N_{used} stands for the number of active subcarriers in the current symbol,

$\mathrm{Re}_0(i,j,k)$ and $\mathrm{Im}_0(i,j,k)$ denote the ideal point in the complex plane related to the k^{th} subcarrier associated with the j^{th} time-domain OFDM symbol within the i^{th} subframe, and $\mathrm{Re}(i,j,k)$ and $\mathrm{Im}(i,j,k)$ denotes the observed point in the complex plane related to the k^{th} subcarrier associated with the j^{th} time-domain OFDM symbol within the i^{th} subframe. The RCE value should be within specific limits, which depend on modulation type, for minimizing problems at receiver.

Specifically, the main steps described by the standard for RCE evaluation provide for: detection of the subframe of interest, symbol timing recovery (synchronization), coarse and fine frequency offset estimation and compensation, channel frequency response estimation and equalization, and actual constellation recognition.

Although not strictly required by the standard, it can be helpful considering other parameters specifically addressed to modulation quality. Major solutions available on the market allow EVM to be measured according to the following relation [II.14]:

$$EVM = \frac{\sum_{\substack{k=-N_{used}/2 \\ k\neq 0}}^{N_{used}/2} \left\{ \left(\mathrm{Re}(i,j,k) - \mathrm{Re}_0(i,j,k)\right)^2 + \left(\mathrm{Im}(i,j,k) - \mathrm{Im}_0(i,j,k)\right)^2 \right\}}{\sum_{\substack{k=-N_{used}/2 \\ k\neq 0}}^{N_{used}/2} \left\{ \mathrm{Re}_0(i,j,k)^2 + \mathrm{Im}_0(i,j,k)^2 \right\}} \qquad \text{(II-3)}$$

While the RCE provides global information on modulation quality, the EVM accounts for the modulation quality for each symbol involved in the analysis.

II.2.2 Proposed approach

The proposed approach has two different measurement configurations, namely auto-detection and user-defined configuration. When auto-detection is activated, guard interval, occupied bandwidth, modulation schemes, frame structure and frame duration are automatically detected. In the user-defined configuration, specific values for the aforementioned parameters have to be provided. In both configurations, the transmission mode and carrier frequency of the signal under analysis have to be *a-prior* known. In particular, if the FDD mode is involved, the carrier frequency refers to the transmission channel.

Furthermore, the approach can operate in "single" or "continuous" mode. In "single" mode, one single measurement is performed, while in "continuous" mode repeated measurements are executed. The measurement process can be supervised through a user-friendly graphical interface (GUI).

For the sake of clarity, the main stages of the approach, sketched in the block diagram of Fig. II.2, are separately and detailed described in the following.

II.2.2.A Digitization

Any data acquisition system (DAS) with an analog input bandwidth greater than few units of gigahertz, a sample rate faster than 10 GS/s and a nominal vertical resolution not smaller than 8 bits is eligible for directly digitizing the RF signal to be analyzed. Solutions that meet these technical features are widespread on the market, and commonly used in telecommunication laboratories. Moreover, its memory

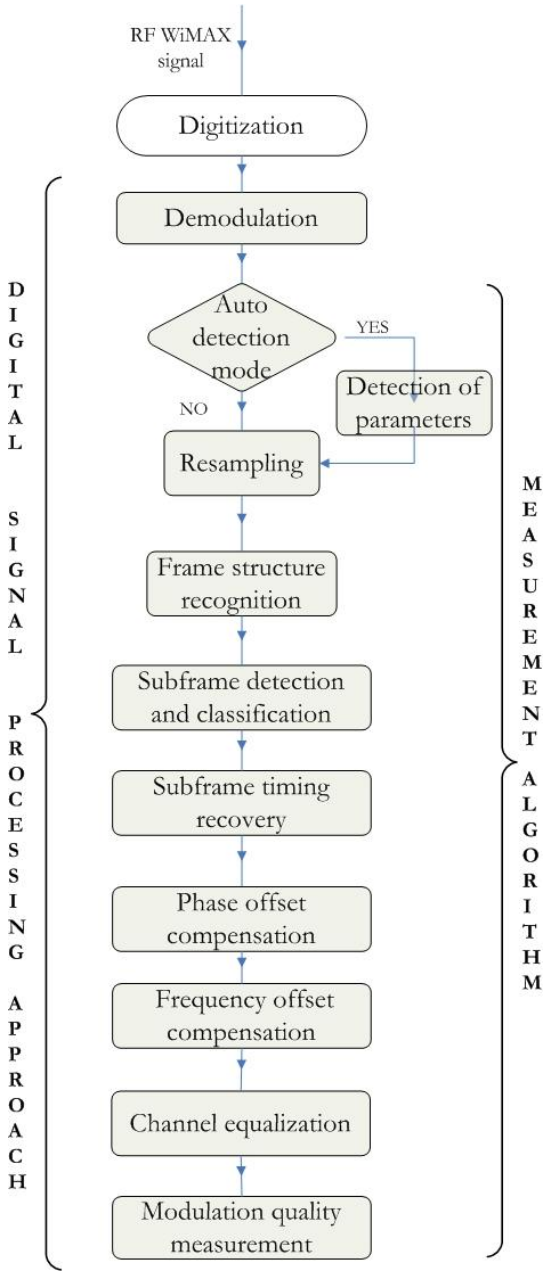

Fig. II.2 Block diagram of the proposed digital signal processing approach.

depth has to be

chosen in such a way as to allow the time interval of interest (including one or more frames) to be completely observed.

II.2.2.B Quadrature Demodulation

Quadrature demodulation [II.16] extracts the baseband I and Q components from the digitized WiMAX signal. Incoherent demodulation is adopted, which relies on the following model (Fig. II.3):

$$s(nT) = I'(nT) * \cos(2\pi(f_0 + \Delta f)nT + \varphi) + Q'(nT) * \sin(2\pi(f_0 + \Delta f)nT + \varphi) \quad \text{(II-4)}$$

where f_s stands for the sampling rate, φ is a constant-phase term, f_o the nominal carrier frequency of the

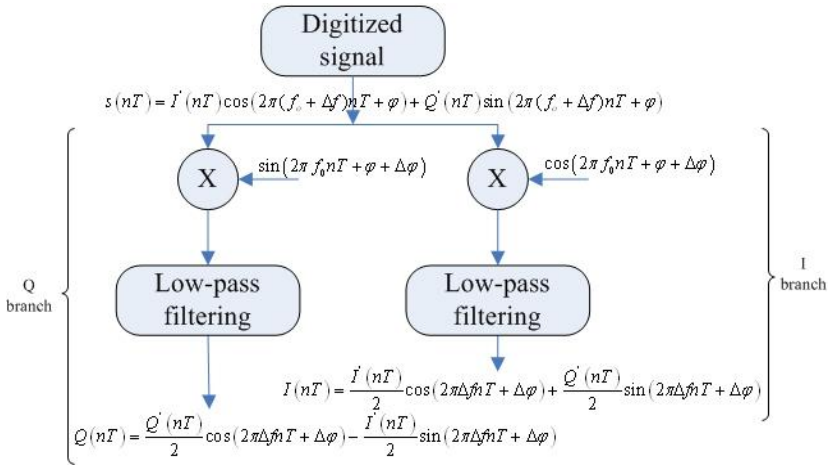

Fig. II.3 Quadrature demodulation scheme.

transmitted signal, Δf the carrier frequency offset, $\Delta\varphi$ the phase offset, and n is the discrete time variable. With regard to the I branch, the digitized signal is multiplied by a discrete-time co-sinusoidal carrier, the frequency of which is equal to f_0. The multiplication gives rise both to a baseband component and a high-frequency component, and a low-pass fifth-order Butterworth filter is applied to retain only the baseband component (also called I component). As for the Q branch, the orthogonal version (also called the Q component) of the aforementioned baseband component is furnished as a result of similar operations. The cut-off frequency of the low-pass filter has to be chosen according to the widest WiMAX channel bandwidth (i.e. 28 MHz); moreover, high stopband attenuation is recommended. If the FDD mode is involved, the filter allows only the signal related to the transmission channel of interest to be retrieved.

II.2.2.C Auto-detection

Guard interval g, expressed as a fraction of the useful part, T_b, of a time-domain OFDM symbol as well as channel bandwidth are automatically evaluated in this stage. They allow both T_b and the duration of

the cyclic prefix, expressed as $T_g = g * T_b$, to be assessed. Let us recall that the duration of the whole time-domain OFDM symbol is $T_s = T_g + T_b$. The adopted iterative procedure works as follows:

- the ratio between the adopted sample rate, f_s, and each of the admissible generation frequencies, according to the standard guidelines [II.2], is calculated. Multiplying each of the obtained values by the standard number of samples included in the useful part of a time-domain OFDM symbol, for the given generation frequency, provides the actual number of samples, *N*, characterizing the useful part of any time-domain OFDM symbol in the acquired record;
- the values of *N* and *M* (*M* = *g***N*, number of samples included in the cyclic prefix) are determined for each admissible generation frequency-guard interval couple; *P* = *N* + *M* gives the number of samples peculiar to the whole time-domain OFDM symbol;
- the presence of the cyclic prefix is exploited. In particular, a time window embracing *M* samples in the acquired record is considered, the first sample of which is supposed to mark the beginning of a time-domain OFDM symbol. The autocorrelation function between the window and another one of the same length, located at the end of the enlisted time-domain OFDM symbol, is evaluated. Other *P*-1 autocorrelation functions are calculated moving both windows forward, one sample at a time. The greatest value, *x*, among those assumed by all *P* functions is found. The procedure is iterated for each admissible generation frequency-guard interval couple. A sequence x_i (*i=1,…,m*, *m* being the number of admissible couples) is obtained, and the couple with which the greatest value is associated, is taken into account for finally fixing the guard interval and channel bandwidth.

II.2.2.D Resampling

A correct and efficient working of the approach calls for baseband components characterized by a sample rate equal to a integer multiple, *z*, of the generation frequency of the input WiMAX signal. This condition is not met in most practical cases, due both to the unknown symbol rate of the signal and limited adjustment of the adopted hardware. This is the reason why a digital resampling algorithm has to be applied to both components.

To gain a new sample rate, equal to $\frac{Y}{W} f_s$ and capable of meeting the aforementioned condition, the following steps are taken:

- upsampling by *Y*: insertion of zeros between two successive samples;
- low-pass filtering: polyphase FIR filter plays an anti-aliasing function before decimation;
- decimation by *W*: every W^{th} sample of the filtered sample is picked out.

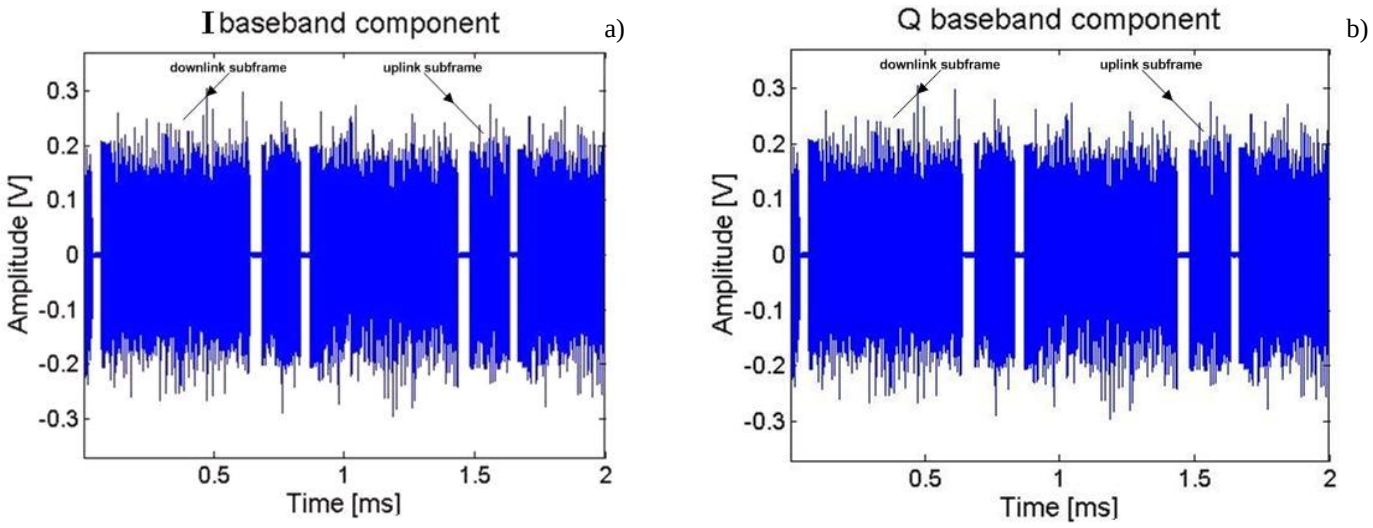

Fig. II4 a) I and b) Q baseband component after resampling.

Many experimental tests, conducted for different values of channel bandwidth and guard interval, have pointed out that $\tilde{z}$ equal to 8 is the good tradeoff between computational burden and accuracy. A typical evolution versus time of resampled I and Q components in the TDD mode and bursty frame structure is given respectively in Fig. II.4a and Fig. II.4b.

II.2.2.E Frame structure recognition and subframe detection

For frame structure recognition, the presence of time gaps in the baseband components is checked. A gap is identified as a series of consecutive samples, the values of which are below a suitable threshold, set to 3% of the peak power characterizing the considered baseband component. If time gaps are found, their first and last sample allow the detection respectively of the end of the previous subframe and the beginning of the successive one. If no time gap emerges, a continuous frame structure is active, and an innovative procedure, designed and implemented by the authors, is applied for subframe detection. Its main stages are:

- calculation of the envelop power (EP) according to
  $$EP(n) = I(n)^2 + Q(n)^2 \quad \text{(II-5)}$$
- application of a moving average filter on the obtained envelop power. For each subframe, the preamble, the mean power of which is twice greater than that of the remaining part, is thus emphasized (Fig. II.5). A rough estimate of preamble location is achieved by singling out the samples in the filter output that overcome a threshold equal to 10 % of the peak power. The values of the discrete-time variable associated to all selected samples (Fig. II.6) are gathered into the vector *SI* as follows:

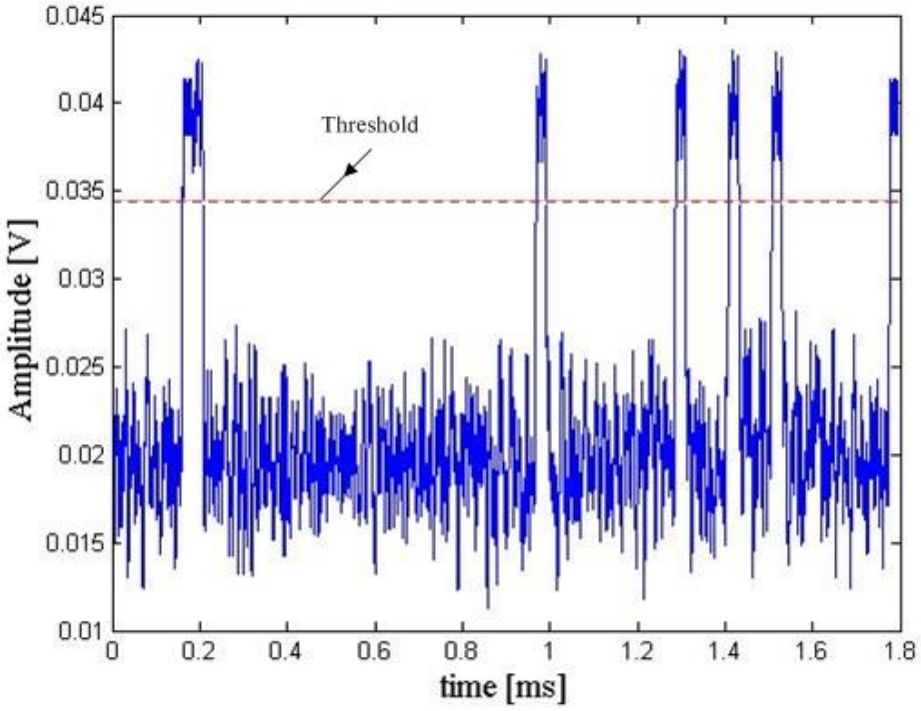

Fig. II.5 Moving average filter output. The dashed line shows the threshold set to 10% of the peak power.

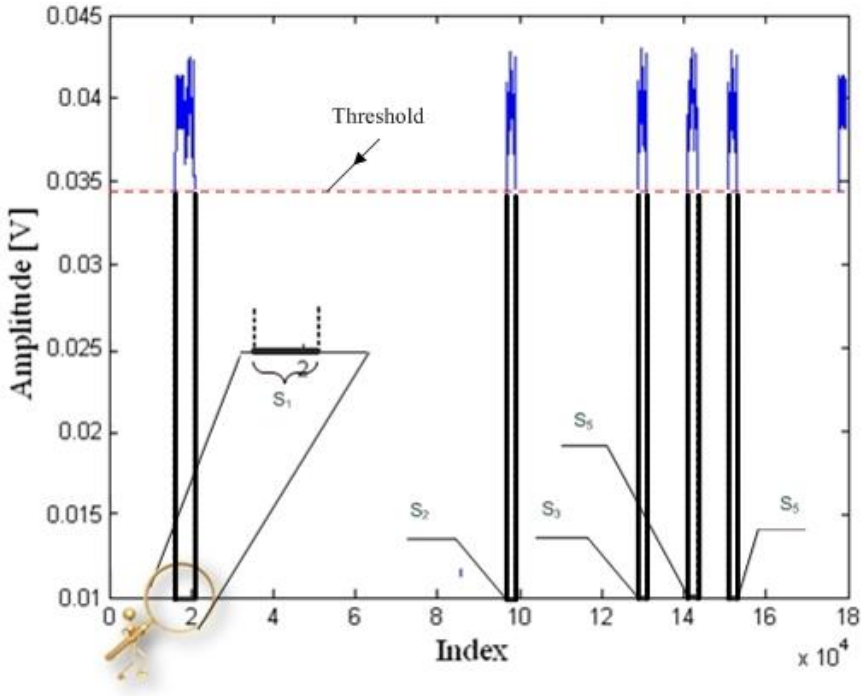

Fig. II.6 Values of the discrete-time variable associated to the samples above the threshold (dashed line). s1 collects the values related to the first preamble, s2 those related to the second preamble, and finally s5 those related to the last detected preamble.

$$SI = \bigcup_{i=1}^{L} s_i \qquad \text{(II-6)}$$

where the element s_i stands for the values (an entire block) of the discrete-time variable peculiar to the *i*-th preamble; *L* is the number of detected subframes;

- calculation of a new vector *DI*, the elements of which are given by

$$DI_j = SI_{j+1} - SI_j, \qquad j = 1,..,r-1 \qquad \text{(II-7)}$$

where *r* is the dimension of the vector *SI*. All elements of *DI* have the same value (equal to 1) but those corresponding to the beginning of each preamble (i.e. the beginning of each detected subframe). Due to the continuous structure, the end of a subframe is pointed out by the sample positioned before the beginning of the successive preamble.

II.2.2.F Subframe classification

Downlink subframes are distinguished from uplink ones through the analysis of their preamble. If the number of active subcarriers characterizing the first time-domain OFDM symbol is 50, as it is for a long preamble, a downlink subframe is encountered, otherwise, if 100 active subcarriers are detected, a short preamble of an uplink subframe is found.

II.2.2.G Subframe timing recovery

After detecting a subframe, all samples within a time interval T_I, centered on its onset and characterized by a time extent much smaller than the time-domain OFDM symbol duration, are taken into account. Then, starting from the first sample of the interval, a portion of the subframe, the duration of which is equal to that of a whole time-domain OFDM symbol, is selected. The cyclic prefix of the symbol is removed, and the FFT of the remaining part is calculated. Since both long and short preambles are characterized by QPSK modulation, the subset of all FFT bins related to active carriers gives rise to known QPSK points on the complex plane. Due to the lack of synchronization, the positions of the detected points on the complex plane may be much different from the expected ones. The detected points are thus rotated of a certain amount, estimated as the average of the phase deviations of the actual points with respect to the related ideal ones, and finally normalized.

The procedure is applied to all the other portions of the subframe, always covering a whole time-domain OFDM symbol, which are obtained moving forward the beginning of the portion considered above, one sample at a time, up to the end of T_I. For each portion, the EVM characterizing the final points is evaluated. The time instant associated with the beginning of the portion, in correspondence of which the

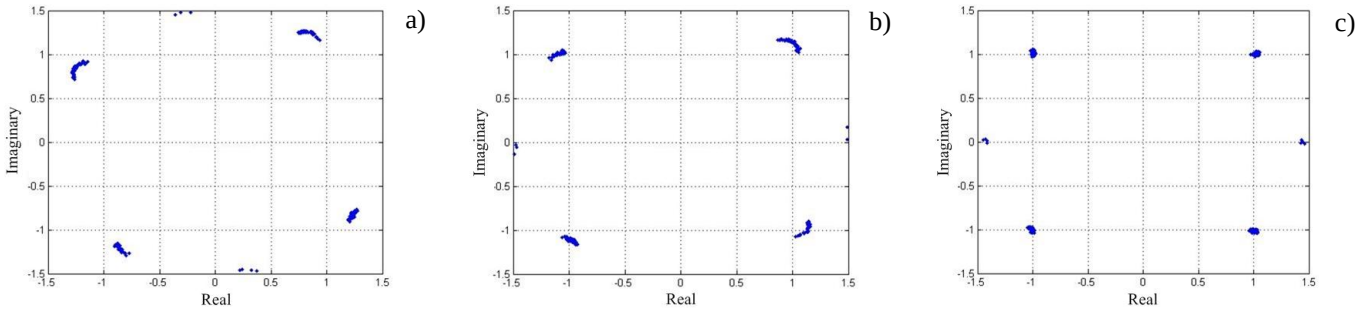

Fig. II.7 OFDM symbol, characterized by QPSK modulation, as it appears on the complex plane a) before and after b) phase offset and c) carrier frequency offset compensation.

minimum EVM value is attained, i.e. the smallest scattering of the points, is elected as true initial time of the subframe. Very fine synchronization is typically achieved with T_I including about 20 samples.

II.2.2.H Phase Offset estimation and compensation

This stage aims at measuring and compensating the phase offset introduced by the incoherent quadrature demodulation. For each subframe, the first time-domain OFDM symbol of the preamble (the only one in an uplink subframe) is exploited; IEEE 802.16d-2004 standard, in fact, fixes the ideal position, in terms of amplitude and phase on the complex plane, of the active subcarriers associated with it. Thus, the angle between the actual and ideal position is assessed, and the desired phase offset is estimated through an average process and suitably compensated. As an example, Fig. II.7a shows typical detected points on the complex plane, while Fig. II.7b gives their position after phase offset compensation and normalization.

II.2.2.I Carrier frequency offset estimation and compensation

Carrier frequency offset [II.17] is a typical issue in quadrature demodulation. It refers to the difference between the actual carrier frequency of the input signal and that of the local oscillator, used to generate the sine and cosine waveforms in the demodulation stage. As a matter of the fact, the carrier frequency often experiences slight variations around its nominal value. Differently from the phase offset, which introduces a constant and rigid rotation of all frequency-domain OFDM symbols on complex plane, the carrier frequency offset causes different rotation angles. A typical effect is depicted in Fig. II.7b.

To estimate and compensate a possible carrier frequency offset, a proper procedure is applied to each subframe. Pilot subcarriers of the obtained frequency-domain OFDM symbols are in particular exploited. For each frequency-domain OFDM symbol and for each pilot subcarrier, the difference between the phase characterizing the nominal position on the complex plane associated with the subcarrier, fixed by

the standard, and that peculiar to the actual one is first evaluated (referred to as subcarrier phase error). Then, all the subcarrier phase errors in a given frequency-domain OFDM symbol are averaged, obtaining the symbol phase error. The evolution of the symbol phase error versus time within the subframe is calculated (phase error trace). The slope ($\Delta\varphi$) of the obtained trace finally gives the desired frequency offset:

$$\Delta f = \frac{\Delta\varphi f_s}{2\pi P} \tag{II-8}$$

Compensation is straightforwardly accomplished in the time domain according to

$$S(n)_{new} = (I(n) + jQ(n)) * e^{-j2\pi\Delta f n} \tag{II-9}$$

Typical compensation results are shown in Fig. II.7c.

II.2.2.J Channel equalization

Attention is focused either on the time-domain OFDM symbol transmitted through 100 active carriers, which is the second time-domain OFDM symbol of the long preamble of the downlink subframe, or the unique time-domain OFDM symbol of the short preamble of the uplink subframe. For each of the 100 subcarriers, proper complex coefficients to compensate gain and phase are obtained as difference between the actual and ideal position of the detected points on the complex plane. They give information about the behavior of the channel at some frequencies inside the occupied bandwidth, and a linear interpolation algorithm is thus exploited in order to reconstruct the whole frequency response exhibited by the channel. Channel equalization for each obtained frequency-domain OFDM symbol of the subframe can thus be carried out.

To mitigate other detrimental time-varying effects, such as those related to momentary fading, a further equalization is conducted. To this aim, a new estimate of the actual gain and phase characterizing the channel is obtained from the current frequency-domain OFDM symbol. In particular, only the eight pilot subcarriers are monitored.

II.2.2.K Estimation of modulation quality parameters

The value of RCE is gained through the application of expression (II-2) to the active subcarriers. Non standard parameters can be evaluated as well. As an example, the RCE related to a subset of frequency-domain OFDM symbols characterized by the same modulation scheme, as well as the EVM related to each frequency-domain OFDM symbol, can be obtained. In the auto-detection configuration, the estimated value of all considered parameters is also presented to the user.

II.2.3 Performance assessment

To assess the performance of the proposed approach, a number of experiments has been executed on laboratory WiMAX signals. A suitable measurement station has been set up to the purpose (Fig. II.8). Moreover, major solutions already available on the market have been taken into account for a comparative analysis.

II.2.3.A Measurement station

The measurement station (Fig. II.8) has been equipped with a vector signal generator (ESG), namely Agilent Technologies *ESG E4438C*^{TM} (250 kHz – 6 GHz output frequency range), with arbitrary waveform generation capability (80 MHz modulation bandwidth, 16 bit vertical resolution, 8 MSample memory depth), a signal analyzer (MXA), namely Agilent Technologies *N9020A*^{TM} (20 Hz – 8.4 GHz input frequency range), with digital demodulation capability (25 MHz analysis bandwidth, 12 bit vertical resolution) and operating as a VSA, a real-time spectrum analyzer (RSA), namely Tektronix *3408A*^{TM} (DC - 8 GHz input frequency range), with digital demodulation capability (36 MHz analysis bandwidth, 12 bit vertical resolution), and a digital scope (SDA), namely LeCroy *SDA6000A*^{TM} (DC - 6 GHz input analog bandwidth, 8 bit vertical resolution, 20 GS/s maximum sample rate, 100 MSample memory depth). All instruments have been interconnected to a processing and control unit through a 100 Mbit/s IEEE 802.3 standard interface.

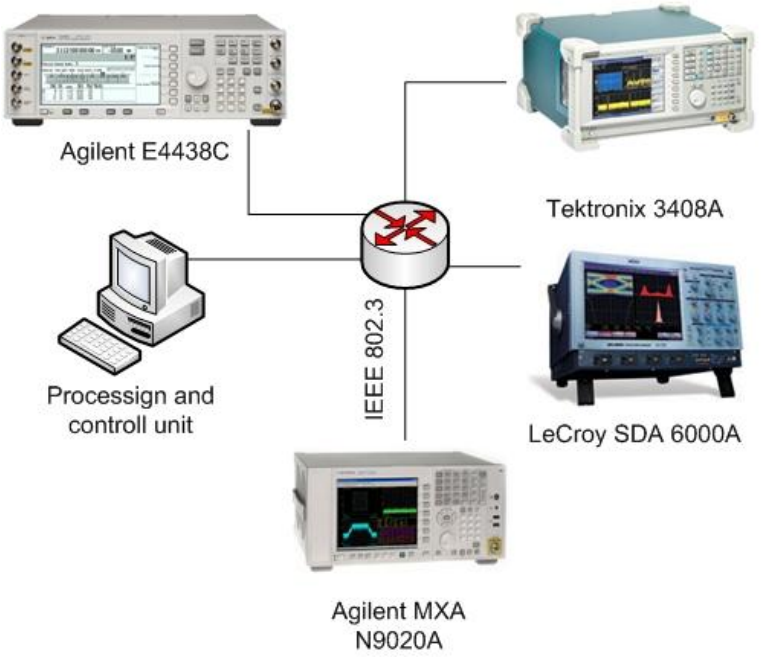

Fig. II.8 Measurement station.

WiMAX signals compliant with IEEE 802.16d-2004 have first been generated by means of an appropriate signal studio software running on the processing and control unit. They have been downloaded into the local memory of the ESG, which has produced them in analog form at radiofrequency [II.10]. The RF signal has been routed to the RSA and MXA as well as to the SDA. A sample rate equal to 10 GS/s and the maximum vertical resolution have been exploited as default setting for signal digitization by SDA. The digitized signal has been retrieved by the processing and control unit, on which the Matlab® software implementing both the proposed approach and GUI has run.

II.2.3.B Application examples

For the sake of clarity, the typical output of the proposed approach is shown in Fig. II.10a. Two

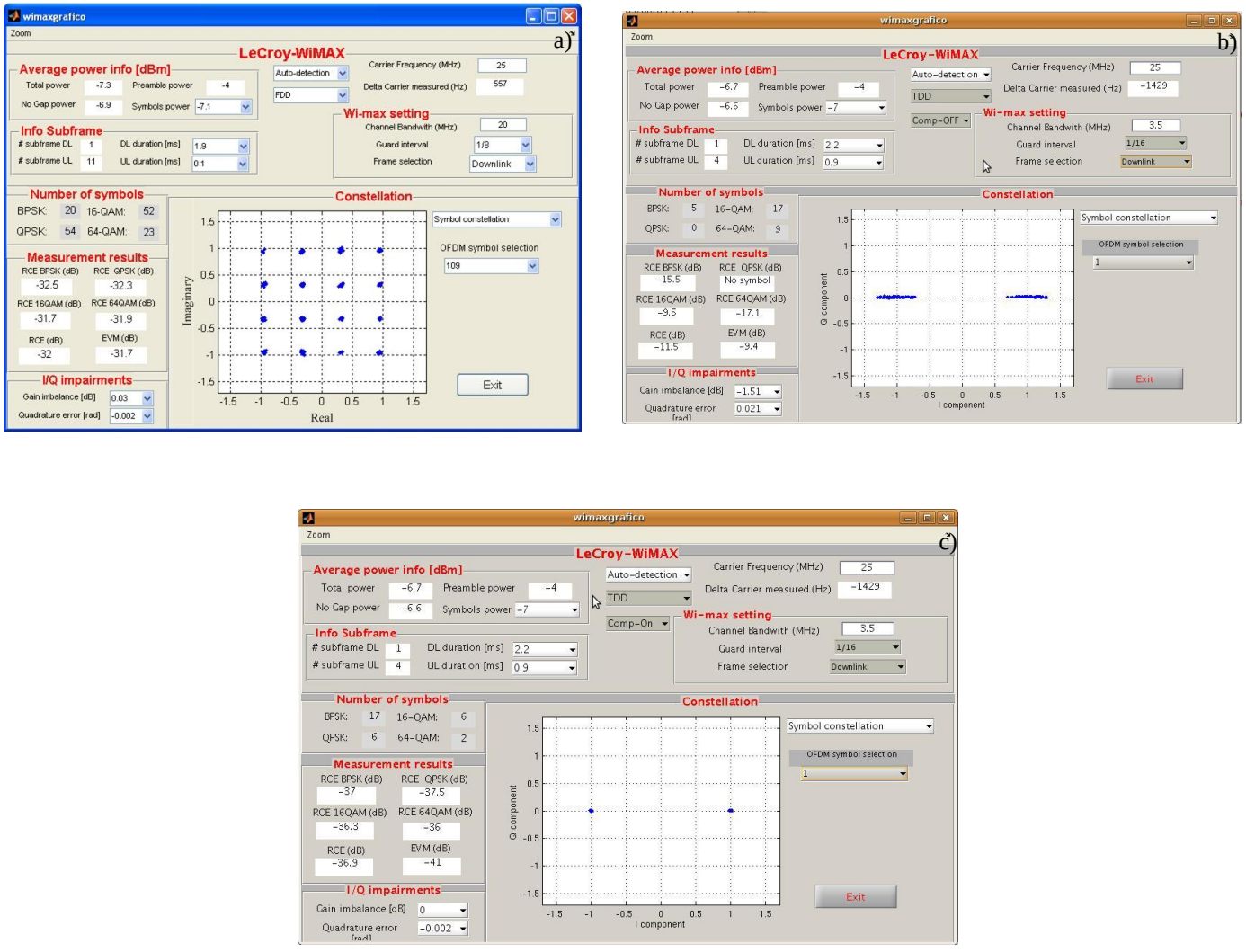

Fig. II.9 Typical output of the proposed approach through the GUI. It refers to a WiMAX signal characterized by the TDD transmission mode a) and TDD without a) and with b) activation of correction stages.

application examples are considered to the purpose. The first example concerns a WiMAX signal characterized by TDD transmission mode and continuous frame structure with (Fig. II.9a) and without (Fig. II.9b) phase and carrier frequency offset compensation. It is worth noting that the compensation stages play a key role throughout the measurement chain. The second example, instead, refers to a WiMAX signal exhibiting FDD transmission mode and bursty frame structure (Fig. II.9c).

In both examples, the GUI clearly offers to the user information both on the structure of each analyzed subframe, like channel bandwidth, guard interval, duration, number of time-domain OFDM symbols, and related modulation quality parameters (RCE and EVM). Moreover, the constellation display of each symbol on the complex plane is also allowed.

II.2.3.C Comparative analysis

Performance of the proposed approach has been compared to that offered by major solutions

Tab. II.1 Main features of the considered measurement solutions.

	89601A™	***RSA-IQWIMAX™***	**Proposed approach**
Operative mode	Uplink & Downlink	Uplink & Downlink	Uplink & Downlink
Input parameters	Channel Bandwidth	Channel bandwidth	Channel Bandwidth
	Guard interval	Guard interval	Guard interval
	Frame duration	Frame duration	-
Auto-detection mode	NO	YES (Channel bandwidth, guard interval and frame duration are automatically evaluated)	YES (Channel bandwidth, guard interval and frame duration are automatically evaluated)
Output results	Constellation diagram	Constellation diagram	Constellation diagram
	Modulation scheme	Modulation scheme	Modulation scheme
	Average RCE(EVM) (Error vector magnitude averaged over all OFDM symbols)	Average EVM (Error vector magnitude averaged over all OFDM symbols)	Average EVM (Error vector magnitude averaged over all OFDM symbols)
	RCE(EVM) for each OFDM symbol	EVM for each OFDM symbol	EVM for each OFDM symbol
	-	-	Total RCE (Relative Constellation Error averaged over all symbols and subframes)
	-	-	Single RCE (Relative Constellation Error averaged over all symbols characterized by the same modulation scheme)
	-	-	Number of downlink and uplink subframes
	-	-	Duration of downlink and uplink subframe
	Peak RCE (EVM)	-	-
	Pilot carrier RCE (EVM)	-	-

Tab. II.2 Mean and experimental standard deviation of 50 EVM values related to a WiMAX signal characterized by a power level equal to -10 dBm and bursty frame structure, for different values of channel bandwidth and guard interval.

Channel Bandwidth [MHz]	Guard Interval	Power level equal to -10 dBm in bursty frame structure											
		Agilent Technologies solution				Tektronix solution				Proposed approach			
		Average [dB]		Standard deviation [dB]		Average [dB]		Standard deviation [dB]		Average [dB]		Standard deviation [dB]	
		TDD	FDD	TDD	FDD	TDD	FDD	TDD	FDD	TDD	FDD	TDD	FDD
2.5	1/4	-39.12	-38.12	0.05	0.04	-40.11	-39.32	0.05	0.03	-39.91	-38.92	0.08	0.07
	1/8	-38.95	-39.21	0.06	0.01	-41.12	-40.11	0.06	0.05	-39.11	-39.22	0.06	0.04
	1/16	-39.84	-39.52	0.08	0.06	-41.21	-40.21	0.02	0.01	-39.12	-39.35	0.05	0.06
	1/32	-39.73	-39.32	0.04	0.05	-41.10	-41.52	0.04	0.09	-39.51	-39.78	0.02	0.03
5.50	1/4	-39.13	-39.31	0.06	0.07	-42.13	-42.45	0.04	0.04	-39.20	-39.65	0.03	0.01
	1/8	-38.95	-38.26	0.07	0.03	-41.63	-41.22	0.04	0.03	-39.44	-40.01	0.05	0.06
	1/16	-39.84	-39.45	0.09	0.03	-40.54	-40.85	0.03	0.02	-38.46	-38.62	0.09	0.02
	1/32	-39.76	-39.32	0.08	0.02	-40.82	-40.16	0.02	0.08	-39.94	-39.40	0.06	0.07
10	1/4	-39.18	-39.85	0.07	0.09	-40.77	-40.66	0.03	0.06	-39.93	-39.11	0.06	0.06
	1/8	-38.94	-38.91	0.08	0.1	-41.15	-40.50	0.03	0.07	-39.81	-39.50	0.02	0.03
	1/16	-39.88	-39.41	0.02	0.04	-40.96	-41.06	0.02	0.03	-39.77	-39.65	0.01	0.02
	1/32	-39.76	-39.36	0.03	0.03	-40.28	-40.81	0.02	0.09	-39.38	-39.21	0.08	0.05
15	1/4	-39.12	-39.11	0.05	0.04	-41.54	-40.25	0.04	0.05	-39.93	-40.01	0.07	0.09
	1/8	-38.93	-38.14	0.02	0.02	-41.96	-41.24	0.04	0.05	-39.64	-39.64	0.08	0.1
	1/16	-39.84	-39.51	0.06	0.08	-40.83	-40.83	0.03	0.04	-39.81	-39.11	0.09	0.04
	1/32	-39.75	-39.30	0.03	0.06	-40.01	-39.95	0.03	0.08	-39.20	-38.91	0.02	0.02
20	1/4	-39.12	-39.61	0.04	0.03	-40.80	-40.01	0.01	0.10	-39.33	-39.22	0.05	0.05
	1/8	-38.93	-38.80	0.02.	0.01.	-40.23	-40.30	0.02	0.05	-39.15	-39.92	0.03	0.05
	1/16	-39.86	-39.16	0.09	0.08	-40.71	-39.12	0.05	0.05	-39.53	-39.23	0.06	0.06
	1/32	-39.71	-39.35	0.08	0.03	-41.32	-39.32	0.04	0.02	-39.12	-39.69	0.05	0.05

available on the market and specifically addressed to WiMAX signal analysis. In particular, the software developed by Litepoint for the Tektronix RSA, namely *RSA-IQWIMAX™*, and that offered by Agilent Technologies, installed on the MXA, namely *89601A™*, have been considered.

Main features of all measurement solutions are given in Tab. II.1. It is worth stressing that the proposed approach measures both the RCE and EVM, according to the standard guidelines, while the others only the EVM, often referred to as RCE. This is the reason why the comparative analysis has been conducted only in terms of EVM.

A number of tests has been conducted on WiMAX signals characterized by different values of channel bandwidth and guard interval. Different transmission modes, subframe structures, and power levels, namely -10 dBm (high), -20 dBm (medium), and -40 dBm (low), have been considered as well. With regard to the TDD transmission mode, signals characterized by a downlink subframe including 31 time-domain OFDM symbols, 17 BPSK, 6 QPSK, 6 16-QAM and 2 64-QAM modulated, and an uplink subframe containing 41 time-domain OFDM symbols, modulated according to a QPSK (12 symbols), 16-QAM (16

Tab. II.3 Mean and experimental standard deviation of 50 EVM values related to a WiMAX signal characterized by a power level equal to -20 dBm and bursty frame structure, for different values of channel bandwidth and guard interval.

Channel Bandwidth [MHz]	Guard Interval	Power level equal to -20 dBm in bursty frame structure											
		Agilent Technologies solution				Tektronix solution				Proposed approach			
		Average[dB]		Standard deviation [dB]		Average [dB]		Standard deviation [dB]		Average[dB]		Standard deviation [dB]	
		TDD	FDD	TDD	FDD	TDD	FDD	TDD	FDD	TDD	FDD	TDD	FDD
2.5	1/4	-37.12	-38.92	0.06	0.03	-39.82	-39.45	0.02	0.02	-39.26	-38.91	0.02	0.07
	1/8	-36.90	-38.52	0.07	0.04	-40.84	-40.85	0.02	0.04	-38.98	-39.22	0.03	0.05
	1/16	-37.84	-39.65	0.05	0.06	-40.51	-41.35	0.03	0.024	-39.25	-39.92	0.04	0.05
	1/32	-36.26	-39.12	0.07	0.02	-42.63	-41.22	0.05	0.08	-38.82	-39.65	0.07	0.04
5.50	1/4	-37.13	-39.32	0.09	0.06	-41.59	-41.84	0.06	0.04	-39.14	-39.45	0.08	0.04
	1/8	-37.07	-39.01	0.04	0.07	-40.46	-40.30	0.02	0.02	-38.57	-39.56	0.04	0.05
	1/16	-36.78	-39.48	0.06	0.07	-40.58	-40.66	0.02	0.02	-38.98	-39.46	0.08	0.09
	1/32	-36.26	-39.61	0.08	0.04	-41.12	-39.97	0.02	0.06	-38.53	-38.95	0.05	0.09
10	1/4	-37.84	-39.80	0.07	0.04	-40.84	-41.00	0.04	0.05	-38.32	-40.01	0.07	0.08
	1/8	-36.93	-38.48	0.09	0.01	-39.25	-39.15	0.03	0.04	-39.84	-39.75	0.03	0.08
	1/16	-37.94	-39.65	0.07	0.1	-39.56	-39.96	0.03	0.08	-38.66	-39.95	0.04	0.01
	1/32	-36.02	-40.01	0.06	0.06	-41.68	-39.56	0.04	0.05	-38.52	-39.58	0.05	0.01
15	1/4	-36.20	-39.65	0.08	0.05	-40.11	-39.45	0.06	0.06	-39.85	-39.74	0.09	0.01
	1/8	-37.81	-38.93	0.09	0.04	-40.32	-40.32	0.05	0.04	-39.19	-39.65	0.08	0.05
	1/16	-37.80	-38.84	0.07	0.08	-39.53	-39.35	0.05	0.04	-38.53	-38.95	0.08	0.04
	1/32	-37.33	-38.75	0.03	0.04	-40.66	-40.22	0.05	0.08	-38.09	-38.56	0.09	0.02
20	1/4	-38.64	-39.20	0.05	0.09	-39.88	-39.95	0.03	0.08	-39.28	-39.58	0.09	0.02
	1/8	-37.90	-38.93	0.06	0.07.	-39.77	-39.52	0.03	0.05	-39.14	-38.98	0.06	0.02
	1/16	-37.03	-38.90	0.06	0.07	-40.12	-39.71	0.03	0.03	-39.95	-39.65	0.07	0.08
	1/32	-36.90	-38.75	0.07	0.06	-40.62	-40.20	0.02	0.04	-38.33	-39.35	0.08	0.07

symbols) and 64-QAM (13 symbols) scheme have been considered; the carrier frequency has been set equal to 3.5 GHz.

As for the FDD transmission mode, downlink and uplink channels have been transmitted with a carrier frequency equal respectively to 3.5 GHz and 3.530 GHz, emulating an actual operating scenario. Moreover, the signals have consisted of a downlink subframe including 90 time-domain OFDM symbols and an uplink subframe containing 86 time-domain OFDM symbols, which have been divided among seven uplink user bursts.

Both the analyzers and SDA have always been regulated in such a way as to optimally meet the main features of the signal under analysis. Concerning the proposed approach, the SDA has been regulated as follows: 10 GS/s sample rate, 50 MSample memory depth, 8 ms acquisition time.

The results are provided in terms of average and experimental standard deviation of 50 EVM values obtained in consecutive tests on the same signal. In particular, the outcomes achieved in TDD transmission mode are

Tab. II.4 Mean and experimental standard deviation of 50 EVM values related to a WiMAX signal characterized by a power level equal to -40 dBm and bursty frame structure, for different values of channel bandwidth and guard interval.

Channel Bandwidth [MHz]	Guard Interval	Power level equal to -40 dBm in bursty frame structure											
		Agilent Technologies solution				Tektronix solution				Proposed approach			
		Average[dB]		Standard deviation [dB]		Average [dB]		Standard deviation [dB]		Average[dB]		Standard deviation [dB]	
		TDD	FDD	TDD	FDD	TDD	FDD	TDD	FDD	TDD	FDD	TDD	FDD
2.5	1/4	-38.12	-39.24	0.06	0.04	-38.91	-40.10	0.05	0.04	-38.71	-40.11	0.05	0.07
	1/8	-37.75	-38.82	0.04	0.04	-38.75	-40.25	0.04	0.05	-38.15	-39.22	0.06	0.04
	1/16	-38.48	-39.40	0.07	0.09	-38.68	-40.45	0.06	0.03	-38.39	-39.35	0.03	0.06
	1/32	-39.96	-39.31	0.05	0.05	-38.56	-39.85	0.07	0.08	-38.88	-39.47	0.04	0.03
5.50	1/4	-38.13	-39.33	0.09	0.01	-37.57	-41.30	0.08	0.04	-38.77	-39.56	0.05	0.04
	1/8	-38.92	-39.00	0.05	0.01	-38.65	-41.37	0.01	0.05	-38.24	-39.48	0.07	0.06
	1/16	-39.84	-38.01	0.03	0.08	-37.42	-40.50	0.03	0.06	-38.45	-38.32	0.05	0.06
	1/32	-38.08	-38.76	0.03	0.02	-38.17	-40.32	0.06	0.03	-38.96	-39.85	0.07	0.07
10	1/4	-37.45	-39.80	0.02	0.03	-38.46	-40.25	0.07	0.04	-38.53	-39.58	0.06	0.05
	1/8	-37.74	-38.94	0.04	0.07	-37.84	-41.45	0.07	0.02	-38.12	-39.74	0.03	0.08
	1/16	-37.27	-39.85	0.07	0.01	-37.29	-40.74	0.06	0.04	-38.35	-39.58	0.04	0.06
	1/32	-37.99	-39.45	0.04	0.08	-37.63	-40.25	0.03	0.09	-37.98	-39.95	0.08	0.03
15	1/4	-36.13	-39.74	0.04	0.06	--38.11	-40.40	0.06	0.03	-38.04	-39.31	0.07	0.03
	1/8	-36.92	-38.65	0.09	0.06	-39.04	-39.90	0.07	0.04	-37.95	-40.04	0.07	0.07
	1/16	-36.41	-39.44	0.04	0.04	-38.95	-40.30	0.08	0.04	-38.29	-39.65	0.02	0.07
	1/32	-39.74	-39.15	0.03	0.07	-38.76	-41.01	0.06	0.05	-38.16	-39.52	0.03	0.05
20	1/4	-37.75	-38.98	0.02	0.1	-38.88	-39.80	0.05	0.09	-37.33	-39.47	0.02	0.09
	1/8	-37.56	-38.93	0.09	0.04.	-38.87	-38.98	0.07	0.05	-37.46	-39.50	0.09	0.04
	1/16	-37.78	-39.54	0.09	0.02	-37.55	-39.47	0.05	0.09	-38.48	-40.52	0.04	0.03
	1/32	-37.95	-39.47	0.07	0.08	-37.63	-40.22	0.06	0.01	-38.15	-39.82	0.07	0.03

shown in Tab. II.2, Tab. II.3 and Tab. II.4 for bursty and in Tab. II.5 for continuous frame structure; those obtained in the FDD transmission mode are summarized in Tab. II.2, Tab. II.3 and Tab. II.4 for bursty and in Tab. II.6 for continuous frame structure.

From the analysis of all results, the following considerations can be drawn.

- With special regard to a bursty frame structure, the results provided by the proposed approach always concur with those assured by the two competitive solutions.
- Both Litepoint and Agilent Technologies solution fail in the presence of a continuous frame structure, while the proposed approach exhibits quite the same performance as in the case of bursty frame structure. Good reliability is evidenced.
- In the auto-detection mode, the proposed approach is always successful in determining the actual channel bandwidth, guard interval and frame structure.
- Litepoint solution sometime fails in singling out the subframe type (downlink or uplink), with special regard to the uplink subframe.

Tab. II.5 Mean and experimental standard deviation of 50 EVM values related to a WiMAX signal characterized by the FDD transmission mode and continuous frame structure, for different values of power level, channel bandwidth and guard interval.

Channel Bandwidth [MHz]	Guard Interval	FDD transmission mode and continuous frame structure					
		Power level equal to -10 dBm		Power level equal to -20 dBm		Power level equal to -40 dBm	
		Average [dB]	Standard deviation [dB]	Average [dB]	Standard deviation [dB]	Average [dB]	Standard deviation [dB]
2.5	1/4	-38.24	0.03	-38.63	0.03	-38.61	0.04
	1/8	-38.82	0.07	-38.31	0.09	-38.54	0.07
	1/16	-38.75	0.06	-38.67	0.04	-38.65	0.08
	1/32	-38.65	0.03	-38.57	0.06	-38.73	0.03
5.50	1/4	-38.73	0.08	-38.34	0.08	-38.65	0.04
	1/8	-38.65	0.04	-38.71	0.04	-38.48	0.07
	1/16	-38.01	0.05	-38.53	0.08	-38.43	0.05
	1/32	-38.76	0.07	-38.75	0.07	-38.82	0.03
10	1/4	-38.81	0.02	-38.35	0.04	-38.73	0.08
	1/8	-38.45	0.03	-38.52	0.07	-38.91	0.06
	1/16	-38.82	0.03	-38.56	0.02	-38.64	0.06
	1/32	-38.55	0.06	-38.53	0.03	-38.55	0.01
15	1/4	-38.93	0.05	-38.65	0.08	-38.11	0.05
	1/8	-38.52	0.08	-38.65	0.02	-38.17	0.02
	1/16	-38.65	0.01	-38.85	0.04	-38.69	0.02
	1/32	-38.52	0.03	-38.67	0.07	-38.50	0.08
20	1/4	-38.81	0.3	-38.46	0.03	-38.74	0.08
	1/8	-38.52	0.06	-38.98	0.04	-38.50	0.04
	1/16	-38.62	0.03	-38.73	0.05	-38.52	0.02
	1/32	-38.71	0.07	-38.64	0.07	-38.44	0.06

- Experimental standard deviations exhibited by the proposed approach are very close to those characterizing the results furnished by the other solutions. Satisfying repeatability is experienced.
- Neither the proposed approach nor the other solutions allow real time operation. Tab. II.VII summarizes the required computation time in terms of mean and experimental standard deviation obtained through 50 independent measurements in single shot acquisition.

II.2.4 Processing time

Proper experiments have been carried out in order to measure the processing time of the proposed method. In particular, the processing time has been evaluated analyzing different WiMAX signal lengths (acquisition record), and for each one of them the time elapsed for fulfilling all stages, from demodulation stage until the modulation quality assessment, has been calculated. Personal computer (PC), characterized by a Intel Core 2 Duo and 3 GB of RAM has been utilized for processing all acquisition records, while LeCroy SDA 6000A has been exploited for digitizing the incoming signal. Acquisition record length

Tab. II.6 Mean and experimental standard deviation of 50 EVM values related to a WiMAX signal characterized by the TDD transmission mode and continuous frame structure, for different values of power level, channel bandwidth and guard interval.

Channel Bandwidth [MHz]	Guard Interval	TDD transmission mode and continuous frame structure					
		Power level equal to -10 dBm		Power level equal to -20 dBm		Power level equal to -40 dBm	
		Average [dB]	Standard deviation [dB]	Average [dB]	Standard deviation [dB]	Average [dB]	Standard deviation [dB]
2.5	1/4	-38.34	0.01	-39.56	0.04	-37.98	0.06
	1/8	-38.26	0.03	-38.58	0.04	-38.85	0.02
	1/16	-39.28	0.05	-38.15	0.05	-38.76	0.04
	1/32	-38.91	0.06	-39.85	0.05	-37.98	0.05
5.50	1/4	-39.30	0.07	-38.31	0.02	-38.65	0.03
	1/8	-39.01	0.03	-39.39	0.02	-38.32	0.02
	1/16	-39.31	0.05	-38.45	0.03	-38.45	0.02
	1/32	-38.67	0.02	-38.23	0.08	-38.56	0.02
10	1/4	-38.81	0.03	-38.53	0.07	-38.55	0.02
	1/8	-38.65	0.03	-38.51	0.06	-38.48	0.01
	1/16	-38.85	0.04	-38.65	0.01	-37.99	0.08
	1/32	-38.95	0.02	-38.81	0.04	-38.95	0.02
15	1/4	-38.57	0.08	-38.68	0.03	-38.71	0.04
	1/8	-38.82	0.04	-38.38	0.03	-38.42	0.01
	1/16	-39.61	0.02	-38.67	0.06	-38.33	0.09
	1/32	-38.43	0.07	-38.15	0.08	-38.62	0.03
20	1/4	-38.18	0.1	-38.54	0.01	-39.14	0.08
	1/8	-38.30	0.03	-38.81	0.03	-38.97	0.03
	1/16	-38.32	0.01	-38.34	0.04	-38.67	0.05
	1/32	-38.22	0.05	-38.82	0.07	-38.29	0.02

belongs to the range [5, 10, 15, 20, 25, 50, 100] MSample has been selected for taking advantage of LeCroy features in terms of memory depth. Fig II.11 shows the obtained processing time versus acquisition record. It is worth noting that no result is provided for acquisition record length greater or equal than 50 MSample. Unfortunately, above of this threshold (acquisition record length ≥50 MSample) a memory overflow issue arises. However, thanks to a linear increase, experienced from achieved results, it is possible to estimate the processing time when in input is provided an acquisition record length greater than 50 MSample. Fig. II.10 sketches processing time for all acquisition records, in which red bars are estimated supposing a processing time linear increase. From these results the following considerations can be drawn:

- acquisition record length above of 50 MSample doesn't allow to accomplish all proposed method stages;
- acquisition record equal to 25 MSample provides processing time of nearly 2.5 minute;

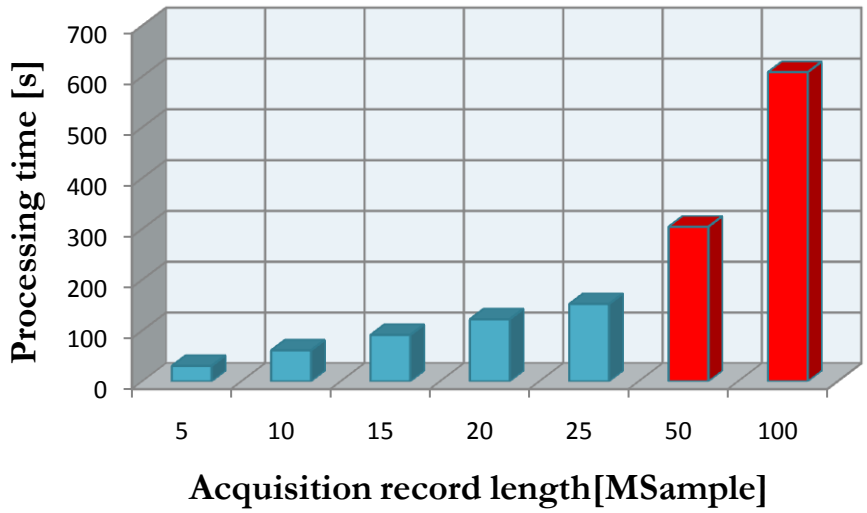

Fig. II.10 Processing times versus acquisition record length: red and blue bars stand for guessed and measured processing times respectively

- linear relation between the acquisition record length and processing time is extracted, which allows to estimate processing time of 6 minute for acquisition record of 100 MSample;
- a parallel implementation of the proposed method allows efficiently reduce the processing times for all record acquisition lengths involved into analysis.

II.2.5 Conclusion

A digital signal processing approach for modulation quality measurement of WiMAX transmitters compliant with IEEE 802.16d-2004 standard has been presented. It provides for a direct digitization of the RF input signal, and makes use of an original measurement algorithm for the estimation of the main parameters related to modulation quality. To this aim, only a general-purpose acquisition hardware, characterized by a suitable input bandwidth, sample rate and vertical resolution, is required. A number of digital scopes and data acquisition systems, offered by many manufactures and often present in typical telecommunication laboratories, can prove appropriate.

With respect to major competitive solutions, the novelty and attractiveness of the approach mainly rely on its independency of a specialized hardware, such as a VSA or RSA, and on the modular and open structure of the measurement algorithm that makes any further improvement and upgrade an agile task.

Satisfying performance, in terms of repeatability and reliability, has been exhibited in a number of experiments on laboratory WiMAX signals in different operating conditions, as regards to the channel bandwidth, power level, and frame structure. Furthermore, a comparative analysis has given evidence of the approach's efficacy with respect to two relevant measurement solutions available on the market. In

particular, the approach has provided reliable results also in the presence of WiMAX signals characterized by a continuous frame structure, in the analysis of which the other two solutions have always failed.

II.3 Second measurement method: blind signals separation

In-service measurements, usually adopted for maintaining or troubleshooting wireless digital telecommunications systems, proved to be a difficult task in the presence of multiple signals interfering with one another. This is particularly true for modern telecommunication systems that do not use an own licensed band, but rather share an unlicensed band with other systems, such in the case of those based on the standard IEEE 802.11x (Wi-Fi), IEEE 802.15.4 (ZigBee) or IEEE 802.15 (Bluetooth). Such overcrowded radio spectrum may give rise to harmful and undesired malfunctioning of wireless systems and networks, resulting in dropped or noisy connections, lost channels and poor reception. This is true not only, as expected, for systems and networks exploiting unlicensed bands, but also for those operating in regulated, and apparently protected, bands. In such conditions, in service testing at physical layer for maintenance and performance assessment purposes, a very pressing demand at the present time, might be impossible. In particular, measuring the power spectrum of the wideband radio signal, which is the fundamental step for gaining the values of relevant frequency domain quantities like channel power, occupied bandwidth and carrier frequency, might provide unfeasible results.

Several methods and techniques have been already proposed in literature, based either on parametric [II.20][II.21] or non parametric [II.22][II.23] approaches, aimed at assuring reliability and repeatability in power spectrum measurements of signals compliant with several wireless communication standards. Most of them, however, suffer from undesired performance degradation in the presence of signals interfering both in time and frequency domain with the useful one, thus proving unsuitable for in-service testing. Moreover, measurement solutions available on the market [II.18][II.19] are mainly oriented to interference hunting and require either to disable traffic on the channel to be analyzed or wait a quiet time of the useful signal to get valid measurement of the interference.

A first solution to this aim is given in [II.24]. Taking into account some attractive characteristics of multiple-input multiple-output (MIMO) systems, [II.24] shows how a typical eigenvalues decomposition based algorithm is capable of measuring the power spectrum of a given number of wideband radio signals impinging on a uniform linear array (ULA) of antennas. In particular, they combined the use of the multiple signal classification (MUSIC) algorithm with spatial diversity for a preliminary estimation of the direction of arrival (DOA) of the involved signals and a successive separation and measurement of their power spectrum. The number of involved signals has to be given, thus making the suggested solution unsuitable in actual measurement conditions. It is worth noting that MUSIC algorithm was firstly proposed

to estimate the direction of arrival (DOA) of a number of signals modeled either as sinusoids or sum of complex exponential functions and impinging on an uniform linear array (ULA) of receiving antennas [II..25],[II.26]. The earliest works were mainly concerned with theoretical and simulative analysis [II.27]-[II.30]; very few experimental results were given. More recent papers have extended MUSIC capabilities also to wideband signals, but still focusing the attention only to DOA measurements [II.31]-[II.34]. To the best of the authors' knowledge, no use of the MUSIC algorithm for estimating the power spectrum of wideband signals and measuring their relevant parameters has been proposed yet.

Stemming from this first experience, taking also into account the promising results presented in [II.35], a new eigenvalues decomposition based method, capable of executing a blind separation of the power spectra peculiar to signals that interfere in time and frequency domain, is proposed. To this aim, the method first estimates the number of signals of interest through the use of the Aikake's information criterion (AIC) [II.36][II.37], and then applies the MUSIC algorithm to gain the desired power spectra from which the measurement information is derived [II.34].

II.3.1 Problem statement

In-service testing at physical layer of wireless communications systems and networks usually relies on the measurement of parameters defined in the frequency domain; to this aim, reliably estimating the power spectrum of all involved signals is mandatory. Common estimation approaches work with success if the acquired waveform consists of (i) a single signal (the desired one) or (ii) coexisting signals (multiple signals including the desired one) that can be separated either in the time (e.g. bursty non-overlapped signals, Fig II.11a or frequency (e.g. signals occupying non-overlapped portion of the spectrum, Fig. II.11b

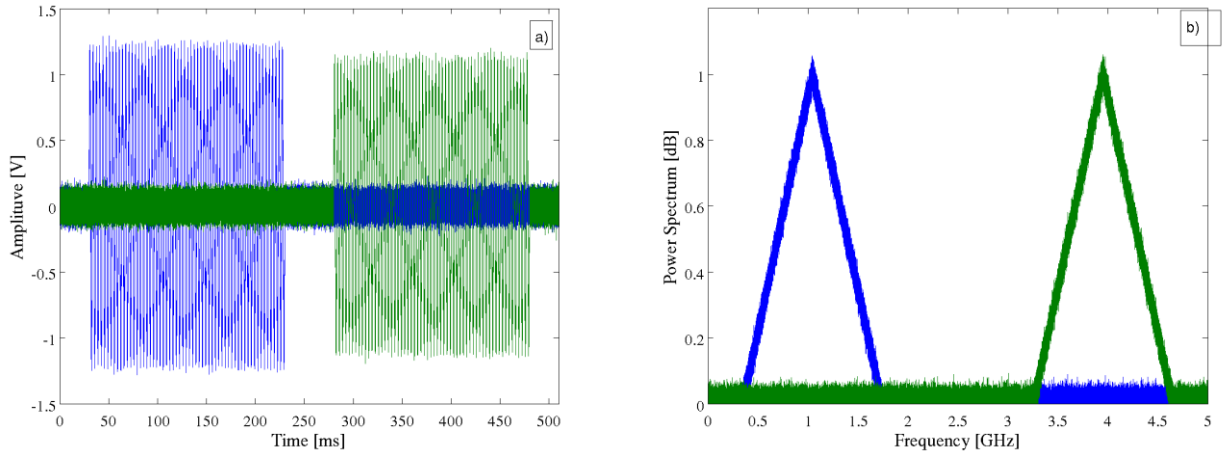

Fig. II.11 Common estimation approaches work with success when coexisting signals can be separated either in the time (a) or frequency (b) domain.

domain. On the contrary, they provide unreliable results when signals interfering both in the time and frequency domain are considered (Fig. II.12).

Unfortunately, such operating conditions are becoming more and more frequent due to the diffusion of wireless communications systems and networks sharing the same or contiguous frequency bands to provide wideband connectivity. Most of interferences are unintentionally produced by other legitimate activities; nevertheless, their effect on the quality of service of the victim systems may be withering. Typical sources of undesired and/or unintentional interference can be found in (i) improperly configured or unauthorized transmitters, (ii) coverage area overlapping of different systems, (iii) intermodulation generated by other transmitters, fences, roofs, antennas or connectors, and (iv) overload or noise sidebands from legitimate transmitters.

It is worth noting that interference problems could arise not only in unlicensed bands but also in regulated bands. As an example of unlicensed scenario, let us consider the one involving wireless local area networks (WLANs) compliant with the IEEE 802.11x standard. They can usually be set to operate in one among eleven channels allocated in the frequency range from 2401 MHz up to 2484.5 MHz (referred to as Industrial, Scientific and Medical band). In particular, each channel has a nominal bandwidth of 22 MHz and the related carrier frequency is shifted by 5 MHz with respect to that of the previous one. Due to the increasing number of access points (devices providing wireless access to internet), all the available channels are usually exploited and frequency domain overlap condition is usually met. Similar overlap conditions are encountered also in cellular networks operating in the universal mobile telecommunications system (UMTS) licensed band; users simultaneously transmit data in the same frequency band and are

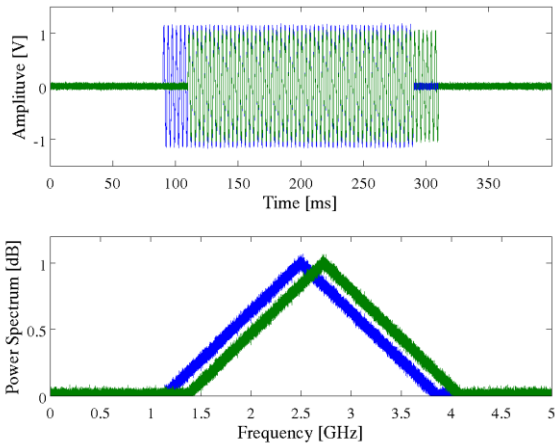

Fig. II.12 Common estimation approaches fail when coexisting signals interfere both in the time and frequency domain.

distinguished from one another only by a unique code. With no information about the code, the number of involved signals (users) is unknown and their power spectra cannot be separated.

II.3.2 Theoretical background

Theoretical fundamentals about signal model along with main characteristics of AIC and MUSIC algorithms are given below. More specifically, the signal model is explained with regard to a uniform linear array (ULA) of antennas [II.24] and the main steps of AIC [II.37] and MUSIC [II.25], mandated respectively to the number estimation and parameters measurement of the signals, are described in detail.

II.3.2.A Signal Model

Let us assume that d wideband signals, each of which characterized by its own bandwidth B_k, impinge on the ULA array from an azimuth angle ϑ_k, with k=1,..,d. The ULA array is defined as a set of m (with *m* greater than *d*) identical receiving antennas arranged on a single line with uniform spacing equal to p. Moreover, the signals, emitted by d sources, are assumed to be ergodic and stationary zero-mean stochastic processes.

Under these assumptions, the signals received at the m antennas are a linear combination of the d impinging signals and noise, and the generic received signal $r_i(t)$ on the i-*th* antenna can be expressed as

$$r_i(t) = \sum_{k=1}^{d} a_{ik} s_k(t - \tau_{ik}) + n_i(t) \qquad \text{(II-10)}$$

where $s_k(t)$ is the k-*th* impinging signal, a_{ik} is the k-th amplitude response, τ_{ik} is the propagation delay of the k-*th* signal on the i-*th* antenna, and finally $n_i(t)$ is the additive white Gaussian noise. If the received signal is acquired for a certain period T, eq. (1) can approximately be represented by its Fourier series,

$$r_i(t) = \sum_{l=0}^{l_{max}} R_i(f_l)\, e^{j2\pi f_l t} \qquad \text{(II-11)}$$

where $R_i(f_l)$ are the Fourier coefficients, and l_{max} stands for the index corresponding to the maximum frequency component involved in $r_i(t)$.

By applying the Fourier transforms to both sides of eq. (II-10) and assuming that the observation period is longer than the propagation delay of each signal across the array ($\tau_{ik} \ll T$), the propagation delay can be transformed to phase shift, and the eq. (II-10) becomes:

$$R_i(f_l) = \sum_{k=1}^{d} a_{ik} e^{-j2\pi f_l \tau_{ik}} S_k(f_l) + N_i(f_l) \quad \text{(II-12)}$$

where $S_k(f_l)$ and $N_i(f_l)$ are the Fourier coefficients of sk(t) and ni(t), respectively. If similar operations are applied on received signal of each antenna of the array at a generic frequency f_l, eq. (II-12) can be written in matrix notation as:

$$\mathbf{R}(f_l) = \mathbf{A}(f_l)\mathbf{S}(f_l) + \mathbf{N}(f_l) \quad \text{(II-13)}$$

$R(f_l)$ and $N(f_l)$ are the $m \times 1$ vectors.

The columns $A_k(f_l)$ of the matrix $A(f_l)$, referred to as direction vectors of the source, are expressed by:

$$A_k(f_l) = [1\ e^{-j2\pi f_l \tau(\vartheta_k)} \ldots\ e^{-j2\pi f_l (m-1)\tau(\vartheta_k)}]^T \quad \text{(II-14)}$$

where the propagation delay, $\tau(\vartheta_k)$, is defined by $\frac{2\pi p}{c}\cos(\vartheta_k)$, c stands for the propagation speed of light and p is chosen according to Shannon spatial theorem, i.e.:

$$p \leq \frac{\lambda_{max}}{2} \quad \text{(II-15)}$$

where λ_{max} stands for the longest wavelength to be analyzed.

II.3.2.B MUSIC fundamentals

MUSIC is a parametric and incoherent method originally proposed to estimate the direction of arrival (DOA) of narrowband signals and successively extended in order to make possible its application also in the presence of wideband signals. As for the other parametric methods, MUSIC exploits the eigenstructure of the covariance matrix to evaluate the DOA of each signal impinging on the array. To this aim, the wideband signal is decomposed in a set of narrowband signals by means of a filters bank and the covariance matrix is calculated as

$$\boldsymbol{Z}(f_l) = E\left[\left(\boldsymbol{A}(f_l)\boldsymbol{S}(f_l) + \boldsymbol{N}(f_l)\right)\left(\boldsymbol{A}(f_l)\boldsymbol{S}(f_l) + \boldsymbol{N}(f_l)\right)^H\right] \quad \text{(II-16)}$$

where f_l is the center frequency of the generic filter of the bank; the superscript H denotes matrix transpose conjugation, and E [ ] is the expected value operator.

In the assumption of Gaussian, zero-mean noise uncorrelated with the signals, eq. (II-16) can be written:

$$\boldsymbol{Z}(f_l) = \boldsymbol{A}(f_l)\boldsymbol{Q}(f_l)\boldsymbol{A}(f_l)^H + \boldsymbol{\sigma^2}(f_l)\boldsymbol{I} \quad \text{(II-17)}$$

where $\boldsymbol{Q}(f_l) = E[\boldsymbol{S}(f_l)\boldsymbol{S}(f_l)^H]$, $\boldsymbol{Z}(f_l)$, and $\boldsymbol{\sigma^2}(f_l)$ stand for the covariance matrix of impinging, received and noise signals, respectively.

To refine the estimate of matrix $\boldsymbol{Z}(f_l)$, the received signal $r_i(t)$ is divided into K segments, referred to as *snapshots*, whose duration is equal to P (with $P = T/K$). Thanks to the snapshots, the covariance matrix $\boldsymbol{Z}(f_l)$ can be evaluated, for each frequency, by means of the following expression:

$$\boldsymbol{Z}(f_l) = \frac{1}{K}\sum_{j=1}^{K} \boldsymbol{R}_j(f_l)\boldsymbol{R}_j(f_l)^H \quad l = 0,..,l_{max} \tag{II-18}$$

Let $\lambda_1(f_l),\dots,\lambda_m(f_l)$ and $V_1(f_l),\dots,V_m(f_l)$ be, respectively, the eigenvalues and eigenvectors of the matrix $\boldsymbol{Z}(f_l)$. It is easy to demonstrate, for each frequency component involved in $r_i(t)$, that:

I. $\lambda_1(f_l) \geq \cdots \geq \lambda_m(f_l)$, i.e. the eigenvalues can be collected in an ordered set;
II. the average value of the lowest eigenvalues, $\lambda_{d+1}(f_l),\dots,\lambda_m(f_l)$, allows to estimate $\boldsymbol{\sigma^2}(f_l)$;
III. $\boldsymbol{C}(f_l) = \{V_{d+1}(f_l),\dots,V_m(f_l)\} \perp \{A_1(f_l),\dots,A_d(f_l)\}$, i.e. the noise space is orthogonal to the signals space;
IV. the covariance matrix can be decomposed as $\boldsymbol{Z}(f_l) = \boldsymbol{V}(f_l)^H \Delta(f_l)\boldsymbol{V}(f_l)$, with $\boldsymbol{V}(f_l) = [V_1(f_l),\dots,V_m(f_l)]$ and $\Delta(\mathrm{f_l}) = diag\{\lambda_1(f_l),\dots,\lambda_m(f_l)\}$.

Thanks to the propriety III, the d desired directions of arrival minimize the ordinary Euclidean distance between signals and noise space (i.e. minimize the scalar product of $\boldsymbol{C}(f_l)$ by $\boldsymbol{A}(f_l)$) expressed as

$$\boldsymbol{h}(\vartheta, f_l)^2 = |\boldsymbol{A}(f_l)^H \boldsymbol{C}(f_l)|^2 \tag{II-19}$$

II.3.2.C Aikake's Information Criterion fundamentals

AIC belongs to a wide family of methods that take advantage from information theoretical criteria (ITC). The basic idea underlying these criteria is the identification, inside a defined set of likelihood functions, of the one that better represents the distribution of N observations of the same statistical process. The criterion adopted to select the best likelihood function distinguishes the ITC criteria from one another. In particular, AIC method points out the likelihood function $\mathrm{LF}\left(\widetilde{\boldsymbol{Z}(\mathrm{f_l})}\middle|\overline{\mathbf{p}(\mathrm{f_l})}\right)$ that minimizes the expression

$$\mathbf{AIC}\left(\widetilde{\boldsymbol{Z}(f_l)}\middle|\overline{\mathbf{p}(f_l)}, \tilde{\mathrm{k}}\right) = -2\log\left(\mathrm{LF}\left(\widetilde{\boldsymbol{Z}(f_l)}\middle|\overline{\mathbf{p}(f_l)}\right)\right)^{m-\tilde{k}} + 2\tilde{k}\,(2m-\tilde{k}\,) \tag{II-20}$$

where $\tilde{k}$ stands for the number of parameters in the statistical model, $\widetilde{\boldsymbol{Z}(f_l)}$ is the *actual* (measured) covariance matrix and $\overline{\mathbf{p}(f_l)}$ are the constraints to be met for the minimization of the likelihood function for each frequency component f_l. The couple $\left(\overline{\mathbf{p}(f_l)}, \tilde{\mathrm{k}}\right)$ that minimizes the eq. (II-20) has to be found; the obtained value of $\tilde{k}$ provides the desired number of signals present in the received signal.

II.3.3 Proposed method

The proposed method (Fig. II.13) allows the estimation of the power spectrum of each impinging signal present in the received signal, thus making it possible to measure typical quantities (channel power, bandwidth and carrier frequency). To this aim, no information about either the number or characteristics of the involved signals is necessary. However, to achieve the best tradeoff between computational burden and analysis reliability, the method has to be applied on a limited frequency range (in the following referred to as analysis range and defined by the frequency interval from the lowest (F_{min}) to the highest (F_{max}) frequency value of interest). This is not a relevant limitation, since the analysis is only restricted to those frequency components which result to be significant in the received signal. For the sake of clarity, the operating steps of the method will be presented below with reference to an application example.

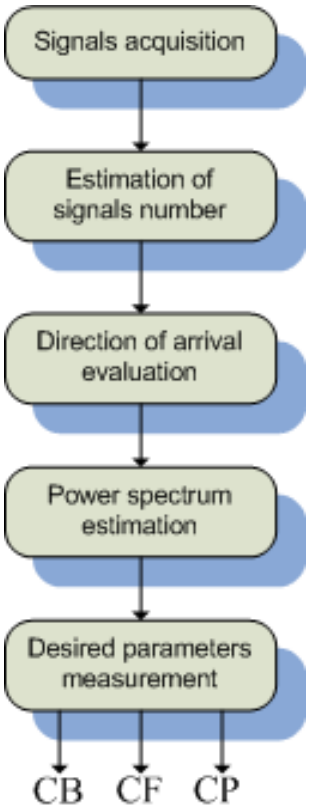

Fig. II.13 Block diagram of the proposed method.

II.3.3.A Acquisition of signals

The first step of the method consists of digitizing the signals received by means of the ULA of m antennas with a proper data acquisition system, the characteristics of which, in terms of sample rate and memory depth, have to be carefully chosen. As for the application example, it refers to a received signal consisting of d=2 interfering signals compliant with the UMTS standard and referred in the following as UM1 and UM2. They impinge on an ULA of m=6 antennas from two azimuth angles of 30° and 60°, respectively. UM1 and UM2 have been characterized by nominal channel power equal to -30 dBm and -40 dBm with the same carrier frequency (2.1 GHz) and channel bandwidth (4.2 MHz). No further additive white Gaussian noise has been added on the signals. Received signal on each antenna has been generated according to what stated in Section V; in particular, each signal has been digitized through LeCroy® SDA6000 (maximum sample rate equal to 20 GS/s and memory depth of 16 M-points), the sample rate and memory depth of which have been set to 10 GS/s and 1 M-points, respectively. As an example, Fig. II.14 shows the power spectrum obtained by applying traditional DFT algorithm on the signal received by the antennas.

No information about the number and spectral contribute of each impinging signal can be extracted, and channel power measurements could provide unexpected results.

II.3.3.B Estimation of the number of signals

Once the digitization step is over, the number of impinging signals has to be evaluated thanks to the approach provided by AIC. To this aim, the m received signals are divided into K snapshots and the actual covariance matrix $\widehat{\boldsymbol{Z}(f_l)}$ can be estimated according to eq. (9) for all the frequency components.

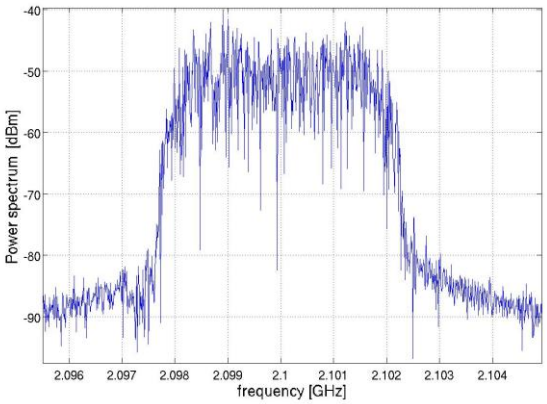

Fig. II.14 Power spectrum obtained by means of traditional DFT algorithm of two interfering UMTS signals. No information about number of involved signals can be retrieved, as well as no reliable measurement of their parameters can be carried out.

With regard to the constraints $\overline{\mathbf{p}(f_l)}$, they can be expressed in terms of eigenvalues and eigenvectors of $\widetilde{\boldsymbol{Z}(f_l)}$. In particular, if the observations on each antenna are linearly independent from one another, the logarithm of likelihood function related to actual covariance matrix can be expressed, after some straightforward elaborations, as

$$\log\left(\mathrm{LF}\left(\widetilde{\boldsymbol{Z}(f_l)}\middle|\overline{\mathbf{p}(f_l)}\right)\right) = -\mathrm{N}\log\left(\det\left(\widetilde{\boldsymbol{Z}(f_l)}\right) - \widetilde{\boldsymbol{Z}(f_l)}^{-\mathrm{H}}\widetilde{\boldsymbol{Z}(f_l)}\right) \quad \text{(II-21)}$$

where $\overline{\mathrm{p}(\mathrm{f_l})} = \left\{\overline{\lambda_1(\mathrm{f_l})}, \dots, \overline{\lambda_\mathrm{m}(\mathrm{f_l})}, \overline{\sigma^2(\mathrm{f_l})}, \overline{\mathrm{V_1}(\mathrm{f_l})}, \dots, \overline{\mathrm{V_m}(\mathrm{f_l})}\right\}$.

It is possible to demonstrate, as discussed in [II.31], that the logarithm of the likelihood function in eq. (II-21) is minimized if the parameters $\overline{\mathrm{p}(\mathrm{f_l})}$ are given by:

$\overline{\lambda_\mathrm{i}(\mathrm{f_l})} = \lambda_\mathrm{l}(\mathrm{f_l})$, with i=1,.., $\tilde{\mathrm{k}}$;

$\overline{\sigma^2(\mathrm{f_l})} = \frac{1}{\mathrm{m}-\tilde{\mathrm{k}}}\sum_{\mathrm{i}=\tilde{\mathrm{k}}+1}^{\mathrm{m}}\lambda_\mathrm{l}(\mathrm{f_l})$;

$\overline{\mathrm{V_j}(\mathrm{f_l})} = \mathrm{V_j}(\mathrm{f_l})$, with $\mathrm{j} = 1, \dots, \mathrm{m}$.

Under these assumptions, eq. (II-20) can be rewritten as

$$\mathbf{AIC}\left(f_l, \tilde{k}\right) = -2\log\left(\frac{\prod_{i=\tilde{k}+1}^{m}\lambda_i(f_l)}{\overline{\boldsymbol{\sigma^2}(f_l)}}\right)^{m-\tilde{k}} + 2\tilde{k}(2m-\tilde{k}) \quad \text{(II-22)}$$

Due to the wideband nature of signals, the information about the number of signals can be achieved by means of all frequency included in the analysis range, as demonstrated in [II.37]. Thus, the eq. (II-22) becomes:

$$\mathbf{AIC}\left(\tilde{k}\right) = -2\sum_{l=0}^{l_{max}}\log\left(\frac{\prod_{i=\tilde{k}+1}^{m}\lambda_i(f_l)}{\overline{\boldsymbol{\sigma^2}(f_l)}}\right)^{m-\tilde{k}} + 2\tilde{k}(2m-\tilde{k}) \quad \text{(II-23)}$$

The number of impinging signals is, finally, estimated by determining the value d^* of the parameter $\tilde{\mathrm{k}}$ that minimizes the expression (II-23):

$$d^* = \underbrace{\min}_{\tilde{k}=1,..,m}\ \mathbf{AIC}(\tilde{k}) \quad \text{(II-24)}$$

Thanks to the eq. (II-24), the two wideband signals involved in the application example have properly been estimated.

II.3.3.C DOA evaluation

Thanks to some attractive properties of the actual covariance matrix, it is possible to evaluate the DOA of each impinging signal through the MUSIC algorithm [II.35][II.29][II.32]. In particular, DOA values can be gained by minimizing the ordinary Euclidean distance between signals and noise subspaces, according to the eq. (II-19).

The reciprocal of $h(\vartheta, f_l)^2$ is referred to as pseudo-spectrum, since it gives no information about the actual signal power spectrum, but only about the DOA of the signals. The d^* local maxima emerging from the evolution of $1/h(f_l)^2$versus ϑ are, in fact, the desired DOA's at the frequency f_l. This procedure has to be applied for each frequency of the analysis range in order to obtain the rough pseudo-spectrum expressed as

$$\boldsymbol{h}^2(\vartheta) = \sum_{l=0}^{l_{max}} \left|\boldsymbol{A}(f_l)^H \boldsymbol{C}(f_l)\right|^2 \qquad \text{(II-25)}$$

The rough pseudo-spectrum is successively smoothed through a suitable moving average filter in order to enhance the performance of MUSIC algorithm in DOA estimating and singling out as much as possible the d^* local maxima of $h^2(\vartheta)$. With regard to the application example, Fig. II.15a and Fig. II.15b show the obtained rough and smoothed pseudo-spectrum, respectively; rough pseudo-spectrum presents a residual ripple around the DOA of two signals, thus preventing an easy estimation of the DOA values by means of the local maxima detection. On the contrary, thanks to the effect of the smoothing filter, the ripple on the peaks is reduced and usually removed; it is so possible of singling out the azimuth position of the impinging signals.

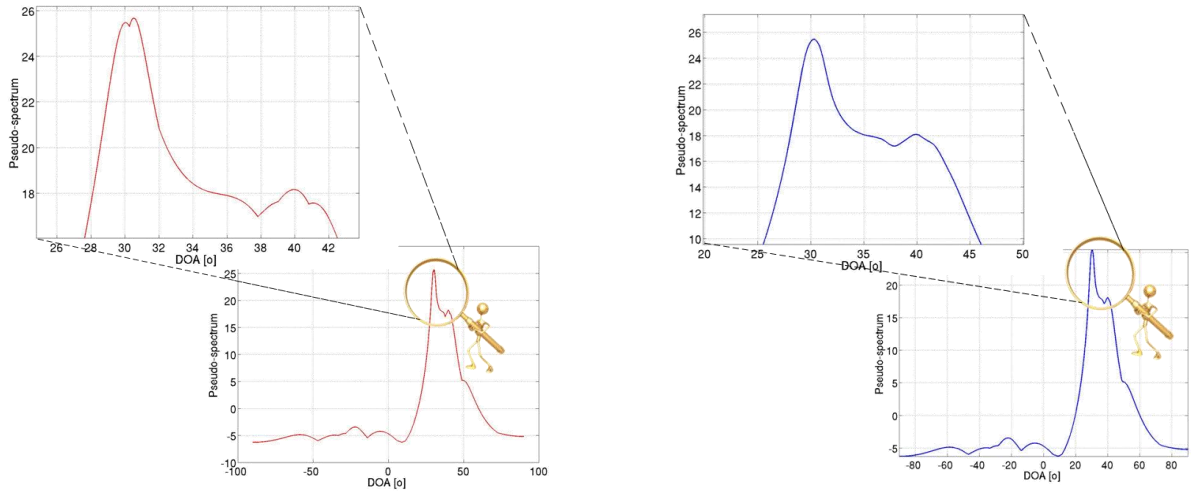

Fig. II.15 Rough (a) and smoothed (b) pseudo-spectrum obtained for two UMTS signals with azimuth angles respectively of 30° and 40°.

With regard to the considered application example, two local maxima are experienced, corresponding to DOA values equal to 29.8° and 40.1°.

II.3.3.D Power spectrum estimation

Once DOA's have been estimated, the power spectrum of each impinging signal can be gained by inverting the eq. (II-17) with respect to matrix $Q(f_l)$, according to

$$\boldsymbol{Z}(f_l) = \frac{1}{K}\sum_{j=1}^{K} \boldsymbol{S}_j(f_l)\boldsymbol{S}_j(f_l)^H = [\boldsymbol{A}(f_l)^H\boldsymbol{A}(f_l)]^{-1}\boldsymbol{A}(f_l)^H\boldsymbol{V}(f_l)^H\Delta(f_l)\boldsymbol{V}(f_l)\boldsymbol{A}(f_l)[\boldsymbol{A}(f_l)^H\boldsymbol{A}(f_l)]^{-1} \quad \text{(II-26)}$$

The k-th entry of the main diagonal of matrix $Q(f_l)$ is, in fact, associated with the portion of the power spectrum of k-th impinging signal at the frequency component f_l. In this way, by gathering the k-th entry for all values of f included in the analysis range, the whole estimated power spectrum of the k-th wideband signal can be measured.

$$RMSE = \sqrt{\frac{1}{l_{max}}\sum_{l=0}^{l_{max}} \left(\frac{\hat{\boldsymbol{S}}(f_l) - \boldsymbol{S}(f_l)}{\boldsymbol{S}(f_l)}\right)^2} \quad \text{(II-27)}$$

Fig. II.16a and Fig. II.16b show the power spectrum of UM1 and UM2, respectively, reconstructed by applying eq. (II-26), whereas Tab. II.7 summarizes the results provided for the root mean square error (RMSE) evaluated according to eq.(II.27), where $\hat{S}(f_l)$ stands for the estimated Fourier coefficient and $S(f_l)$ is the nominal Fourier coefficient evaluated by applying a traditional DFT on one signal at time.

With regard to the signals involved in the application example, RMSE values lower than 0.6% for both signals assure the reliability of the method in separating and extracting the power spectrum for each of them.

Tab. II.7 Results provided by the proposed method for the application example.

	CB[MHz]	CP [dBm]	CF [MHz]	RMSE [%]
UM1	4.23	-30.8	2100	0.6
UM2	4.21	-40.6	2100	0.4

II.3.3.E Measurement of the desired parameters

Once the power spectrum of each impinging signal has been estimated, parameters measurements are carried out by means of very straightforward procedures given below.

Referring to the channel bandwidth (CB), the power included in the whole analysis range is considered 100% of the total power of the signal. Hence, the two frequency values, f1 and f2, which make each of the two frequency intervals [Fmin, f1] and [f2, Fmax] contain 0.5% of the total power, are found. The difference f2 - f1 provides the required bandwidth.

As for the carrier frequency (CF), it has been set equal to the frequency capable of assuring a power value equal to the 50% of total power.

With regard to the channel power (CP), the frequency interval, centered at the obtained carrier frequency of the monitored channel and whose extent is as wide as the channel spacing of the specific system, is first established. Then, the desired power is obtained by summing the power spectrum coefficient over the aforementioned frequency interval.

With reference to the considered example, the obtained results of CP, CF and CB are given in Tab. II.7; remarkable concurrence with the nominal values can be noticed.

II.3.4 Experimental results

A number of tests have been carried out in order to assess the method's capability of suitably estimating the number of impinging signals and their power spectrum along with the aforementioned parameters. The same parameters have been measured, one signal at a time, also through a high performance spectrum analyzer RSA3308A™ (RSA) by Tektronix (up to 8 GHz input frequency band, 12 bit vertical resolution, 25 dBm maximum input power). It has been possible to draw a comparative analysis between the results provided by the proposed method and those granted by the RSA, taken as reference.

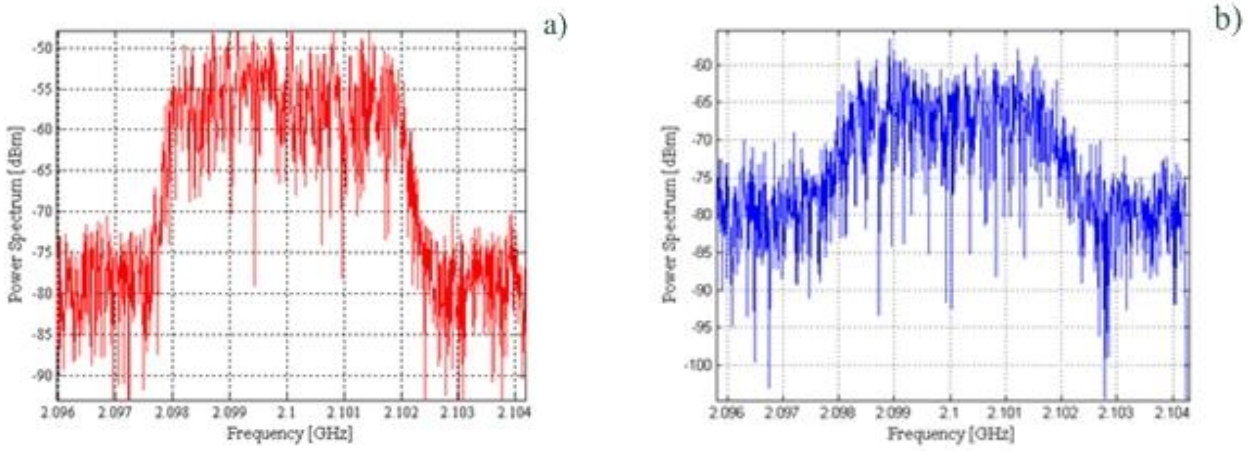

Fig. II.16 Power spectrum respectively of UM1 a) and UM2 b) reconstructed by means of proposed method.

Typical operating scenarios have, in particular, been emulated, in which interference can usually be encountered.

Tests has been conducted for different values of Signal-to-Noise Ratio (SNR), expressed as

$$\mathrm{SNR}=10^{*}\log\left(\frac{\sum_{i=1}^{n}\mathrm{S_i}}{N_0}\right) \qquad \text{(II-28)}$$

where S_i stands for the nominal channel power of the *i*-th impinging signal and N_0 is the noise power. The same SNR values have been considered for each scenario in order to assess the method's performance in the presence of different *(i)* signal types and *(ii)* interference conditions in the frequency domain (partial and full spectra overlap). In particular, SNR values run from -10 dB up to 10 dB, with a step of 2dB. Moreover, three ULA configurations have been investigated, in the following referred to as *critical* (*m* equal to 6), *normal* (*m* equal to 8), and *good* (*m* equal to 10).

Method's performance has thus been assessed through the following figures of merit:

- estimated number of signals d^*;
- estimated direction of arrival ϑ^*;
- *RMSE* of the power spectrum of each signal involved in the analysis;
- difference Δ_X% between estimated ($\hat{X}$) and nominal (X) signal parameter (measured through the RSA), expressed in relative percentage terms:

$$\Delta_X\% = \left|\frac{\hat{X}-X}{X}*100\right| \qquad \text{(II-29)}$$

II.3.4.A ULA emulation

As stated above, the first step of the method is mandated to digitize the signals that impinge on the ULA array. To this aim, the ULA has been emulated by means of a measurement station consisting of a digital acquisition system (DAS), namely SDA 6000A™ by LeCroy®, and a radio-frequency vector signal generator, namely ESG E4438C™ by Agilent Technologies (250 kHz-6 GHz output frequency range, 12 bit vertical resolution, 10 MSamples memory depth). In particular, the DAS has been used to achieve a master version of each impinging signal, from which *m* delayed replicas (i.e. $s_k(t-\tau_{ik})$) have been generated.

The nominal azimuth angle of each signal has been used to evaluate the propagation delays τ_{ik} to be adopted in eq. (1). Propagation delay has successively been transformed in phase shift $A_k(f_l)$ in the frequency domain thanks to the eq. (II-14); delayed replicas are, finally, attained as the product of the

Tab. II.8 Signals setting configuration in first scenario

	WC1	*OF1*	*OF2*	*OF3*
CB [MHz]	20	16.6	16.6	16.6
CP [dBm]	-30	-35	-32	-40
$\vartheta[°]$	10	20	40	60

discrete time Fourier transforms (DFT) of the master version by the corresponding $A_k(f_l)$, and applying an inverse DFT on the result of multiplication. Moreover, the availability of the master version of each signal impinging on the ULA has made it possible to achieve its nominal power spectrum to be adopted in *RMSE* evaluation.

II.3.4.B First scenario

As first example, wideband signals generated by four wireless networks operating according to different channels of the IEEE 802.11b/g standard have been taken into account. In particular, two signals, referred to as OF1 and OF2, have been associated with the transmissions on the channels 8 and 9 according to the IEEE 802.11g standard; the other two signals, referred to as OF3 and WC1, have shared the same channel (equal to 10) but have been transmitted according to the IEEE 802.11g and IEEE 802.11b standard, respectively. The other parameters of the signals, in terms of channel bandwidth, channel power and azimuth angle, are given in Tab. II.8.

Results provided by the proposed method in tests conducted in the c*ritical* configuration are shown in terms of estimated number of signal (Fig. II.18), *RMSE* (Fig. II.17), $\Delta_{CB}\%$ (Fig. II.19) and $\Delta_{CP}\%$ (Fig. II.20). It is worth highlighting that:

- the number of signals d^* involved into the analysis has reliably been estimated only for SNR

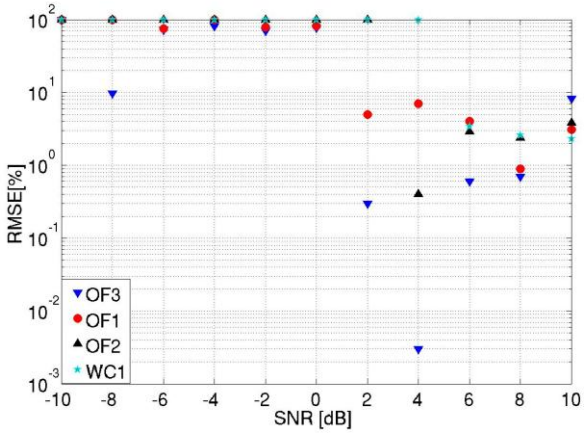

Fig. II.17 Results, in terms of RSME, provided by the proposed method for tests conducted in critical configuration in first scenario.

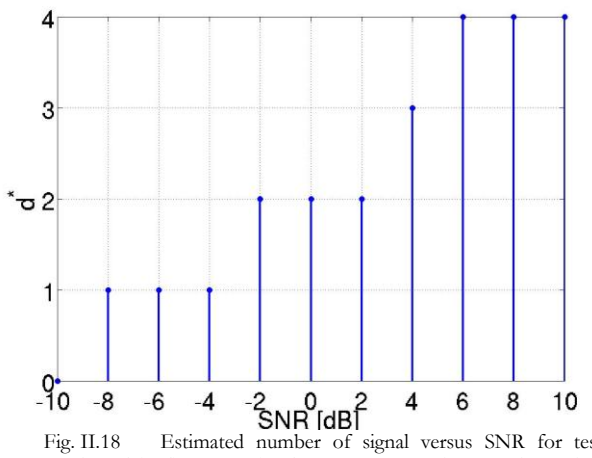

Fig. II.18 Estimated number of signal versus SNR for tests conducted in first scenario; for SNR greater than -10 dB, at least one signal has been singled out.

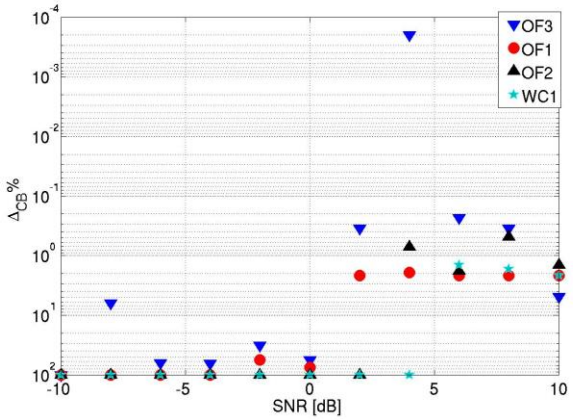

Fig. II. 19 Differences between estimated and nominal channel bandwidth for tests conducted in critical configuration in first scenario.

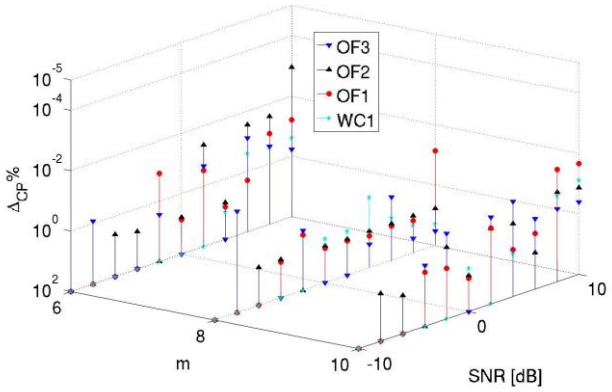

Fig. II.20 Results, in terms of Δ_{CP}%, obtained in different ULA configurations for SNR values varying in the interval from -10 to 10 dB.

equal or greater than 6 dB, while only two signals have been detected upon the SNR varying within the interval -2 dB-2 dB; the method has been capable of detecting at least one signal for SNR values greater than -10 dB;

- DOA estimate of detected signals have always been good; differences between nominal and measured values of the azimuth angle never greater than 0.4° have, in fact, been attained;
- estimates of CP and CB of the d^* detected signals have concurred with the nominal values for each SNR condition; $\Delta_{CP}\%$ and $\Delta_{CB}\%$ values as low as 1% and 6% have, in fact, been experienced also when the method have not succeeded in correctly estimating d. As an example, for tests conducted with a SNR value equal to -4 dB and in the *good configuration*, the method has detected two among four signals (OF3 and OF2 in Fig. II.21). The corresponding results of CB and CP has allowed to obtain $\Delta_{CP}\%$=2.1% and $\Delta_{CB}\% = 2.5\%$ for OF3 and $\Delta_{CP}\%$=2.2% and $\Delta_{CB}\% = 2.3\%$ for OF2;
- the method has been capable of reliably reconstructing the power spectrum of each signal involved in the analysis. In fact, RMSE values always lower than 4% have been experienced for correctly detected signals.

In order to assess the effect of the number of ULA antennas, further tests have been conducted in the other two configurations (*normal* and *good*). From the obtained results, the following considerations can be drawn:

- the whole set of four signals has correctly been estimated for SNR values as low as 4 dB, thus granting a slight performance improvement with respect to the *critical* condition;

- the method has not succeeded in detecting the signal characterized by the lowest channel power for SNR values varying in the interval from -2 dB up to 2 dB. A number of signals equal to 2 has been obtained for SNR value below -2 dB;
- reliable measurements of DOA, CB and CP (Fig. II.21) have been achieved independently from the SNR condition, thus highlighting their independence from the number of ULA antennas;
- similar results of RMSE have been attained for different SNR values in all the measurement configurations.

II.3.4.C Second scenario

The second scenario has considered three wideband signals (in the following referred to as WC1, WC2 and WC3) generated according to the UMTS standard. In particular, all the signals have been characterized by the same carrier frequency and channel bandwidth equal to 2.1 GHz and 4.2 MHz, respectively; with regard to the channel power, different nominal values have been set (-10 dBm for WC1, -20 dBm for WC2, and -30 dBm for WC3).

As stated above, the spectral analysis based on the traditional DFT approach would provide such a power spectrum that only one signal could apparently be perceived from it, thus preventing any further analysis on the number of impinging signals or measurement of their parameters. On the contrary, thanks to the proposed method, it has been possible to single out the power spectrum of each signal, as shown in Fig. II.21.

Performance of the method in terms of d^* estimated number of signals for tests conducted in *critical*, *normal* and *good* configurations has been shown in Fig. II.22. It has been possible to notice that:

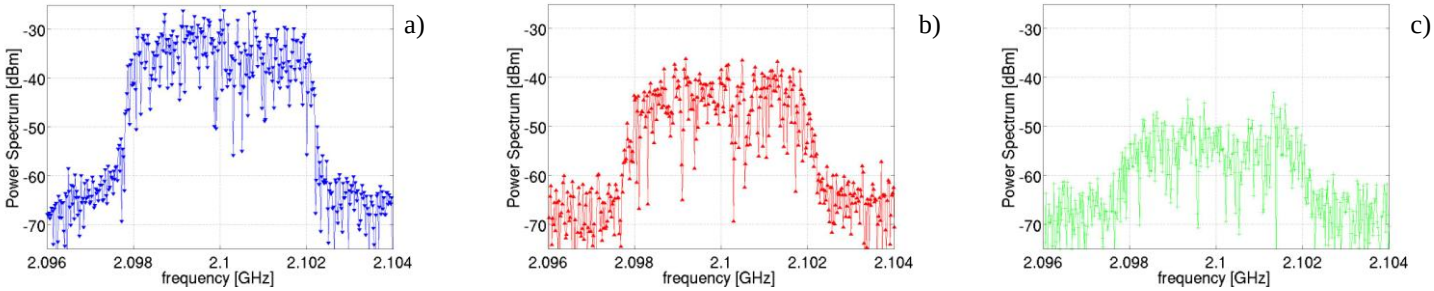

Fig. II.21 Power spectrum of WC1 a), WC2 b), and WC3 c) reconstructed by means of the proposed method for tests conducted in second scenario.

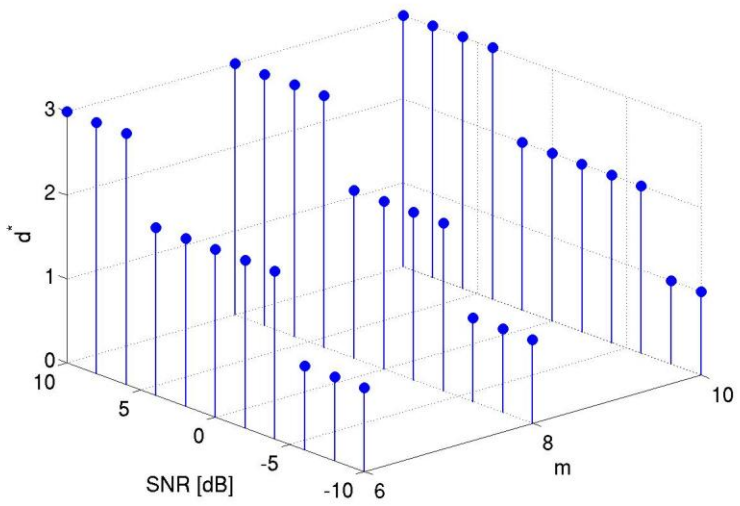

Fig. II.22 Evolution of d^* versus SNR for critical (m=6), normal (m=8), and best (m=10) configurations for tests conducted in second scenario.

- as expected, the number of ULA antennas slightly affects the method's performance. In tests conducted in *normal* configuration, the correct number of signals has, in fact, been obtained for SNR values greater than 4 dB, while the same performance can be gained in *critical* configuration for SNR values at least of 6 dB.

  The further addition of two antennas (*good* configuration) in the ULA has not allowed an enhancement of the performance with respect to the *normal* configuration; no real improvement in the estimation both of $\Delta_{CP}\%$ (Fig. II.23) and $\Delta_{CB}\%$ (Fig. II.24) has been experienced moving from 6 up to 10 ULA antennas. In fact, $\Delta_{CP}\%$ and $\Delta_{CB}\%$ have never exceeded 11% in all the configurations, thus allowing reliable measurements;
- remarkable concurrence between reconstructed power spectra and nominal ones has been

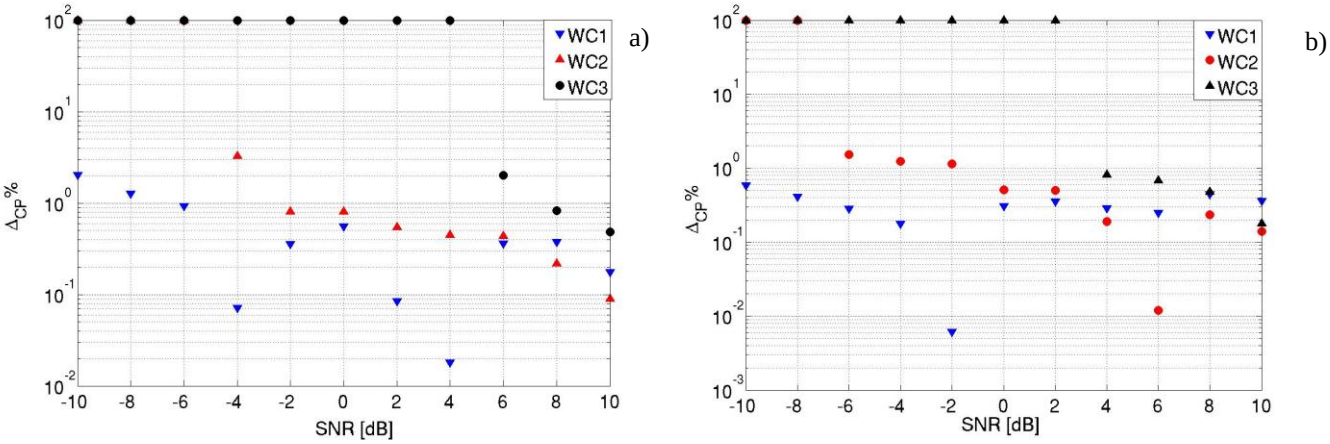

Fig. II.23 Evolution of $\Delta_{CP}\%$ versus SNR for *critical* a) and *good* b) configurations for tests conducted in second scenario.

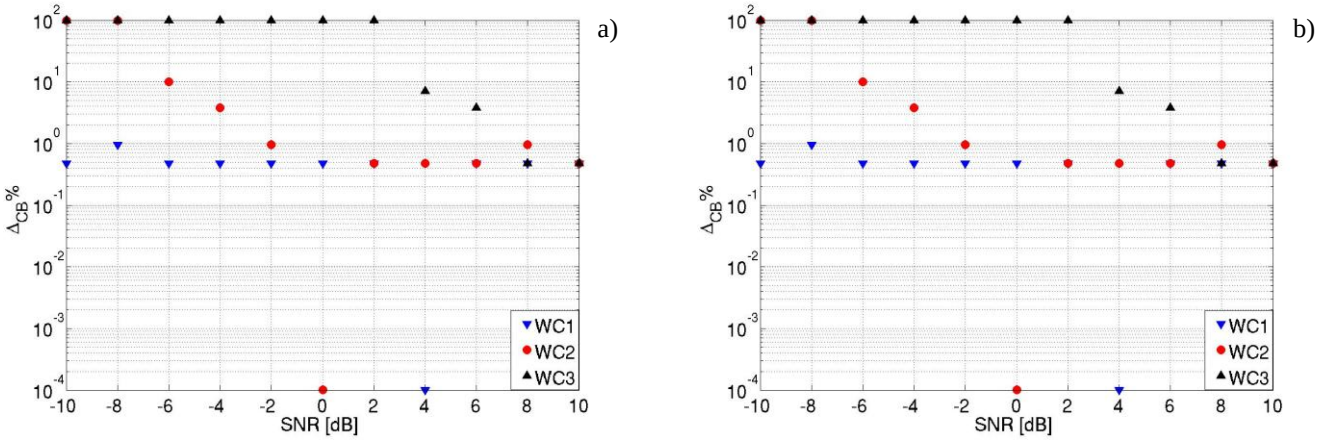

Fig. II.24 Evolution of Δ_{CB}% versus SNR for *critical* a) and *good* b) configurations for tests conducted in second scenario.

experienced; RMSE values never exceeding 5% have, in fact, been measured.

II.3.4.D Third scenario

Third example has referred to a typical situation that can be encountered in actual transceivers of wireless communications systems. Many systems can, in fact, present functioning anomalies after some years, due to aging effect of their internal components, such as mixer, amplifier, converter, and so on. In this way, harmful phenomena like transmitter spectral mask distortion or power leak in adjacent frequency bands could arise, thus generating non-intentional interference for other communication systems. Such conditions have been emulated in a further scenario consisting of an interfering narrowband signal (NS) and three wideband signals compliant with IEEE 802.11g standard. In particular, the carrier frequency of NS has been set equal to 2.462 GHz, while the wideband signals have respectively been associated with channel 8 (OF1), 9 (OF2), and 10 (OF3). Further information about signals parameters is given in Tab. II.9.

The proposed method has been capable of separating the power spectrum of each signal and carrying out reliable measurements of channel bandwidth and channel power also for tests conducted in this scenario. It is, in fact, worth evidencing that:

Tab. II.9 Signals setting configuration in third scenario

	NS	OF1	OF2	OF3
CB [MHz]	0	16.6	16.6	16.6
CP [dBm]	-30	-30	-32	-40
ϑ[°]	10	-10	30	50

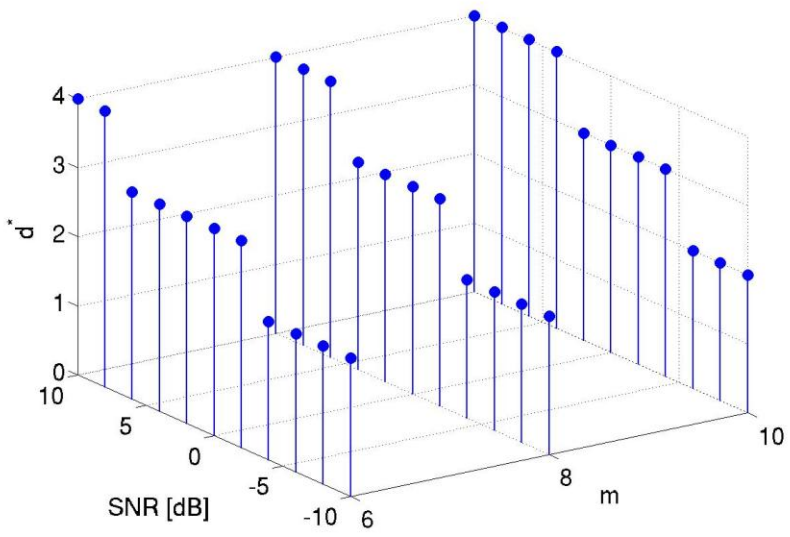

Fig. II.25 Evolution of d^* versus SNR for critical (m=6), normal (m=8), and best (m=10) configurations for tests conducted in third scenario.

- the proposed method has correctly estimated the number of signals (Fig. II.25) for SNR values greater than 8 dB, independently of the measurement configuration. Increasing the number of antennas has allowed performance improvement, providing the desired values of d^* for SNR values greater than 6 dB and 4 dB for tests conducted in *normal* and *good* configurations, respectively;
- channel power and channel bandwidth of all signals have reliably been measured for SNR≥8 dB. Values of Δ_{CP}% and Δ_{CB}% always lower than 5% have, in fact, been obtained;
- the proposed method has succeeded in measuring the desired parameters of all detected signals also in the presence of an underestimation of their number. Δ_{CP}% and Δ_{CB}% values never exceeding respectively 10% and 6% have, in fact, been obtained;
- RMSE values always lower than 3% have been encountered, thus assuring notable concurrence between the reconstructed power spectra and reference ones.

Tab. II.10 Signals setting configuration in fourth scenario

	WM1	OF1
CB [MHz]	24	16.6
CP [dBm]	-10	-25
ϑ[°]	30	40

II.3.4.E Fourth scenario

Two wideband signals, transmitted according with IEEE 802.16d-2004 [22] (WiMAX fixed and referred as WM1) and IEEE 802.11g standard (referred as OF1), are taken into account. OF1 signal emulates a power leak due to the non-linearity of transmitter amplifier, whose gives rise a rigid translation of the power spectrum towards a higher frequency band. In this case, OF1 power spectrum should be centered around the frequency of 2.462 GHz (eleventh channel of IEEE 802.11g standard), but, because of cited drawback, it is pushed upwards to the central frequency of 3.5 GHz, in which the WiMAX systems typically operate. More details about the two signals are summarized in Tab. II.10.

Thanks to the proposed method, the presence of unexpected interfering signal can be discovered, because two signals are estimated, and the typical parameters, associated with WiMAX signal can be reliably measured yet. In particular, the results obtained through the wide experimental phase evidence that:

- no signal (Fig. II.26), in *critical* configuration, is estimated for SNR values below of -8 dB, and only if the SNR is equal or greater than 8 dB the right d^* value is detected. The addition of two antennas (m equal to 8) assures a performance improvement, thus providing the correct d^* estimation for SNR ≥6 dB. Further increase of antennas (*good* configuration) doesn't affect the final performance;

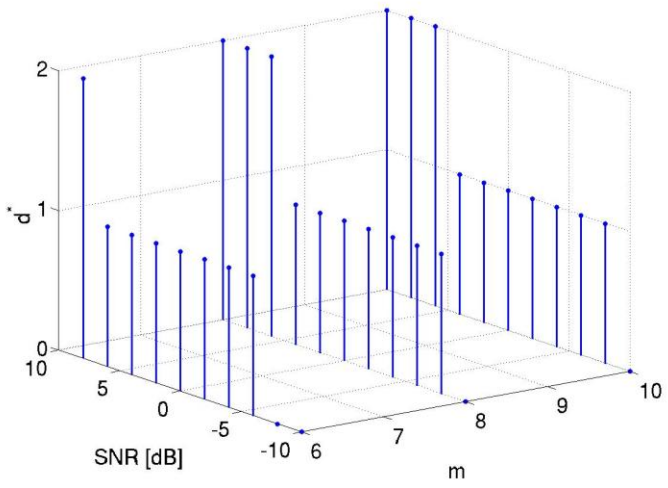

Fig. II.26 Evolution of d^* versus SNR for critical (m=6), normal (m=8), and best (m=10) configurations for tests conducted in fourth scenario.

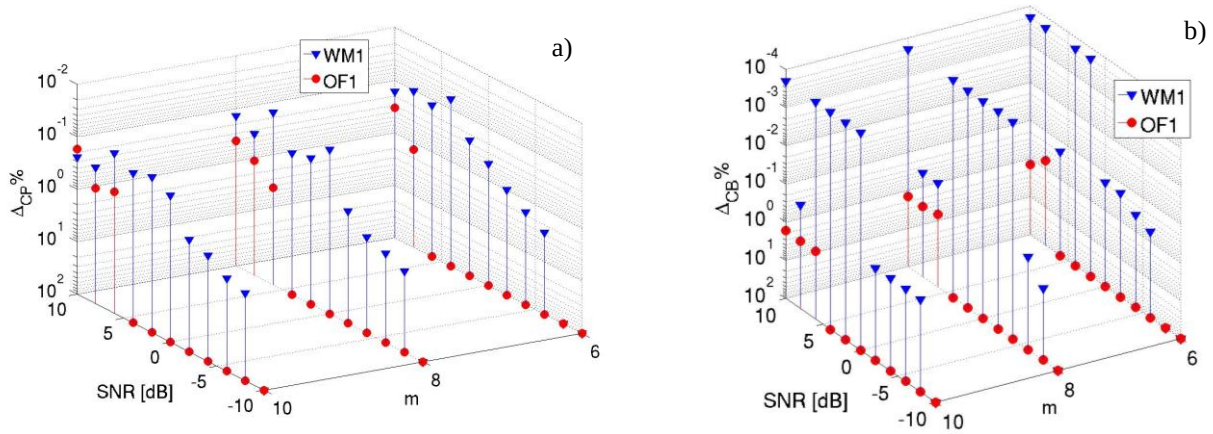

Fig. II.27 Evolution of Δ_{CP}% a) and Δ_{CB}% b) versus SNR for tests conducted in fourth scenario.

- reliable measurements of channel power and channel bandwidth are achieved when the number of signals involved into analysis is exactly estimated, thus providing Δ_{CP}% and Δ_{CB}% values always lower than 3% and 1%, respectively (Fig. II.27);
- DOA's values in concurrence with nominal ones allow to reliably reconstruct the power spectrum of each signal; RMSE values around of 5% has been experienced;
- Δ_{CP}% and Δ_{CB}% values never exceed both 10%, when the proposed method gives a *d** underestimation.

II.3.5 Processing time

Proposed method processing times have been evaluated for different analysis band and number of signals involved in the analysis. More specifically, analysis band from 22 up to 82 MHz with step equal to 5 MHz and centered at 2.437 GHz has been analyzed in two operating conditions; that is, in presence of two (Fig. II.28a), and three OFDM wideband signals (Fig. II.28b) compliant to IEEE 802.11g standard. Each wideband signal is characterized by the features summarized in Tab. II.11, where OF_i (with i runs from 1 up to 3) stands for the i-*th* signal. Moreover, critical (m equal to 6), normal (m equal to 8) and best (m equal

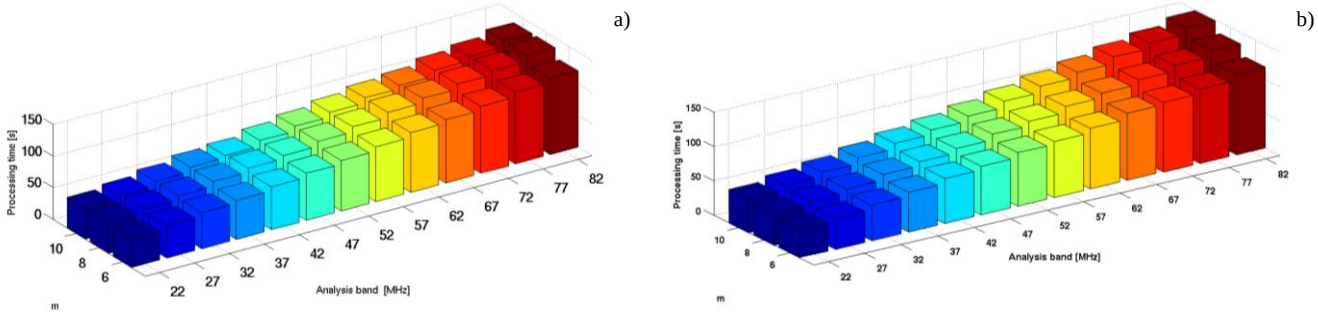

Fig. II.28 Processing times versus analysis band and *m,* in presence of two a) and three b) OFDM wideband signals

Tab. II.11 Signals setting configuration for processing times evaluation

	OF_1	OF_2	OF_3
CF [GHz]	2.437	2.442	2.447
CB [MHz]	16.6	16.6	16.6
CP [dBm]	-10	-12	-15
ϑ[°]	-5	25	45

to 10) ULA configurations are taken into account. The obtained results lead to the following considerations:

- linear growth of processing times versus analysis band is experienced, independently from both ULA configuration and number of signals involved into analysis;
- slight increase of processing times is achieved when three signals have to estimated; as an example for m=10 and 82 MHz as analysis band, the processing time between both operating conditions differs of only 20 s;
- for each analysis band, the processing time doesn't abruptly change with the number of ULA antennas;
- processing time equal to 150 s (almost 2.5 minute) is provided when all analysis band is analyzed through an ULA array characterized by 10 antennas;
- proposed method could take advantage of parallel implementation of some stage in order to reduce the whole processing time.

II.3.6 Conclusion

A new method based on eigenvalues decomposition approach has been proposed for in-service testing at physical layer of wireless communications systems and networks. In particular, the method allowed the measurement of relevant parameters of wideband signals interfering both in time and frequency domain. In such conditions, traditional approaches, principally based on parametric and non-parametric estimators, had no success in parameters measurement. On the contrary, the proposed method has suitably assured the reconstruction of the power spectrum of each involved signal, thus allowing the execution of reliable measurements.

Experimental tests, aimed at assessing the method's performance and carried out emulating different configurations of the ULA, have evidenced that the proposed method provides results very close to those granted by a high performance spectrum analyzer independently from the signal typology

(wideband and narrowband) and interference condition (partial or full power spectra overlap). Method's performance depends both on the SNR values and the number *m* of ULA antennas. In particular, the increase of *m* from 6 to 8 has allowed the method to suitably operate also in worst SNR conditions, while the further addition of 2 antennas in the emulated ULA has not provided significant performance enhancement. Reliable measures of channel power and channel bandwidth have always been gathered for each impinging signal properly detected; differences between measured and reference values of CP and CB, expressed in relative percentage terms, never greater than 10% has been attained. Finally, values of RMSE always lower than 5% have highlighted that the reconstructed power spectra concur with the reference ones.

II.4 References

[II.1] D. J. Shyy, M. Jamie, R. M. Tamer, "WiMAX RF planner," *Proc. of Testbeds and Research Infrastructures for the Development of Networks & Communities* 2009, Washington DC, USA, April 6-8, 2009, pp. 1-3.

[II.2] L. Garber "Mobile WiMax: The Next Wireless Battle Ground" Computer Volume 41, Issue 6, June 2008 pp. 16-18 Digital Object Identifier 10.1109/MC.2008.201.

[II.3] A. Ghosh, D.R. Wolter, J.G. Andrews, R. Chen, "Broadband Wireless Access with WiMax/802.16: Current Performance Benchmarks and Future Potential, " Volume 43, Issue 2, Feb. 2005 Page(s):129 – 136 Digital Object Identifier 10.1109/MCOM.2005.139151.

[II.4] A. Yarali, B. Mbula, A. Tumula "WiMAX: A key to bridging the digital divide," *Proc. of SoutheastCon*, 2007, Richmond, VA, March 22-25, 2007, pp. 159-164.

[II.5] J. Zhang, C. Wang, "RF transceiver of WiMAX base station for 802.16d" *Proc. of Microwave and Millimeter Wave Technology*, 2008, Nanjing, China, April 21-24, 2008, pp. 124-126.

[II.6] IEEE 802.16™-2004, *Standard for local and metropolitan area networks – Part 16: Air interface for fixed broadband wireless access systems.* (Revision of IEEE Std 802.16-2001) June 2004, ISBN 0-7381-4069-4 SH95246.

[II.7] B.Bennett, P.Hemmingsand, B.A.Hamilton, *"Operational considerations of deploying WiMAX technology as a last-mile tactical communication system*," *Proc of Military Communications Conference* 2006, Oct 17-20. 2006, pp. 1-7.

[II.8] "*WiMAX Concepts and RF Measurements – IEEE 802.16-2004 WiMAX PHY layer operation and measurements"*, Application Note Agilent, 2005. Agilent Technologies Literature 5989-2027 EN.

[II.9] "Using Error Vector Magnitude Measurements to Analyze and Troubleshoot Vector-Modulate Signals," Product note 89400-14, 2000. Agilent Technologies Literature 5965-2898E.

[II.10] L.Angrisani, M.D'Apuzzo, M.D'Arco, *"A digital signal processing approach for modulation quality assessment in WiMAX systems"*Proc. of IMTC 2007, Vancouver, May 1-3. 2007, pp. 1-6.

[II.11] L.Angrisani, M.D'Arco, M.Vadursi, "Error vector-based measurement procedures for RF digital transmitters troubleshooting," *IEEE Trans. Instrum. Meas.*, vol. 54, no. 4, pp. 1381-1387, Aug. 2005.

[II.12] 802.11 *IEEE Standard for Information technology — Part 11: Wireless LAN Medium Access Control (MAC) and Physical Layer (PHY) specifications—Amendment 1: High-speed Physical Layer in the 5 GHz band.*

[II.13] "IEEE 802.11 Wireless LAN PHY Layer RF operation and measurement," Application Note, 2001. Agilent Technologies Literature 5988-5411EN.

[II.14] J.Lei, D.Gang, Z.Ping, "EVM measurement algorithm for OFDM transmitters," *Proc of International Symposium on Communications and Information Technologies* 2006, Toulouse, France, Oct 18-20, 2006, pp. 102-107.

[II.15] Agilent N7613A Signal studio for 802.16-2004 (WiMAX) technical overview, 2006. Agilent Technologies Literature 5989-2152 EN.

[II.16] K.C. Ho, Y.T. Chan, R. Inkol, "A digital quadrature demodulation system," *IEEE Trans. Aerospace and Electronic Systems* vol. 32, no. 4, pp. 1218-1227, Oct. 1996.

[II.17] Z. Zhang, K. Long, M. Zhao, L. Yuanan," Joint frame synchronization and frequency offset estimation in OFDM systems" *IEEE Trans. on Broadcasting*, vol 51, no. 3, pp. 389-392, Sept. 2005.

[II.18] "Fundamentals of Interference in Mobile Networks, " Application note, Tektronik, 2GW-14758-0, 2001

[II.19] "Hunting for Sources of Interference in Mobile Networks," Application note, Tektronik, 2GW-14759-0, 2001

[II.20] L. Angrisani, M. D'Apuzzo, M. Vadursi, "Power Measurement in Digital Wireless Communication Systems through Parametric Spectral Estimation," *IEEE Trans. on Instrumentation and Measurement*, vol.55, No.4, August 2006, pp.1051-1058.

[II.21] L. Angrisani, A. Napolitano, M. Vadursi, "True-Power Measurement in Digital Communications Systems Affected by In-Channel Interference," *IEEE Trans. on Instrumentation and Measurement*, vol.58, No.11, November 2009.

[II.22] L. Angrisani, M. D'Apuzzo, M. D'Arco, "New digital signal-processing approach for transmitter measurement in third generation telecommunication systems," *IEEE Trans.on Instrum. And Measur.*, Vol. 53 no. 3, June 2004, pp. 622-629.

[II.23] L. Angrisani, M. D'Apuzzo, M. D'Arco, "A New Method for Power Measurements in Digital Wireless Communication Systems," *IEEE Trans. on Instrum. and Measur.*, vol.52, no.4, Aug. 2003, pp.1097-1106.

[II.24] A. Leopoldo, A. Napolitano, R.S. Lo Moriello, "Measuring true signal parameters in digital wireless systems in the presence of in-channel interference," in *Proc. IEEE I2MTC*, Victoria Island, BC, May 12 15, 2008, pp. 1588 1593.

[II.25] R. Schmidt, "Multiple emitter location and signal parameter estimation," IEEE Trans. Antennas Prop., vol. AP-34, pp. 276 280, Mar. 1986.

[II.26] F. Li , K. Tam, Y. Wu, "Determining the number of sources in signal processing," *in Proc. Signal Processing*, Aug 21 25, 2000, vol. 1, pp.413-420.

[II.27] J. Luo, Z. Zhang, "Using eigenvalue grads method to estimate the number of signal source," in *Proc. Signal Processing*, Aug. 21 25, 2000, vol. 1, pp. 223 225.

[II.28] A. Morrison, B.S. Sharif, S. Sali, and O. R. Hinton, "An iterative DOA Algorithm for a space-time DS-CDMA rake receiver," *Proc. of 3G Mobile Communication Technologies*, London, UK, March 27 29, 2000, pp. 208 212.

[II.29] A. Hirata, T. Morimoto, and Z. Kawasaki, "DOA Estimation of ultra-wideband EM waves with MUSIC and interferometry," *Antennas and wireless propagation letters*, vol. 2, no. 1, pp. 190 193, 2003

[II.30] T. W. Anderson, "Wideband direction of arrival estimation based on fourth-order cumulants," *Proc. of Communication*, *Circuit and Systems,* San Jose, California, July 23-25, 2009, pp. 402-405.

[II.31] P. Stoica, and R. Moses, Introduction to Spectral Analysis. Upper Saddle River, NJ: Prentice Hall, 1997.

[II.32] J. Kusuma, "Parametric Frequency Estimation: ESPRIT and MUSIC," *Proc. of Mathematics subject classification signal*, May 13, 2002.

[II.33] Y.-S Yoon,. L. Kaplan, and J. McClellan, "New signal subspace direction-of-arrival estimator for wideband sources," *IEEE Int. Conf. Acoustics, Speech, and Signal Processing*, Hong Kong, April., 2003, pp. 225 333 .

[II.34] E.Del Re, L. Pietrucci, and S. Marapodi, "On the application of DOA estimation technique to UMTS system," *Proc. of spread spectrum technique and applications*, Prague, Czech Republic, September 2-5, 2002, vol. 2, 2002, pp. 550 554

[II.35] F. Li, H. Liu, and R.J. Vaccaro, "Performance analysis for DOA estimation algorithms: unification, simplification, and observations," *IEEE Trans. Aerospace and Electronic Systems*, vol. 29, no. 4, pp 1170 1184, Oct. 1993

[II.36] A. Leopoldo, A. Napolitano, R.S. Lo Moriello, "Power Spectrum Measurement of Wideband Signals Interfering with One Another in Both Time and Frequency Domain," in *Proc. IEEE I2MTC*, Singapore, May 5-7, 2009, pp. 962-967.

[II.37] H. Akaike,"Information Theory and an extension of the maximum likelihood principle," *Proc. 2nd Inter.Symposium on Information Theory*, Budapest, 1973, pp. 267-281.

[II.38] I. Kopriva, W. Wasylkiwskyj," Estimating number of sub-Gaussian emitters in a narrowband DOA estimation problem by using independent component analysis,". *Proc. of Antennas and propagation*, July 3-8, 2005

[II.39] A. Leopoldo, A. Napolitano," Modulation quality measurement in WiMAX systems through a fully digital signal processing approach,". *in pubblication on IEEE Trans. on Instrumentation and Measurement*

Chapter III

GRID: infrastructure, architecture and services

III.1 What is grid computing?

Grid computing (or, more precisely a "grid computing system") is a virtualized distributed computing environment. Such an environment aims at enabling the dynamic "runtime" selection, sharing, and aggregation of (geographically) distributed autonomous resources based on the availability, capability, performance, and cost of these computing resources, and, simultaneously, also based on an organization's specific baseline and/or burst processing requirements. When people think of a grid, the idea of an interconnected system for the distribution of electricity, especially a network of high-tension cables and power stations, comes to mind. In the mid-1990s the grid metaphor was applied to computing, by extending and advancing the 1960s concept of "computer time sharing." The grid metaphor strongly illustrates the relation to, and the dependency on, a highly interconnected networking infrastructure. It is worth noting that grid computing is an evolving field and, so, there is

not always one canonical, normative, universally accepted, or axiomatically derivable view of "everything grid related," and it follows that we occasionally present multiple views, multiple interpretations, or multiple perspectives on a topic, as they might be perceived by different stakeholders or communities of interest. The precise definition of what exactly this technology encompasses is still evolving and there is not a globally accepted normative definition that is perfectly non overlapping with other related technologies. Grid computing emphasizes (but does not mandate) geographically distributed, multiorganization, utility-based, outsourcer-provided, networking-reliant computing methods. In its basic form, the concept of grid computing is straightforward: with grid computing an organization can transparently integrate, streamline, and share dispersed, heterogeneous pools of hosts, servers, storage systems, data, and networks into one synergistic system, in order to deliver agreed-upon service at specified levels of application efficiency and processing performance. Additionally, or, alternatively, with grid computing an organization can simply secure commoditized "machine cycles" or storage capacity from a remote provider, "on-demand," without having to own the "heavy iron" to do the "number crunching." Either way, to an end-user or application this arrangement (ensemble) looks like one large, cohesive, virtual, transparent computing system [III.1, III.2]. A grid mechanism is an enabling technology for online collaboration and for discovery and access to distributed resources. A grid mechanism is basically a middleware; it is a distributed computing technology. Broadband networks play a fundamental enabling role in making grid computing possible and this is the motivation for looking at this technology from the perspective of communication.

Whereas the Internet is a network of communication, grid computing is seen as a network of computation: the field provides tools and protocols for resource sharing of a variety of IT resources. Grid computing approaches are based on coordinated resource sharing and problem solving in dynamic, multi-institutional virtual organizations.

The enabling factors in the creation of grid computing systems in recent years have been the proliferation of broadband (optical-based) communications, the Internet, and the World Wide Web infrastructure, along with the availability of low cost, high-performance computers using standardized (open) operating systems [III.3, III.4, III.5]. Prior to the deployment of grid computing, a typical business application had a dedicated platform of servers and an anchored storage device assigned to each individual server. Applications developed for such platforms were not able to share resources, and, from an individual server's perspective, it was not possible, in general, to predict, even statistically, what the processing load would be at different times. Consequently, each instance of an application needed to have its own excess capacity to handle peak usage loads. This predicament typically resulted in higher overall costs than would otherwise need to be the case [III.6]. To address these lacunae, grid computing aims at exploiting the opportunities afforded by the synergies, the economies of scale, and

the load smoothing that result from the ability to share and aggregate distributed computational capabilities, and deliver these hardware based capabilities as a transparent service to the end-user. To reinforce the point, the term "synergistic" implies "working together so that the total effect is greater than the sum of the individual constituent elements." From a service-provider perspective, grid computing is somewhat akin to an application service provider (ASP) environment, but with a much-higher level of performance and assurance [III.7]. Specialized ASPs, known as grid service providers (GSPs) are expected to emerge to provide grid-based services, including, possibly, "open-source outsourcing services." Grid computing started out as the simultaneous application of the resources of many networked computers to a single (scientific) problem [III.4]. Grid computing has been characterized as the "massive integration of computer systems".

The ability to have a cluster, an entire data center, or other resources spread across an area connected by the Internet (and/or, alternatively, connected by an intranet or extranet), operating as a single transparent virtualized system that can be managed as a service, rather than as individual constituent components, likely will, over time, increase business agility, reduce complexity, streamline management processes, and lower operational costs [III.6]. Grid technology allows organizations to utilize numerous computers to solve problems by sharing computing resources.

III.2 Comparison with other technologies

It is important to note that certain IT computing constructs are not grid. In some instances, these technologies are the optimal solution for an organization's problem; in other cases, grid computing is the best solution, particularly if in the long term one is especially interested in supplier-provided utility computing.

The distinction between *clusters* and grids relates to the way resources are managed. In the case of clusters (aggregations of processors in parallel-based configurations), the resource allocation is performed by a centralized resource manager and scheduling system. Also, nodes cooperatively work together as a single unified resource. In the case of grids, each node has its own resource manager and does not aim at providing a single system view [III.7]. A cluster is comprised of multiple interconnected independent nodes that cooperatively work together as a single unified resource. This means all users of clusters have to go through a centralized system that manages the allocation of resources to application jobs. Unlike grids, cluster resources are almost always owned by a single organization. Actually, many grids are constructed by using clusters or traditional parallel systems as their nodes, although this is not a requirement. An example of a grid that contains clusters as its nodes is the NSF TeraGrid [III.8]; Although cluster management systems can deliver enhanced distributed computing services, they are not grids themselves; these cluster management systems have centralized control, complete knowledge

of system state and user requests, and complete control over individual components (such features tend not to be characteristic of a grid proper).

Grid computing also differs from basic *Web services,* although it now makes use of these services. Web services have become an important component of distributed computing applications over the Internet [III.9]. The World Wide Web is not yet in itself a grid, its open, general-purpose protocols support access to distributed resources but not the coordinated use of those resources to deliver negotiated qualities of service [III.10]. So, whereas the Web is mainly focused on communication, grid computing enables resource sharing and collaborative resource interplay toward common business goals. Web services provide standard infrastructure for data exchange between two different distributed applications, whereas grids provide an infrastructure for aggregation of high-end resources for solving large-scale problems in science, engineering, and commerce. While most Web services involve static processing and moveable data, many grid computing mechanisms involve static data (on large databases) and moveable processing. However, there are similarities as well as dependencies. First, similar to the case of the World Wide Web, grid computing keeps complexity hidden—multiple users experience a single, unified experience. Second, Web services are utilized to support grid computing mechanisms. These Web services will play a key constituent role in the standardized definition of grid computing, since Web services have emerged in the past few years as a standards-based approach for accessing network applications. In this context, low-level grid services are instances of Web services (a grid service is a Web service that conforms to a set of conventions that provide for controlled, fault-resilient, and secure management of services) [III.11, III.12].

Grid computing also differs from *virtualization.* Resource virtualization is the *abstraction* of server, storage, and network resources in order to make them available *dynamically* for sharing, both inside and outside an organization. *Virtualization is a step along the way on the road to utility computing* (grid computing) and, in combination with other server, storage, and networking capabilities, offers customers the opportunity to build, according to advocates, an IT infrastructure "without" hard boundaries or fixed constraints [III.13]. Virtualization has somewhat more of an emphasis on local resources, whereas grid computing has more of an emphasis on geographically distributed inter-organizational resources. The universal problem that virtualization is solving in a data center is that of dedicated resources. While this approach does address performance, this method lacks fine granularity. Typically, IT managers take an educated guess as to how many dedicated servers they will need to handle peaks, purchase extra servers, and then later find out that a significant number of these servers are significantly underutilized. A typical data center has a large amount of idle infrastructure, bought and set up online to handle peak traffic for different applications. Virtualization offers a way of moving resources from one application to another dynamically. However, specifics of the desired virtualizing effect depend on the specific

application deployed [III.14]. With virtualization, the logical functions of the server, storage, and network elements are separated from their physical functions (e.g., processor, memory, I/O, controllers, disks, switches). In other words, all servers, storage, and network devices can be aggregated into independent pools of resources. Some elements may even be further subdivided (server partitions, storage LUNs) to provide an even more granular level of control. Elements from these pools can then be allocated, provisioned, and managed, manually or automatically, to meet the changing needs and priorities of one's business. Virtualization can span the following domains [III.13]:

1. Server virtualization for horizontally and vertically scaled server environments.
2. Server virtualization enables optimized utilization, improved service levels, and reduced management overhead.
3. Network virtualization, enabled by intelligent routers, switches, and other networking elements supporting virtual LANs. Virtualized networks are more secure and more able to support unforeseen spikes in customer and user demand.
4. Storage virtualization (server, network, and array-based). Storage virtualization technologies improve the utilization of current storage subsystems, reduce administrative costs, and protect vital data in a secure and automated fashion.
5. Application virtualization enables programs and services to be executed on multiple systems simultaneously. This computing approach is related to horizontal scaling, clusters, and grid computing, in which a single application is able to cooperatively execute on a number of servers concurrently.
6. Data center virtualization, whereby groups of servers, storage, and network resources can be provisioned or reallocated on the fly to meet the needs of a new IT service or to handle dynamically changing workloads [III.13].

Grid computing deployment, although potentially related to a re-hosting initiative, is not just re-hosting. This last implies the reduction of typically a large number of servers (possibly using some older and/or proprietary operating system) to a smaller set of more powerful and more modern servers (possibly running on open-source operating systems). This is certainly advantageous from the operations, physical maintenance, and power and space perspectives. There are savings associated with re-hosting. However, applications are still assigned specific servers. Grid computing, on the other hand, permits the true virtualization of the computing function. Here, applications are not pre-assigned a server, but the "runtime" assignment is made based on real-time considerations.

III.3 GRID Computing: some example

In the following a compilation of popular grid computing related consortiums and projects aimed to provide the latest technologies in *grid computing* is given.

III.3.1 Asia Pacific Grid (ApGrid)

ApGrid [III.145] aims at building an international grid test bed among organizations in the Asia Pacific region and provides venues for sharing and exchanging ideas and information, new projects, and collaboration and interfacing with global efforts.

III.3.2 Grids in Science and Engineering

The general drive for most current grid projects is to enable the resource interactions that facilitate large-scale science and engineering projects such as bioinformatics, high-energy physics data analysis, climatology, large-scale remote instrument operation, and so forth. In addition to government and military projects (NASA, DOE), grids are being developed by an increasing community of people who work together through coordinating organizations such as the GGF. From efforts such as this, grids will become a reality and an important component of the practice of science and engineering.

III.3.2.A DataGrid Project

The DataGrid [III.16] project is funded by the European Union (EU). The objective is to build the next generation computing infrastructure by providing intensive computation and analysis of shared large-scale databases, from hundreds of terabytes to petabytes, across widely distributed scientific communities. The DataGrid project will be included in the new EU grid project (Enabling Grids for E-sciencE, EGEE). EGEE aims to build a service grid infrastructure in Europe available to scientists 24 hours a day.

III.3.2.B Grid Physics Network (GriPhyN)

The GriPhyN Project [III.17] is developing grid technologies for scientific and engineering projects that must collect and analyze distributed, petabyte scale datasets. GriPhyN research will enable the development of Petascale Virtual Data Grids (PVDGs) through its virtual data toolkit (VDT). VDT is an ensemble of grid middleware that aims to make it as easy for users to deploy, maintain, and use grid middleware. Basic grid services including Condor-G® and Globus®. Virtual data tools to work with virtual data, particularly the virtual data system. Utility software such as the Grid Security Infrastructure (GSI)–Enabled OpenSSH, software to update GSI certificate revocation lists, and monitoring software like MonaLisa.

III.3.2.C Particle Physics DataGrid (PPDG)

The Particle Physics DataGrid Pilot (PPDG) [III.18] is a collaboration of computer scientists with a strong record in grid technology and physicists with leading roles in the software and network infrastructures for major high-energy and nuclear experiments.

III.3.2.D Petascale Data-Intensive Computing (Grid Datafarm)

Grid Datafarm [III.19] is a Petascale data-intensive computing project initiated in Japan. The project is the result of collaboration among the High Energy Accelerator Research Organization (KEK), the National Institute of Advanced Industrial Science and Technology (AIST), the University of Tokyo, and the Tokyo Institute of Technology. The challenge involves the construction of a petascale to exascale parallel filesystems exploiting local storages of PCs spread over the worldwide grid.

III.4 GRID Services

Web Services emerged from the need for a simple framework for business-to-business (B2B) computing. Web Services have created an existing service provider industry that has been the goal of the business marketplace for distributed information management [III.19]. Web Services provide a standard means of interoperating between different software applications, running on a variety of platforms and frameworks. A Web Services architecture identifies global elements in a network that are required to ensure interoperability between Web Services [III.20]. Web Service is designed to support interoperable machine-to-machine interaction over a network. It has an interface described by the WSDL. Other systems interact with the Web Service using Simple Object Access Protocol (SOAP) messages, typically using HTTP with an XML serialization in conjunction with other Web standards [III.21]. Message exchange is defined by a Web Service description (WSD). The WSD is a specification of the Web Service's interface, written in WSDL. It defines the message formats, data-types, transport protocols, and transport serialization formats that should be used between the requester agent and the provider agent. It also specifies one or more network locations at which a provider agent can be invoked and may provide some information about the message exchange pattern that is expected [III.22]. The Web Services model is based on the following standards:

- SOAP defines the mechanism for message exchange though XML [III.21] . SOAP uses XML envelopes and a remote procedure call convention. SOAP is a protocol independent so it can exchange messages through HTTP, FTP, or any other network protocol.

- The WSDL defines the XML schema and language used to describe a Web Service. Each Web Service is an entity, which is defined by ports that are service endpoints capable of exchanging a set of messages defined by the port type [III.19].

- The Universal Description, Discovery and Integration (UDDI) and the Web Services Inspection Language (WSIL) provide the mechanism needed to discover WSDL documents [WebServices01]. UDDI is a specification for a registry that can be used by a service provider as a place to publish WSDL documents. Clients can then search the registry looking for services and fetch the WSDL documents needed to access them. WSIL provides a simple way to find WSDL documents on a Web site. These discovery mechanisms are equivalent to the Grid Information Services provided by Globus.

The Web Services model provides two advantages to grid services:

- Support for dynamic discovery and composition of services in heterogeneous distributed environments through WSDL. WSDL provides the mechanism for discovering and defining interface definitions and endpoint implementation descriptions [III.23].

- The widespread adoption of Web Services mechanisms allows the framework to exploit new tools and technologies such as WSDL processors, workflow systems, language bindings, and hosting environments.

A *GRID service* is a Web Service that provides a set of well-defined interfaces and that follows specific conventions. The interfaces address discovery, dynamic service creation, lifetime management, notification, and manageability [III.23].

The basic characteristics that separate a grid service from a Web Service are the following [III.19]:

- A grid service must be an instance of a service implementation of some service type.

- It must have a grid services handle (GSH), which is a type of uniform resource identifier (URI) for the service instance. The GSH is not a direct link to the service instance but, rather, is bound to a grid service reference (GSR). The GSH provides a way to locate the current GSR for the service instance because the GSR may change if the service instance changes or is upgraded.

- A grid service instance must implement the GridService interface with three operations:
  - ✓ *FindServiceData*: for service metadata discovery and information.
  - ✓ *Destroy*: for clients to destroy instances
  - ✓ *SetTerminationTime*: for service lifetime management

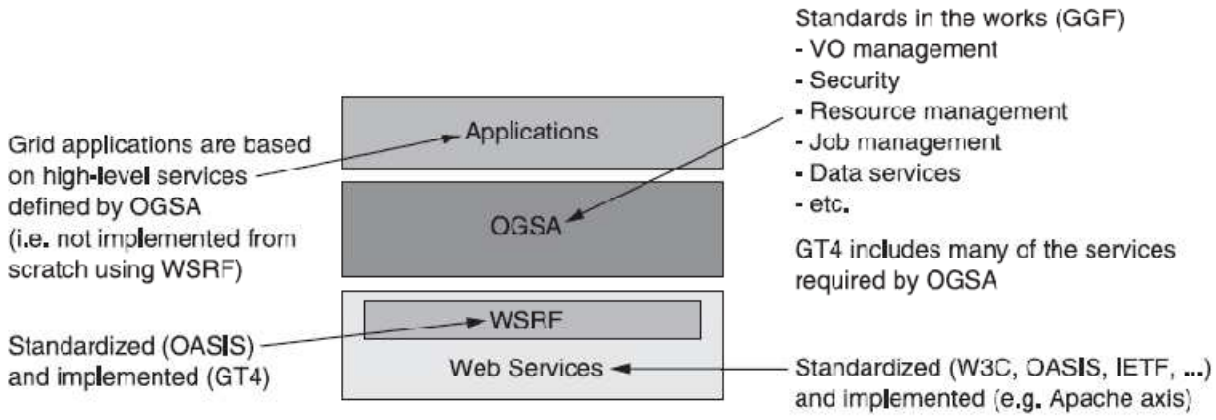

Fig. III.1 GRID Service stack

To this aim a proper architecture has been developed, namely Open Grid Service Architecture (OGSA) [III.19, III.24]. Moreover, to overcome the Web Services limitations, mainly addressed to stateless services, the OGSA have defined the Web Services Resource Framework (WSRF) [III.25]. Hereinafter, a brief description of both is given (Fig. III.1).

III.4.1 OGSA (Open Grid Service Architecture)

A grid system will usually consist of several different components. For example, a typical grid system could have:

- Management Service: To manage what nodes and users are part of each Virtual Organization.
- Resource Discovery and Management Service: So applications on the grid can discover resources that suit their needs, and then manage them.
- Job Management Service: So users can submit tasks (in the form of "jobs") to the Grid.
- And a whole other bunch of services like security, data management, etc.

Furthermore, all these services have to constantly interact. For example, the Job Management Service might consult the Resource Discovery Service to find computational resources that match the job's requirements. With so many services, and so many interactions between them, there exists the potential for chaos. What if every vendor out there decided to implement a Job Management Service in a completely different way, exposing not only different functionality but also different interfaces? It would be very difficult (or nearly impossible) to get all the different software pieces to work together. The solution is standardization: define a common interface for each type of service. For example, take a look at the World Wide Web. One of the reasons why the Web is such a popular Internet application is because it is based on standards (HTML, HTTP, etc.) agreed upon by all the different major players

(Microsoft, Netscape, etc.). Imagine, on the other hand, that you could only use a Microsoft browser to access websites implemented with Microsoft technology (ditto for Netscape, Opera, etc.) It would be definitely un cool. Thanks to standards, we can use our favorite browser (provided it follows standards, which most modern browsers do) to access most of the websites out there (regardless of what technology is used to implement the website).

The Open Grid Services Architecture (OGSA), developed by The Global Grid Forum, aims to define a common, standard, and open architecture for grid-based applications. The goal of OGSA is to standardize practically all the services one commonly finds in a grid system (job management services, resource management services, security services, etc.) by specifying a set of standard interfaces for these services.

The functions are divided into a number of categories, which are listed and described below. Note that the interfaces for these services are not necessarily defined as of yet, and in general the specification will be delegated to other specification documents. The defined functions are:

- ***Service Groups and Discovery Interfaces***—The two-level naming defined by OGSI based on GSHs and GSRs provide a way of accessing a known service, but for a number of reasons, a higher level abstraction is necessary to allow clients to find services. First, the GSH doesn't contain any semantic information, so you can't discover any attributes of a service instance based on this information. Second, one might not have a locator at all, and still need to discover available services, perhaps based on abstract service attributes. Third, the service locator doesn't distinguish between services you are entitled to use, or QoS attributes of a service, etc. For these reasons, registries are often used to attach more semantic content to a group of services. OGSA Platform outlines two approaches to doing registries, one based on attribute naming (i.e., associating meta-data with service listings), and another based on path naming (i.e., organization of services via a hierarchical naming scheme).

- ***Service Domain Interfaces***—A common usage pattern in grid solutions is to create Grid Service collections that together produce a higher order Grid Service interface. Usually this is done in order to implement a domain-specific solution based on more generic lower level services. These are called "Service Domains" in OGSA Platform. This concept of Service Domain generates some requirements for the registration, discovery, selection, filtering, routing, failover, creation, destruction, enumeration, iteration, and topological mapping of service instances within the Service Domain. Building on OGSI service group interfaces, there is a

need to define OGSA Platform interfaces to implement behaviors for filtering, selection, topology, enumeration, discovery, and policy.

- ***Security***—OGSA Platform security mechanisms are primarily focused on integrating and unifying current underlying security systems that are already in use today (e.g., PKI (Public Key Infrastructure) or Kerberos). GGF's OGSA-Sec working group is defining specifications for generic security services, and their mappings to underlying security systems. There is also an effort to stay consistent with the emerging Web Services security framework being defined in other standards organizations (e.g., in OASIS). Given the dynamic nature of virtual organizations, the OGSA Platform security model needs to support the following security disciplines: authentication, confidentiality, message integrity, policy expression and exchange, authorization, delegation, single logon, credential lifespan and renewal, privacy, secure logging, assurance, manageability, firewall traversal, and security at the OGSI level.

- ***Policy—***Many Grid Services will need some form of policy management in order to help direct their actions. For example, if a user needs to consume a computing resource, there may be limits on how long it can be used, or what times of day the user can access the resource. Policies are needed to guide resource usage as well as incorporate business logic and service level agreements. Higher-level policies will be required to be rapresentable in a canonical way which "makes sense" to the underlying lower-level resource. To this end, the OGSA Platform needs to define representations of policy, and the functions needed to implement a policy management system. These representations and functions include: a canonical representation for expressing policies, a management control point for policy lifecycle, an interface that policy consumers can use to retrieve required policies, a way to express that a service is "policy aware," and a way to effect change on a resource. OGSA Platform defines an architecture for this set of services.

- ***Data Management Services***—In the grid environment, there is a great variance in the form of data sources, their location relative to consuming services, their types, and their lifetimes. This diversity adds much complexity when trying to integrate multiple data sources for processing or for management. To this end, it would be useful to define data management interfaces that would abstract the details of accessing a particular set of data from its form. Some of the areas that need to be examined include data access, data replication, data caching services, meta-data catalogs (i.e., specialized registries), schema transformation, and storage.

- ***Messaging and Queuing***—The OGSA Platform is intended to extend the OGSI notification interfaces to support a larger range of semantics for messaging. Semantics might include attributes such as reliability of message transport, ordering semantics, and routing.

- ***Events***—An event represents a state change in a system that might be of interest to some other party. The OGSA Platform is intended to define standard representations and standard ways of processing and communicating events in order to enhance interoperability. This mechanism could be drawn from the work of the OASIS Management Protocol TC.

- ***Distributed Logging***—Distributed logging can be viewed as a special case of messaging, where one entity generates "log artifacts," which may not be used until a later time by some message consumer. OGSA logging can leverage the OGSI notification mechanism, but the semantics of log generation and consumption need to be defined. Logging services need to provide extensions to deal with issues such as the decoupling of log generation from log consumption, putting log records into a common format, filtering and aggregating log records, how long the log records should be kept, and various consumption patterns (e.g., real time vs. historical requirements). To this end, OGSA defines an architecture for OGSA logging services intended to meet these requirements.

- ***Metering and Accounting***—Although different grid deployments use different combinations of services and generally are motivated by different economic and business factors, it is a fairly universal requirement to be able to account for resource consumption and utilization over time and identify how those resources are being used. This information is useful for the purposes of trend analysis, capacity planning, chargeback, evaluation of SLAs, detecting faults, etc. The OGSA Platform metering and accounting interfaces are intended to support this activity, through the following interfaces:
  - ✓ Metering Interface—provides a mechanism to aggregate the metered information from lower level resource (e.g., the operating system accounting logs), in order to unify the resource information across the components involved in the grid application.
  - ✓ Rating Interface—used to translate the metered information into financial terms (e.g., for the purposes of chargeback).
  - ✓ Accounting Interface—helps manage account information (e.g., for end user accounts) based on the rated financial information from the Rating Interface.
  - ✓ Billing/Payment Interface—deals with the transfer of funds.

- ✓ Administrative Services—Although there are no specific requirements listed in OGSA Platform, it is expected that standard interfaces for performing administrative tasks (e.g., software upgrades, backups) in an automatic fashion will be desirable.
- ✓ Transactions—As grid solutions become deployed to support applications with requirements for the coordination of services and service state, there will be a requirement for a transaction service to do this coordination. This is more complicated in the grid environment than in the traditional distributed environment due to the potential latencies across geographies and the fluid nature of virtual organizations. The Web Services community is looking at this, and WS-Transactions has been proposed.
- ✓ Grid Service Orchestration—This refers to the coordination of a set of interacting services in pursuit of performing a single "task." This is also commonly known as workflow. The OGSA Platform is intending to define standard portTypes for launching workflows, as opposed to defining a "one size fits all" workflow language standard. Grid Service factories for different workflow systems can then be defined, allowing clients to use the most appropriate mechanism for their problem domain, yet access and control the workflow in a standard way.

III.4.2 WSRF (Web Service Resource Framework)

WSRF defines the specifications for realizing a stateful Web-Service stemming from a stateless characteristic of classic Web Services (Fig. III.2). A stateful service is a service that has access to, or manipulates, logical stateful resources through the propagation of execution context in headers on

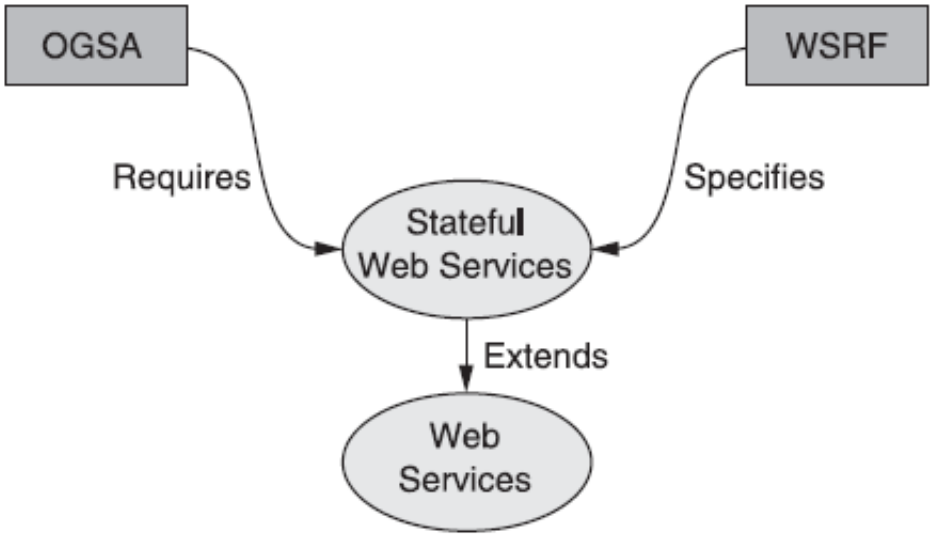

Fig. III.2 Steteful Web Service

message exchanges.

In general, a stateless service enhances reliability and scalability. Thus, stateless services are considered a good practice by the Web Services community [III.26].

WSRF is composed by five specifications that describe the way stateful resources interact with each other.

III.4.2.A WS-ResourceProperties

WS-Resource property defines the constructs by which the state of a WS-Resource can be manipulated through the Web Service interface. A *resource property* maps to an individual component of the resource *state*. WS-ResourceProperties describes WS-Resources by associating stateful resources and Web Services. It also defines methods to retrieve, change, and delete visible properties of a WS-Resource.

III.4.2.B WS-Addressing

WS-Addressing is a construct used to standardize an endpoint reference. An endpoint reference represents the address of a Web-Service deployed over a network endpoint. It is represented as an XML serialization usually returned by a Web Service request to create a new resource. An endpoint reference may contain, besides the Web Service address, metadata such as service description and reference properties.

III.4.2.C WS-Resource Lifecycle

A lifecycle is defined as the period between a WS-Resource creation and destruction that takes into account the following:

III.4.2.C.i Creation

Stateful resources are usually created by a *resource factory*. A *creation* call returns an endpoint reference to the new stateful resource.

III.4.2.C.ii Destruction

Destruction defines the means by which a stateful resource is destroyed and system resources are reclaimed.

III.4.2.C.iii Resource Identifier

Stateful resources must have at least one resource identifier. It is returned as part of the endpoint reference and can be made available to other Web Services in a distributed system.

III.4.2.D WS-ServiceGroup

WS-ServiceGroup is used to organize collections of WS-Resources to build registries or to build services that can perform collective operations. The WS-Service- Group defines the means for managing heterogeneous collections of Web Services. A WS-ServiceGroup uses memberships, rules, constraints, and classifications to define groups. A group is a collection of members that meets some constraints defined using resource properties.

III.4.2.E WS-Resource Security

Security is defined via the WS-Policy and WS-SecurityPolicy specifications, which are part of the Web Services security roadmap. They state the set of policies used to secure message exchanges between clients and Web Services.

III.5 Globus toolkit 4

Globus Toolkit (GT) 4 [III.27] is an open source toolkit organized as a collection of loosely coupled components. These components consist of services, programming libraries and development tools designed for building Grid-based applications according with OGSA specification. It implements most of the services specified into OGSA specific. As shown in Fig. III.3, GT components fall into five broad domain areas: Security, Data Management, Execution Management, Information Services, and Common Runtime.

III.5.1 Security

The GT4 Security components, collectively referred to as Grid Security Infrastructure (GSI), facilitate secure communications and the application of uniform policies across distinct systems.

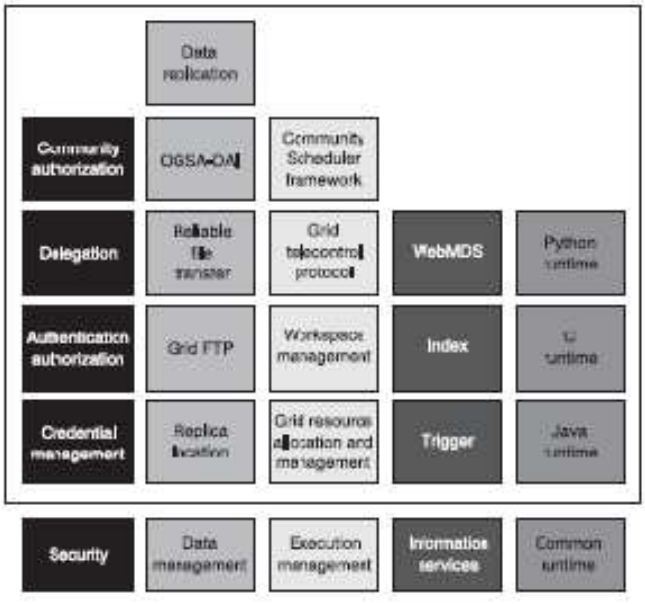

Fig. III.3 GT4 services

- ***Authentication and Authorization:*** Includes libraries and tools for controlling access to services and resources, along with a framework that enables the use of different authorization methods, including user-written methods.

- ***Delegation***: The toolkit includes a service that delegates credentials to a container.

- ***Community Authorization:*** Virtual organizations can use the Community Authorization Service (CAS) to manage authorization policies for VO resources.

- ***Credential Management:*** This component includes SimpleCA, a simple Certificate Authority for users without access to a full-blown CA, and MyProxy, an online credential repository.

III.5.2 Data Management

The Data Management components provide for the discovery, transfer and access of large data.

- ***GridFTP:*** This component includes a fully functional GridFTP server, and several client-side utilities. The GridFTP protocol is specially optimized to transfer large amounts of data between hosts.

- ***RFT:*** The Reliable File Transfer service is a WSRF-enabled service that uses GridFTP internally to move large amounts of data. It provides several interesting features over GridFTP, such as the possibility of resuming interrupted transfers.

- ***Replica Location:*** The Replica Location Service (RLS) allows users to keep track of where different replicas of a dataset are located in a virtual organization.

- ***Data Replication:*** The Data Replication Service (DRS) uses RLS and RFT to guarantee that local copies of replicas are available to the hosts that need them.

- ***OGSA-DAI:*** OGSA Data Access and Integration provides a framework to access and integrate datasets on a Grid which might be available in different formats (plain text files, databases, XML files, etc.). More details are available in the OGSA-DAI website [6].

III.5.3 Execution Management

Execution Management components deal with the deployment, scheduling and monitoring of executable programs, referred to as jobs.

- ***Grid Resource Allocation & Management (GRAM):*** GRAM is the heart of GT Execution Management, providing services to deploy and monitor jobs on a Grid.
- ***Community Scheduler Framework (CSF):*** This component provides a single interface to different resource schedulers such as PBS, Condor, LSF and SGE.
- ***Workspace Management:*** A new component in the toolkit that allows users to dynamically create and manage workspaces on remote hosts.
- ***Grid Telecontrol Protocol:*** This component provides a WSRF-enabled service interface for telecontrol (control of remote instruments).

III.5.4 Information Services

Information Services, commonly referred to as the Monitoring and Discovery System (MDS),includes a set of components to monitor and discover resources in a virtual organization..

- ***Index Service:*** This component is used to aggregate resources of interest to a VO.
- ***Trigger Service:*** Like the Index service, the Trigger service also collects data from resources, but is configured to perform certain actions based on that data.
- ***WebMDS:*** Provides a web browser-based view of data collected by GT4 aggregator services.

III.5.5 Common Runtime

The Common Runtime components provide a set of fundamental libraries and tools for hosting existing services as well as developing new services. Components other than the

- ***C Runtime:*** Includes tools, libraries and a WS hosting environment for C developers.
- ***Python Runtime:*** Includes tools, client libraries and a WS hosting environment for Python developers.
- ***Java Runtime:*** Includes tools, libraries and a service hosting environment for Java developers.

III.6 References

[III.1] T. Myer, "*Grid Computing: Conceptual Flyover for Developers*," IBM Corporation, 1133 Westchester Avenue, White Plains, New York 10604, May 2003.

[III.2] M. McCommon, "*Letter from the Grid Computing Editor: Welcome to the New developerWorks Grid Computing Resource!*" IBM Grid Computing Resource, April 7, 2003.

[III.3] M. Chetty and R. Buyya, "*Weaving Computational Grids: How Analogous Are They With Electrical Grids?*," IEEE Computing in Science and Engineering, July/August 2002.

[III.4] I. Foster and C. Kesselman, "*The Grid: Blueprint for a Future Computing Infrastructure"*, Morgan Kaufmann, 1999

[III.5] I. Foster, C. Kesselman, and S. Tuecke, "*The Anatomy of the Grid: Enabling Scalable Virtual Organizations*," International Journal of High Performance Computer Applications, 15(3), 200 (2001).

[III.6] M. Haney, "*Grid Computing: Making Inroads Into Financial Services*," IBM's Developerworks Grid Library, 24 April 2003, Issue No: Volume 4, Number 5, IBM Corporation, 1133 Westchester Avenue, White Plains, New York 10604.

[III.7] R. Buyya, "*Frequently Asked Questions, Grid Computing Info Centre*," GridComputing Magazine.

[III.8] Grid Computing Info Centre (GRID Infoware), "*Grid Computing, Answers to the Enterprise Architect Magazine Query*," Enterprise Architect Magazine.

[III.9] "*Grid Computing using .NET and WSRF.NET Tutorial*," GGF11, Honolulu, June 6, 2004.

[III.10] I. Foster, "What Is the Grid? A Three Point Checklist," *Argonne National Laboratory and University of Chicago*", 20 July 2002, Argonne National Laboratory.

[III.11] G. Fox, M. Pierce, D. Gannon, and M. Thomas, "*Overview of Grid Computing Environments*", GFD-I.9, Feb 2003.

[III.12] Grid Computing Info Centre (GRID Infoware), "*Grid Computing, Answers to the Enterprise Architect Magazine Query*," Enterprise Architect Magazine.

[III.13] Hewlett-Packard Company, "*HP Virtualization: Computing Without Boundaries or Constraints, Enabling an Adaptive Enterprise*," HP white paper, 2002, Hewlett-Packard Company, 3000 Hanover Street, Palo Alto.

[III.14] M. Smetanikov, "*HP Virtualization a Step Toward Planetary Network*," Web Host Industry Review (theWHIR.com) April 2003, Toronto, Ontario, Canada.

[III.15] Web site: http://www.apgrid.org.

[III.16] Web site: http://eu-datagrid.web.cern.ch/eu-datagrid.

[III.17] Web site: http://www.griphyn.org.

[III.18] Web site: http://www.ppdg.net.

[III.19] Dennis Gannon, Kenneth Chiu, Madhusudhan Govindaraju, and Aleksander Slominski, "*An Analysis of the Open Grid Services Architecture"* Department of Computer Science, Indiana University, Bloomington, IN.

[III.20] M. Paolucci, N. Srinivasan, and K. Sycara, "*OWL Ontology of Web Service Architecture Concepts*", October 2004

[III.21] M. Gudgin, M. Hadley, N. Mendelsohn, J-J. Moreau, and H. Nielsen, *SOAP Version 1.2 Part 1: Messaging Framework*, W3C Recommendation, 24 June 2003.

[III.22] T. Berners-Lee, R. Fielding, L. Masinter, Uniform Resource Identifiers (URI): Generic Syntax, IETF RFC 2396, August 1998.

[III.23] Ian Foster, Carl Kesselman, Jeffrey Nick, and Steven Tuecke, "*The Physiology of the Grid: An Open Grid Services Architecture for Distributed Systems Integration,*" Globus Project, 2002.

[III.24] Dennis Gannon, Kenneth Chiu, Madhusudhan Govindaraju, and Aleksander Slominski, "*An Analysis of the Open Grid Services Architecture,*" Department of Computer Science, Indiana University, Bloomington, IN.

[III.25] Web site: OASIS. http://www.oasis-open.org.

[III.26] Ian Foster, Jeffrey Frey, Steve Graham, Steve Tuecke, Karl Czajkowski, Don Ferguson, Frank Leymann, Martin Nally, Igor Sedukhin, David Snelling, Tony Storey, William Vambenepe, Sanjiva Weerawarana, "*Modeling Stateful Resources with Web Services*", May 2004.

[III.27] B. Sotomayor, L. Childers, "Globus Toolkit 4: Programming java services", Morgan. Kaufmann, 2005, ISBN: 13: 978-0-12-369404-1.

Chapter IV

Proposed GRID Services

IV.1 Introduction

Measurement methods proposed in chapter II have shown satisfying good performance in different operating conditions. At the same time, they suffer from the high computation burden due to the manifold factors, such as processing complexity, number of points to elaborate, and frequencies band to be analyzed. Consequently, high processing times are experienced for fulfilling whole measurement procedures. The development of these methods on GRID architecture, according to GRID Services paradigm, allows to overcome these limitations reducing the processing times. Differently from the current GRID architecture, a new architecture has to be developed in order to allow the interaction between the GRID Services and measurement instrumentation involved during the elaboration. To this aim, innovative strategy is described to make easier the integration of measurement instrumentation with other elements of the GRID environment.

SpeedUp ratio measurements are carried out for both methods to show the advantages provided by the GRID Services with respect to a sequential implementation of the methods. Finally, a brief description of web portal, implemented for taking advantage form services, is provided.

IV.2 Instrumentation GRID

From the point of view of the GRID architecture, measurement instrument could be considered as a resources, which provides one or more services. Nevertheless, suitable operation, such as registration, locating and interacting with instrument require specific mechanisms differently from those adopted for interacting with computational nodes. To allow a proper integration of measurement instruments within GRID environment some elements of the GRID architecture must be revised and integrated:

- ***Resource availability***. The resource availability is one of the key elements of the grid idea. Commonly a consumer makes a resource request on the basis of one or more resource properties. For example, a client may look for an instrument that is able of detecting o generating a particular signal. The ability of a resource to describe what capability, capacity, quality and configuration it is able to offer and under what terms, is in charge of the information protocols. The *information protocols* are necessary also to clients in order to describe the desired resource capabilities and the way they will be used. To integrate an instrument in the resource description framework of the grid architecture, we need to extend the computational resource description with the peculiar attribute metrics of an instrument.

- ***Accessibility and usability***. Once we are able to find and successfully authenticate the desired resource, we have to be able of using it, that is, capable of properly setting the instrument in relation to available functionalities.

- ***Collaboration***. Collaboration with other processing nodes, present within the GRID environment must be death with. In fact, once that the data have been acquired through the measurement instrument, they must be conveyed into GRID for elaboration in parallel way.
  Moreover, it is worth noting that, additional problems, no strictly associated with the instrumentation GRID, but that assume much relevance in presence of instruments, must be solved;

- ***Data storage and transmission.*** The main problem with data storage is that some experiments produces huge amount of data. This is not a problem for a single experiment; however when making serial of such experiments per day, space requirements outgrow usual storage capabilities. The solution could be a combination of two things: firstly, reduce the data to a reasonable amount by means of data reduction, compression or preliminary analysis; secondly, distribute the data among several grid nodes and take precaution that the data can be easily retrieved. Nevertheless, the data amount must be transferred to the grid nodes for

processing, and further problems, such as packet loss, jitter, network latency, and available bandwidth can influence the final performance. Quality of Services mechanism can be applied for overcoming the above drawbacks.

- ***GRID authentication and authorization protocols***. The actual mechanism can be successfully used to map the grid user to the instrument user. The grid Security Infrastructure authentication protocol can be successfully used to authenticate the connections with instruments. However, authorization is often more sophisticated and fine-grained control can be provided over access on Instruments. Overall, a wide range of authorization constraints may be encountered in Instrument control systems.

Few GRID architectures have been developed and proposed in literature to meet the aforementioned requirements, and some of them either introduce additional elements or modify those already present in OGSA. As an example, Grid-enabled Remote Instrumentation with Distributed Control and Computation (GRIDCC), is described along with the main elements involved into proposed GRID architecture.

IV.2.1 GRIDCC (Grid-enabled Remote Instrumentation with Distributed Control and Computation)

Principal components of GRIDCC architecture [IV.1] are depicted in Fig IV.1. We summarize its main elements in the following.

The virtual control room (VCR) is the user interface of a GRIDCC application. Through the VCR users can either monitor and control instruments in real time or submit workflows to the execution

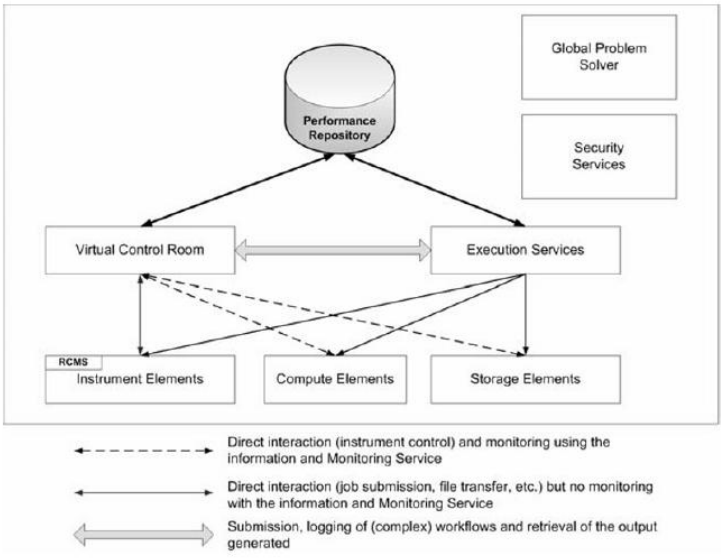

Fig. IV.1 The GRIDCC architecture

services (ES). The VCR has been implemented with a grid portal technology in order to communicate with the underlying grid infrastructure.

The execution services consist of:

- workflow management system (WfMS): service that provides the capability of executing more tasks in sequential order. This is useful when the user has to work with more than one instrument, submitting a job to each one.
- workload management system (WMS), for logging, bookkeeping and service discovery.
- Agreement service (AS) for reservation management.

Through the VCR, the user can define the workflows that must be executed by the ES. Moreover, the ES controls the quality of service, by making resource reservation agreements with the available resources (instrument elements, compute elements or storage elements).

GRIDCC provides two levels of automated problem solving: local problem solver (LPS) and global problem solver (GPS). The former, implemented locally to a given instrument element (IE), works in order to solve malfunctions of the IE in which it is embedded; the latter solves problems related to the whole system, and it is embedded within knowledge-based services. Security services are designed to guarantee security in terms of authentication, authorization and accounting. GRIDCC uses an all-pervasive information and monitoring system (IMS): the run control and monitoring system (RCMS). The performance of this service is critical to the successful operation of the instruments within the GRIDCC architecture. RCMS works on a publish–subscribe model, by passing information to the different components, as they require it. The RCMS also passes information between the different services that make up the IE.

IV.2.1.A The Instrument Element

The term instrument element describes a set of services, which provide the needed interface and implementation that enables the remote control and monitoring of physical instruments. In this context, the IE is a web service interface to monitor and control real instruments. Users view the IE as a set of web services. Web services provide a common language to the cross-domain collaboration and, at the same time, they hide the internal implementation details of accessing specific instruments. That being so, the communications of external entities with the IEs are based on web services standards: WSDL (web services description language) files for describing the services, the information services for discovery and standards for describing workflows (e.g., BPEL4WS), agreements (WS-Agreement), etc. This of course leads to the requirement that the IEs themselves and all the supporting services, like ES

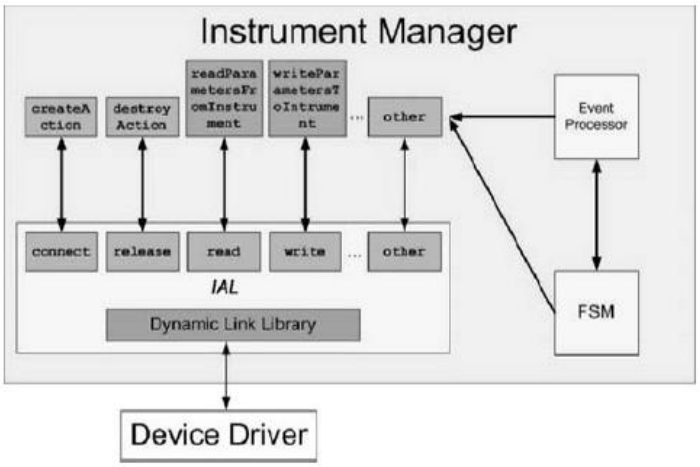

Fig. IV.2 Instrument Manager scheme

and GPS, follow these specifications. On the other hand, the communication between the IEs and the corresponding instruments depends on the installation and can be handled by any network protocol or even by a physical connection, different from one instrument to another.

IV.2.1.B Instrument Managers

An instrument manager (IM, Fig. IV.2) identifies the parts of the instrument element that perform the actual communication with the instruments. IMs act as protocol adapters that implement the instrument-specific protocols for accessing its functions and reading its status. Since the instruments are heterogeneous in nature, there is a need to support many instrument managers in the same container, one instance for each logical set of instruments. Each IM is composed of three subcomponents: the command gateway, the monitor manager and the data mover:

- the command gateway accepts control requests from the virtual instrument grid service and forwards them to the instrument;
- the monitor manager is responsible for collecting monitoring data (status, errors, etc.) and providing it to the information and monitoring service in a common format;
- the data collector component gathers the flow of data (if any) from the instruments; it then passes it to the Data Mover, which provides the interface with any external storage or processing elements;
- the finite state machine reflects the collective state of instruments controlled by the instrument manager; it receives the status from the individual instruments asynchronously and updates its state accordingly.

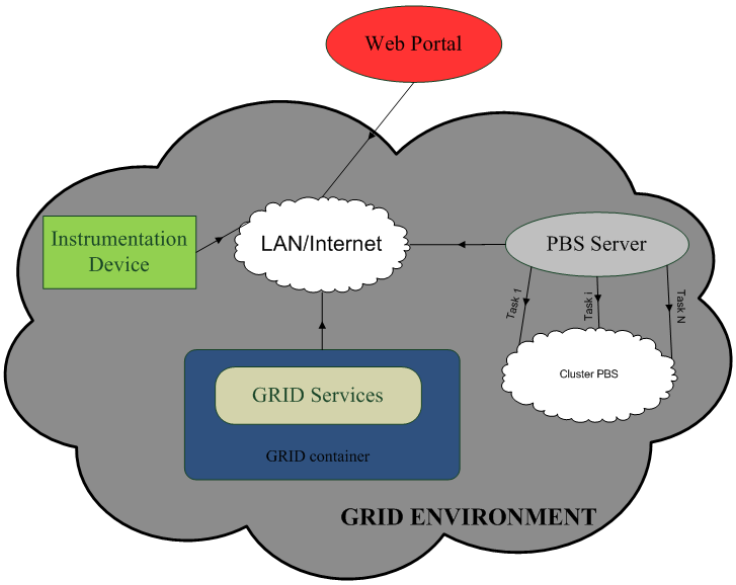

Fig. IV.3 Proposed GRID architecture

If a need for transferring instruments from one instrument element to another arises, then it is sufficient to remove the instrument manager instance from the instrument element and instantiate a new one on the other instrument element. The other services react to this action accordingly. Generally, each instrument manager is collaborating locally with the interfacing services, to translate external requests for control or monitoring into requests that the instruments understand and can react to.

IV.2.2 Proposed GRID architecture

The proposed architecture for integrating the measurement instruments in GRID environment is sketched in Fig. IV.3.

The web portal (WP) is the user-end interface for accessing to GRID Services and resources, such as instrumentation devices (ID) and computational nodes, involved into GRID environment. Through the WP, users can:

- access to GRID Services without taking on the onerous stages defining from OGSA into GSI, but only through a *login* and *logout* procedures;
- select and submit a GRID Service;
- monitoring the state of submitted GRID Service;
- interact with the instrumentation devices (ID) involving into submitted GRID Service.

WP implements the *workflow management service* (WFMS) that allows to drive the submitted measurement procedure along all processing stages: interaction with ID, jobs submission, and results presentation.

To this aim, WP is developed according to grid portal technology for simplifying the integration with the underlying OGSA services, such as GRAM and MDS. The GT4 toolkit has been used for GRID Services implementation.

WP makes use of PBS scheduler for both discovering the presence of suitable ID's, involved into submitted GRID Service, and checking their availability. If one ID is available, the PBS provides to WFMS the information about its URL, otherwise a message of *unavailability* is given back before submitting the GRID Service. URL identifies the Web Service, hosted on ID, through which the user can interact with the instrumentation through the WP. In this way, instruments, characterized by different connection standards, such as RS-232, IEEE 488, and IEEE 802.3, and managed by heterogeneous programming language, like LabVieW, Matlab, and Java, can be transparently added to the GRID. More details about ID and PBS functionalities are provided below.

IV.2.2.A Instrumentation device (ID)

Instrumentation device (Fig. IV.4) stands for a new element of GRID environment. It is composed from a couple of elements, i.e. workstation and measurement instrument (MI). The interaction between workstation and MI can be realized by means of any connection type, depending on the instrument features.

The workstation plays the role of both computational node and interface between the GRID environment and the MI. It generally acts as a computational node, thus waiting for jobs execution through the *pbs_mom*, and, when required, it provides a front-end to set the MI. To this aim, the workstation hosts two software components: instrument Web Service and control driver. The former is developed according to classic Web Service paradigm [IV.2], and it realizes the network front-end

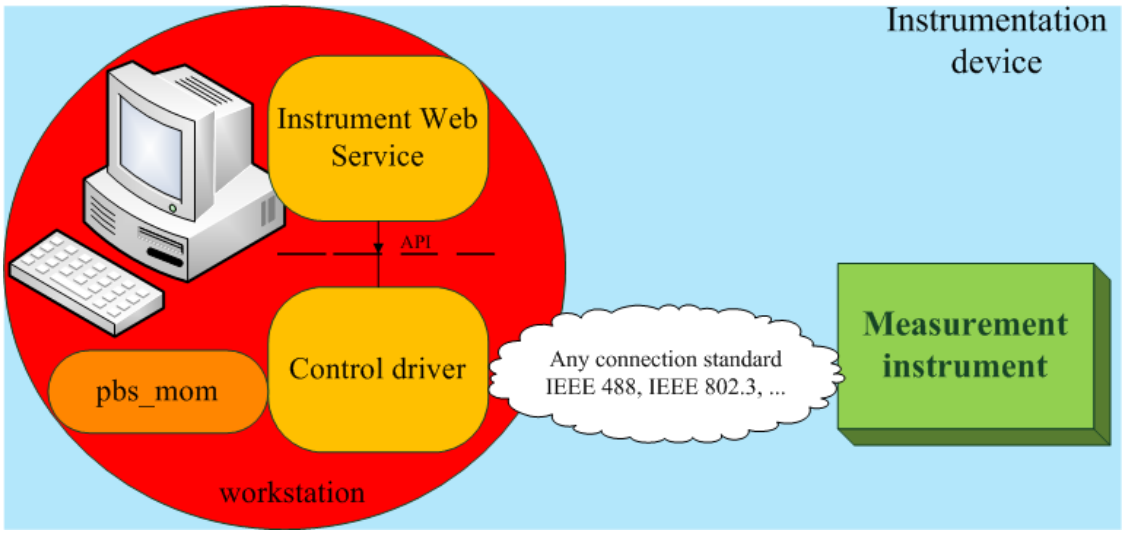

Fig. IV.4 Instrumentation device architecture

between the GRID environment and instrument. The latter, instead, allows to control the instrument functionalities and provides suitable API to be invoked by instrument Web Service. Thanks to that, every incoming request to the instrument Web Service is mapped into a proper control driver API that performs the invocation towards the instrument. It is worth evidencing that this strategy lets to:

- obtain independence from both programming language exploited for instrument control and connection typology; any languages and standards can be utilized;
- separate the instrumentation control from network access tier;
- gain in flexibility when a new instrument has to be added; only the instrumentation Web Service and the driver control must be developed.

IV.2.2.B PBS scheduler

PBS is resource management software, and was developed by NASA to conform to the Portable Operating System Interface for Unix (POSIX) Batch environment standards. PBS allows to perform the following operations:

- accept batch jobs;
- control their attributes;
- preserve and protect the jobs until run;
- deliver jobs output back to the caller.

The four major components in PBS are:

Client side commands are used to submit, control, monitor, or delete jobs and can be installed in any supported platform.

Server (pbs_server) provides the main entry point for batch services such as creating, modifying, and protecting jobs against system crashes. All the clients and other daemons communicate with this server over TCP/IP.

Scheduler (pbs_sched) controls the policies or set of rules used to submit jobs over the network. PBS was designed to allow each cluster to create its own scheduler or policies. When started, the scheduler operates with the server for jobs to be run and the executor for system resource availability.

Job Executor (pbs_mom) is in charge of executing the job by emulating user sessions identical to the user's login session. It delivers the output back to the caller when directed.

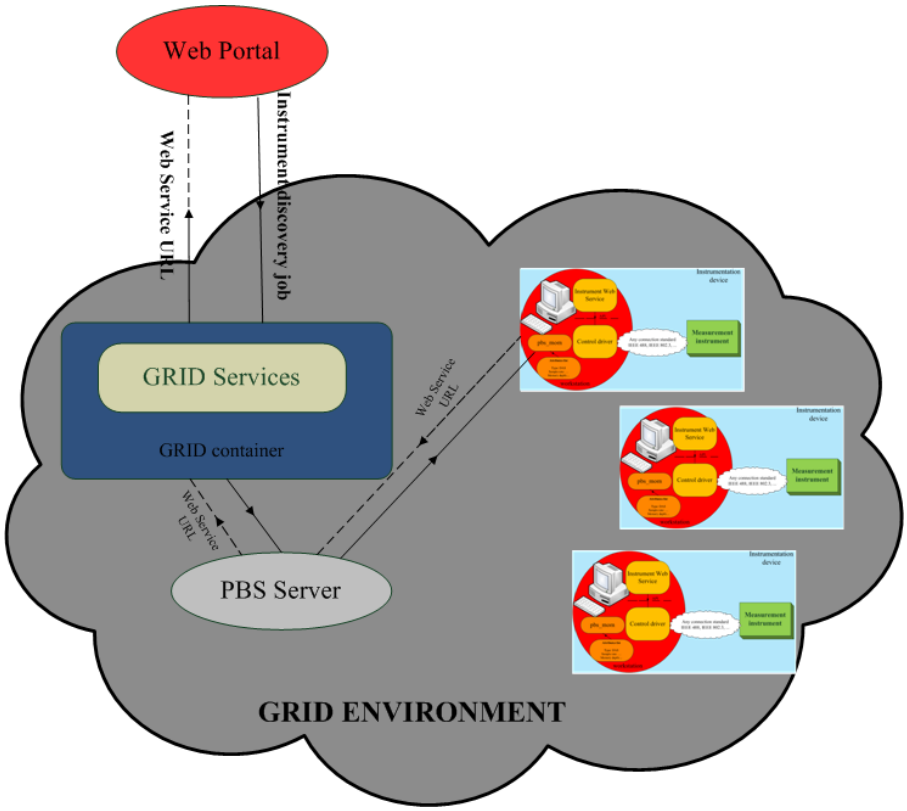

Fig. IV.5 Example of interaction between WP and instrumentation device

As for the control attributes, they describe, at the client side (i.e. computational node) the capabilities of the node, such as number of CPU, hard disk and RAM memory available, while at server side the capabilities required to computational nodes for taking in charge the jobs execution. At both sides, these capabilities can be customized and in each node proper attributes can be added. Taking advantage from this mechanism, it is possible insert in each ID node, suitable attributes that describe:

- *instrument type*, i.e. digital acquisition system (DAS), digital generator (DG) or counter (C);
- *capabilities* (referred as vector capabilities), such as maximum sample rate, memory depth, input band pass, maximum generation frequency, and so on;
- *availability*, a boolean value that describes if the instrument is busy or available;
- *URL* associated with the Web Service hosted on ID.

In this way, when an instrument is required during the execution of GRID Service, the WFMS calls the PBS server submitting a *instrument discovery job* (Fig. IV.5) with input parameters: instrument type and capabilities vector. If *pbs_server* finds an ID available (i.e. with availability attribute equal to true) that matches the input parameters. It sets the availability attribute to false and gives back its URL attribute, which allows to univocally identify the instrument into GRID environment; otherwise the *unavailable* string is given back and a *hibernate procedure* starts. The hibernate procedure saves the state of all GRID

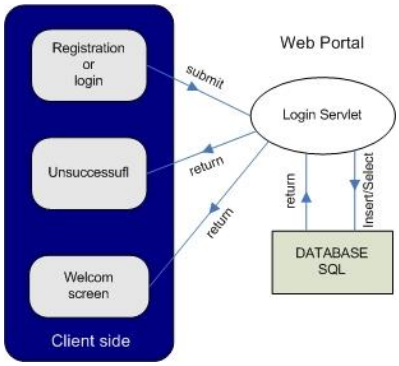

Fig. IV.6 Web page generated for login mechanism

Service resources, and in cyclic way checks the availability of instrument. When the instrument turns into availability state, it is immediately reserved and the procedure of GRID Service restarts.

IV.2.2.C Web Portal

The middleware GT4 does not provide any service or tool to generate a WP for accessing the GRID Services. To overcome this lack, the WP has been implemented as java servlet integrated in a java server page (JSP); the JSP is a multiple platform solution to create dynamic HTML web page at server side using the java language. The obtained Web page are, finally, run in Tomcat Web Services Container (WSC). To allow the interaction between the WP and the GRID environment, an instance of GT4 is installed on the machine that hosts the WP.

The main functionalities required to access GRID Services through WP, i.e. registration or login mechanisms and GRID service selection and submission, are provided by two different servlet, referred respectively to as login and application servlet. This latter implements also WFMS functionality, which allows to fulfill all stages of submitted GRID services, among which the interaction with ID.

IV.2.2.C.i Registration or login mechanism

An access procedure is realized to protect and control the hardware and software resources involved into the GRID infrastructure. When the client connects to the WP through a standard HTTP connection, the principal access page is presented. Two options are provided to the client:

1. If the client accesses to the WP for the first time, he has to register in the database of authenticated and admitted client. To this aim, the client must complete a registration form with typical data useful to his identification and authentication (such as name, e-mail address, phone number and so on) and submits the form to a login servlet. The servlet inserts the received data in a registration-table of SQL database, calculates the user ID and password and returns them to the client for successive accesses (Fig. IV.6).
2. If the client is already present in the SQL database, he can access to the implemented GRID Services through user ID and the password previously obtained. The login servlet compare

this data with those contained in the registration table of SQL database. If a complete matching occurs, the client in provided with a welcome page, otherwise, an unsuccessful login screen is given and the access to GRID Services is forbidden. An example of the implemented web page for login is given in Fig. IV. 7.

IV.2.2.C.ii Selection and submission of GRID Service

Once the client is logged into the WP, he can select a GRID Service from those available on welcome page and submit its execution into the GRID infrastructure. As stated above, the client cannot directly require the service submission, since he does not possess on his own terminal the required certificates.

His submission request is thus redirected to the WP application servlet that executes the actual service submission encapsulating the client selection within a new request carried out by an account authenticated and certified in GRID infrastructure. Moreover, the implementation of the application servlet on Tomcat WSC allows multiple submission requests, sent from different clients, to be effortlessly managed, thus granting multithread services execution. Each GRID Service thread is invocated according to the software design pattern, referred to as factory/instance pattern [IV.2],[IV.3], recommended by WSRF (Web Service Resource Framework).

The invocation has been, in particular, split into two main parts mandated respectively to service initialization and execution. With regard to the first part, it accounts for the initialization of GRID Service resources; for all implemented services, the associated resources are measurement_result (i.e. the result obtained from the measurement), and address_ip (i.e. the ip address of the client that has

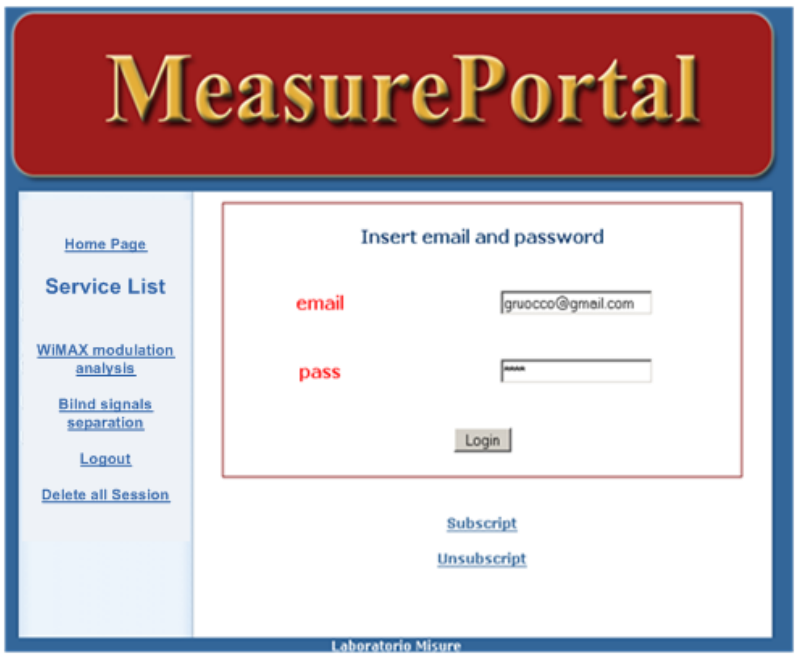

Fig. IV.7 Registration and login mechanism

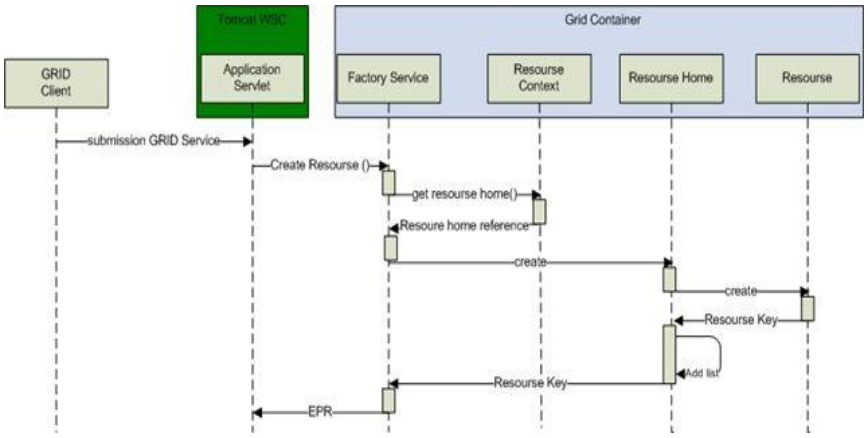

Fig. IV.8 GRID Services initialization according to factory/instance pattern

required the GRID Service). The initialization is carried out through three java classes, referred to as Factory Service, Resource Home and Resource, that interacts to one another as shown in Fig IV.8. In particular, to create new resources, application servlet invokes the createResource method on Factory Service, the location of which is known by means of the associated URI (universal reference identifier). This operation can be accomplished only executing the create method on Resource Home, i.e. the class mandated to manage all the needed resources. To make Factory Service capable of invoking the desired method, Resource Home reference must be obtained by means of a GRID helper class referred to as ResourceContext. Once the Resource Home reference has been achieved, Factory Service can invoke the create method on Resource class, that create the instance of required resource returns an object of type ResourceKey, i.e. a resource identifier (Fig. IV.8). Created resources and associated object are finally added in an internal list of Resource Home; the list allows client to access any available resource though the corresponding identifier. The obtained object along with the URI of the GRID Service is the service End Point Reference (EPR).

Thanks to the obtained EPR, the application servlet can now invoke the methods of the desired GRID Service, i.e. data method and measurement method. The former method manages the whole measurement procedure (WFMS), from data generation and data acquisition to results evaluation. To this aim, the instrument discovery job is invoked, as above described, for looking for the suitable ID. Once that this stage is accomplished, a new jsp page appears to the client, which provides proper fields that allows to modify typical parameters of the adopted instrumentation. It is worth noting that fields are initially completed with default values in order to allow also inexperienced clients to correctly exploit the selected GRID Service.

According to the specific required GRID Service, data method invokes the measurement method necessary to gain the desired measurement results. To this purpose, measurement method distributes the processing stage in parallel tasks that are handled through PBS scheduler. More specifically, the PBS

[2] collects the tasks in a proper queue managed according to a first in first out strategy and schedules their parallel execution on the available processing nodes (cluster PBS). The PBS scheduler uses two files, referred respectively to as prologue and epilogue files, in order to allow all processing nodes to share acquired data among themselves. The former file is used to transfer and store the input signal samples on a processing node, while the latter sends the data resulting from the processing stage to the application servlet that updates the resource measurement_result and delivers its value to the client. The presentation stage is in charge of the WP, which stores the results in a particular record in order to provide them to the client, when they are required.

IV.3 Developed GRID environment

GRID environment has been developed according to the proposed GRID architecture and it includes:

- an ID that includes the LeCroy® data acquisition system, namely SDA 6000A, characterized by a maximum sample rate equal to 20 GS/s, 6 GHz of channel bandwidth, 100 MSample memory depth, and 8 bit of vertical resolution. IEEE 802.3 standard and Matlab are exploited as connection standard and programming language for developing the control driver, respectively;
- an ID that includes the Agilent® digital generator, namely ESG 4438C, characterized by 250 kHz-6 GHz output frequency range. IEEE 802.3 standard and Matlab® are exploited as connection standard and programming language for developing the control driver, respectively;
- five heterogeneous processing nodes, three of which are characterized by processor Intel 2 Core 2.6 GHz and 2 GB of RAM, and the others from mono processor Athlon 64 AMD with 1 GB of RAM.

All GRID environment components are interconnected through 100 Mb/s Ethernet links by a star configuration (Fig. IV.9).

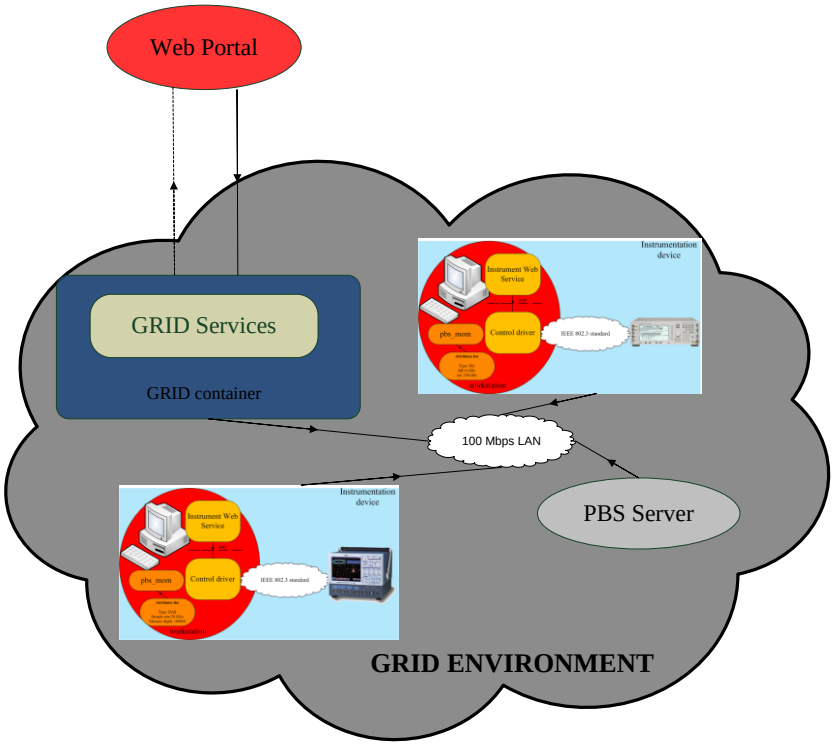

Fig. IV.9 Developed GRID environment

IV.4 GRID Services

Measurement methods, in detail described in Chapter II, have been developed according to the GRID Service paradigm, taking advantage from the proposed GRID architecture. For the sake of clarity, methods for WiMAX signals quality modulation assessment and blind signals separation will be hereinafter referred as *I GRID Service* and *II GRID Service*, respectively. Particular attention is paid on the description of both stages that are executed in parallel way and obtained results in terms of processing times.

IV.4.1 I GRID Service

The operating stages of *I GRID Service* are depicted in Fig. IV.10. The stages, characterized by high elaboration and parallelism property, are divided into multiple jobs to be executed in parallel way. In this way, the computational burden, due to elaboration of long data record can be notably reduced. Demodulation, subframe classification, timing recovery, and phase offset compensation match the above features.

RF WiMAX signal, $s(nT)$, is divided into *NB* blocks (Fig. IV.10), each of which expressed as:

$$s(n_iT) = I_i'(n_iT) * \cos(2\pi(f_0 + \Delta f)n_iT + \varphi) + Q_i'(n_iT) * \sin(2\pi(f_0 + \Delta f)n_iT + \varphi) \quad \text{(IV-1)}$$

where, n_i belongs to the range from Ni up to $N(i+1)-1$, and i runs in the interval $[0, \dots, NB-1]$.

The number of blocks, *NB*, is a configuration parameter and has to be *a-priori* selected, while N value is calculated according to the expression (IV-2)

$$N = floor\left(\frac{L_{tot}}{NB}\right) \quad \text{(IV-2)}$$

L_{tot} indicates the whole length of $s(nT)$. Successively, demodulation scheme, described in Section II.2 is applied on each block for gaining $I_i^{'}$ and $Q_i^{'}$ components. It is worth noting, that the elaboration of each block is independent from one another and hence can be executed in parallel way on different computational nodes. Only the order of blocks has to be hold, in order to allow a correct reconstruction of the $I^{'}$ and $Q^{'}$ components. Attention has to be also made when the $I^{'}$ and $Q^{'}$ are reconstructed at the end of the whole demodulation stage. In fact, the convolution process between i-*th* block and LPF gives rise to a output signal longer than original one, i.e. equal to *N*+*K*, where *K* stands for the LPF length. If the components are reconstruct arranging the $I_i^{'}(n_iT)$ and $Q_i^{'}(n_iT)$ back to back, their length will be greater than L_{tot} and equal to $L_{tot} + NB(K-1)$. To overcome this drawback, a suitable procedure is applied. In particular, the $K-1$ samples at the end of the i-*th* block are added to the $K-1$ samples at the beginning of the next block. In this way, the final length of $I^{'}$ and $Q^{'}$ components will be always equal to L_{tot}, and performance in concurrence with those provide by classic I/Q demodulation scheme are achieved.

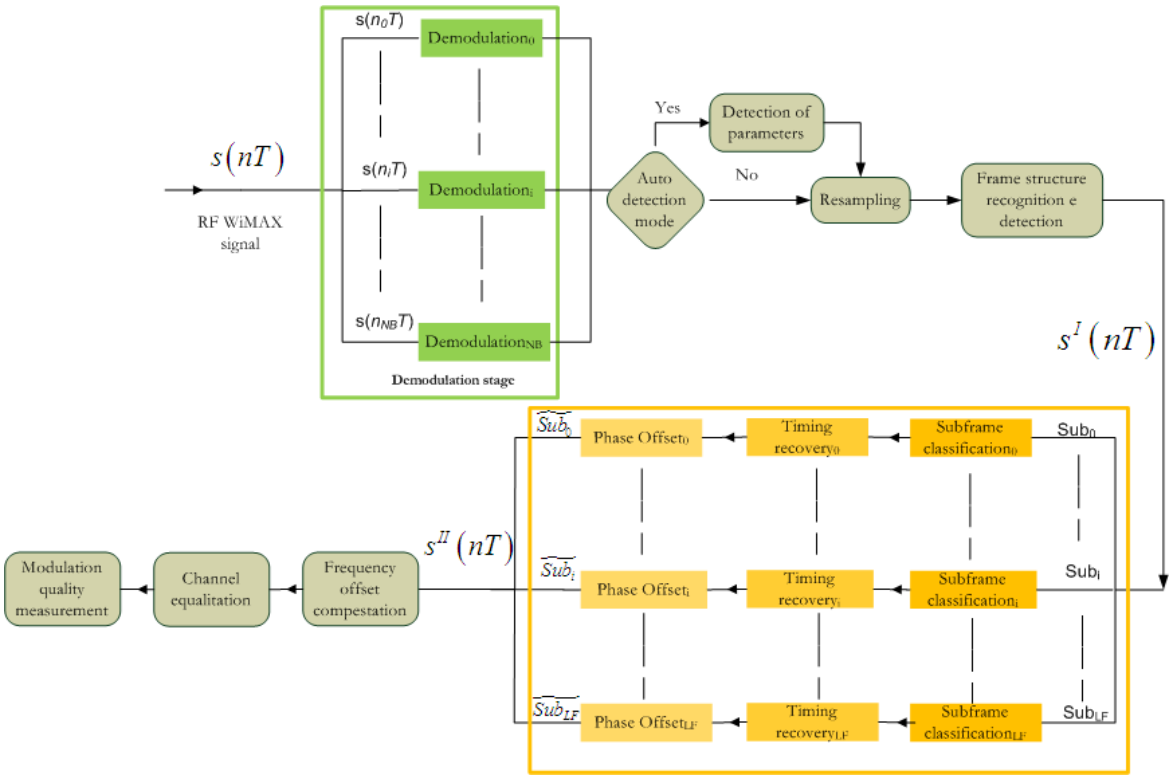

Fig. IV.10 Block diagram of IGRID Service

Once the demodulation stage is fulfilled, the successive stages are executed in sequential mode until the end of the frame structure detection stage. At this point, the number of subframes (LF) involved into acquired signal is detected and their positions also located. This way, it is possible to extract each subframe, the referred to as Sub_i, from the whole signal and executing on each subframe the classification stage, timing recovery stage, and finally phase offset compensation stage in parallel way in order to reduce the computation burden. Elaboration of each subframe is spread on GRID computational nodes, which, take in charge the subframe data, apply the procedures described in Section II.2.2, and finally give back the processed subframe $\widetilde{Sub_i}$. When all subframe are processed, the output signal $s^{II}(nT)$ is reconstructed arranging back-to-back the $\widetilde{Sub_i}$ subframes. The final stages, such as carrier frequency compensation, channel equalization, and modulation quality measurement are accomplished making use of the signal $s^{II}(nT)$.

IV.4.2 II GRID Service

The *II GRID Service* implements the measurement procedure described in Section II.3, making use of GRID Service paradigm in order to reduce the computational burden. Section II.4.F shows that the elaboration time suddenly increases when a wide analysis range has to be analyzed. Due to the characteristics of proposed method, some stages can be spread in parallel way on several computational nodes thus gaining a reduction of whole processing time

These stages have experienced high processing times and can be executed in parallel way have been implemented by multiple jobs. To this aim, FFT evaluation, eigenvalue decomposition stage, and DOA's estimation are properly carried out by multiple jobs elaborating on different computational nodes.

Each signal, $r_i(t)$, received through the m sensors of ULA array is suitable digitized and the samples are forwarded towards a computational nodes. Each node first acquires the samples, and after performs the following operations (Fig. IV.11):

- separation into K snapshots of input samples, each of which referred as $r_{ij}(t)$, where i runs in the range 1,…, m and j from 0 up to K-1;
- evaluation of FFT of each snapshot ($R_{ij}(f_l)$).

At the end, the **R(f)** matrix is composed arranging the FFT's samples of each snapshot along matrix rows (Fig. IV.11), according to the expression (IV-3).

$$R(f_l) = \begin{pmatrix} R_{10}(f_l) & \dots & R_{1K}(f_l) \\ \vdots & \ddots & \vdots \\ R_{m0}(f_l) & \dots & R_{mK}(f_l) \end{pmatrix} \quad \text{(IV-3)}$$

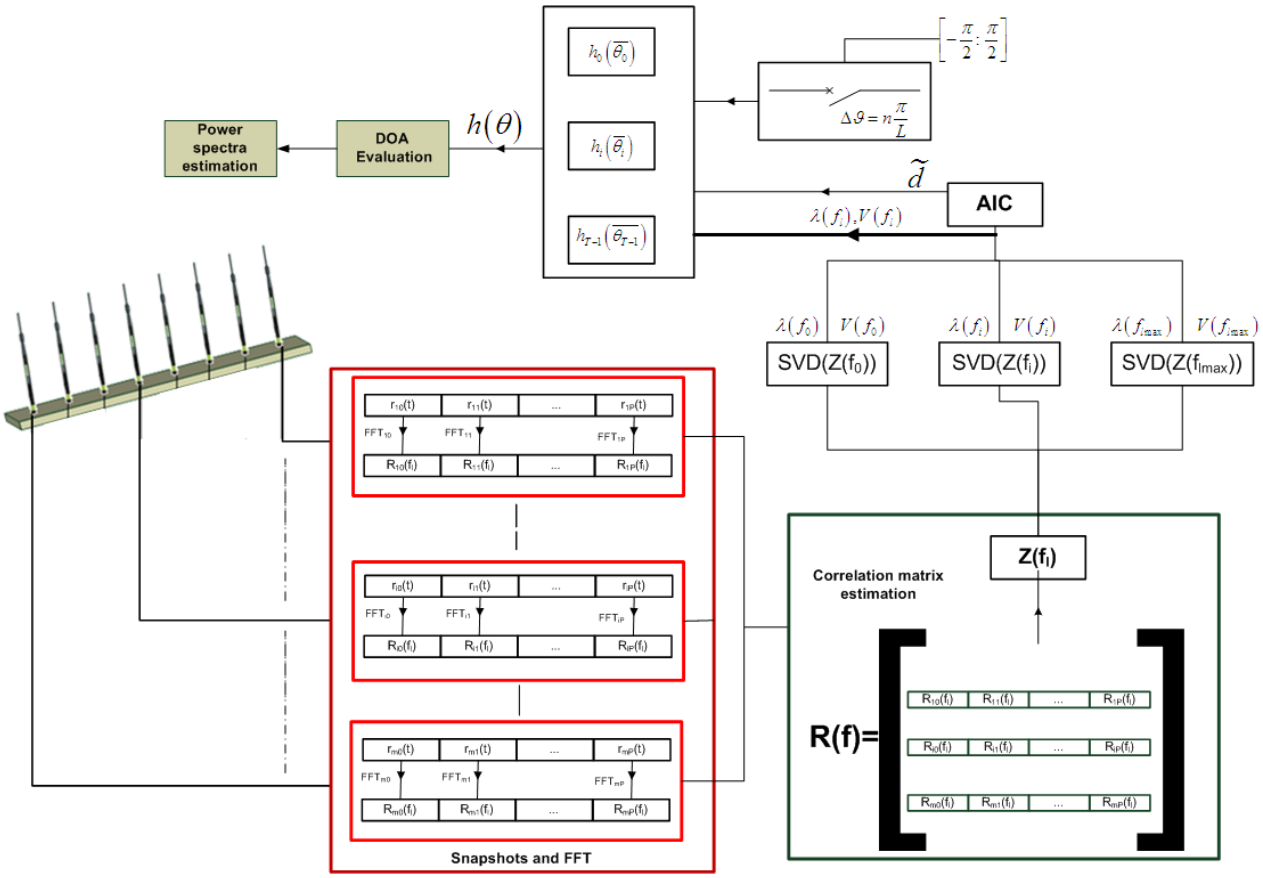

Fig. IV.11 Block diagram of IIGRID Service

Afterwards, covariance matrix $\mathbf{Z(f_l)}$ is straightforwardly evaluated, for each frequency, by means of the expression II-18. The eigenvalues decomposition on $\mathbf{Z(f_l)}$ is executed in parallel way to estimate the number of signals involved into analysis. Each SVD($\mathbf{Z(f_k)}$)) is fed to a computational node providing in output the matrices couple $\boldsymbol{\lambda}(f_k)$, $\mathbf{V}(f_k)$. It is worth noting that, several SVD could be executed on each computational node when any frequencies must be analyzed reducing data file transfer time and, consequently, whole elaboration time. Once all SVD are accomplished, AIC algorithm is executed for evaluating the $\tilde{d}$ number of signals.

The DOA of each signal is successively estimating by means of a suitable procedure, which lets to calculate the pseudo-spectrum in parallel way. First of all, the angles range from $-\pi/2$ up to $\pi/2$ is discretized with step $\Delta\vartheta$, referred as angular resolution and expressed by equation (IV-4).

$$\Delta\vartheta = \frac{\pi}{L} \qquad \text{(IV-4).}$$

L+1 angles are gathered in T vectors, each of which containing A consecutive angular values and expressed by following relation:

$$\bar{\theta}_l = \left[\vartheta_{lA} : \vartheta_{A(l+1)-1}\right] \qquad \text{(IV-5),}$$

where l runs from 0 up to T-1. Each vector is successively forwarded to a computational node to evaluate the equation II.25 and to calculate a piece of the pseudo-spectrum. Arranging back-to-back the output of each node, the whole pseudo-spectrum is constructed and the research of $\tilde{d}$ peaks is accomplished in sequential mode, along with the power spectrum estimation and the measurements of main frequency domain metrics, such as channel power, channel bandwidth and carrier frequency.

IV.5 SpeedUp

In GRID computing, SpeedUp (SU) ratio refers to how much a algorithm, implemented in parallel way, is faster than a corresponding sequential algorithm, i.e. developed by a monolithic approach. SpeedUp is defined by the following expression:

$$SpeedUp = \frac{T_{SP}}{T_{PW}} \quad \text{(IV-6)},$$

where:

- T_{SP} stands for sequential algorithm processing time;
- T_{PW} is the processing time evaluated through parallel algorithm.

SpeedUp provides information about the effectiveness of the parallel algorithm implementation with respect to a sequential one. Higher is the SpeedUp ratio, greater is the reduction of processing time obtained by means of parallel implementation.

IV.5.1 SpeedUp: I GRID Service

I GRID Service SpeedUp ratio is calculated for two acquisition record lengths equal to 50 and 100 MSample, respectively. Different number of blocks, i.e. *NB* equal to {25, 50, 100}, are accounted for each acquisition record length. In particular, *NB* equal to 25 and 50 are utilized with acquisition

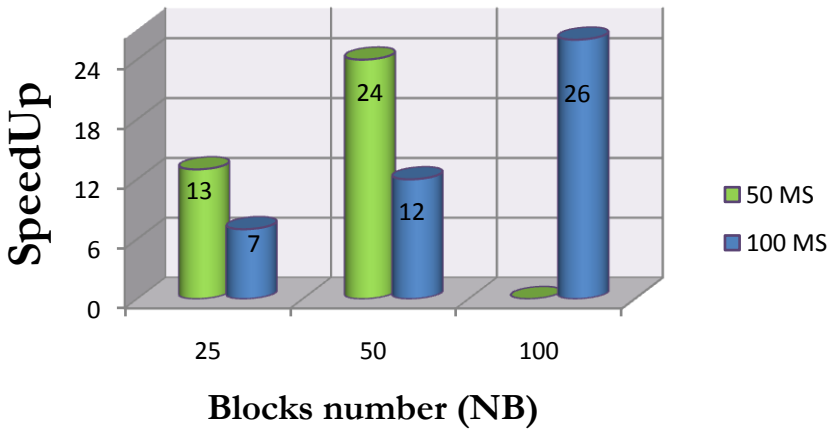

Fig. IV.12 SpeedUp versus NB for acquisition record lengths equal respectively to 50 (green) and 100 (blue) MSample.

record length of 50 MSample, while all *NB* available are exploited with acquisition record length equal to 100 MSample. Fig. IV.12 shows the obtained SU versus NB for both acquisition record lengths; green and blue cylinders stand for acquisition record lengths equal respectively to 50 and 100 MSample. Thanks to the obtained results, the following consideration can be drawn:

- method implementation, as GRID Service, allows to analyze acquisition record lengths greater than 50 MSample, which provide memory overflow issue by means of sequential execution;
- SU of 26 is obtained with NB=100 and acquisition record length equal to 100 Msample; that is, a reduction of 26 times is assessed, decreasing the processing time from 600 s, corresponding to execution of sequential algorithm, to 23 s in the case of parallel implementation;
- almost linear growth versus NB is experienced for both acquisition record lengths. In fact, increasing NB, several demodulation jobs are executed in parallel way, but each one of them elaborates a smaller number of points, which are faster to be both transferred among computational nodes and managed by memory for next elaborations.

IV.5.2 SpeedUp: II GRID Service

SpeedUp values are calculated as regards to *II GRID Service* taking only into account the critical operating conditions evidenced through the analysis carried out in Section II.3.5. In particular, analysis bands from 57 up to 82 MHz are analyzed, and for each frequency bin the SVD evaluation is executed in parallel way. Fig. IV.12 plots the SU versus analysis band for ULA array characterized by 6 (blue

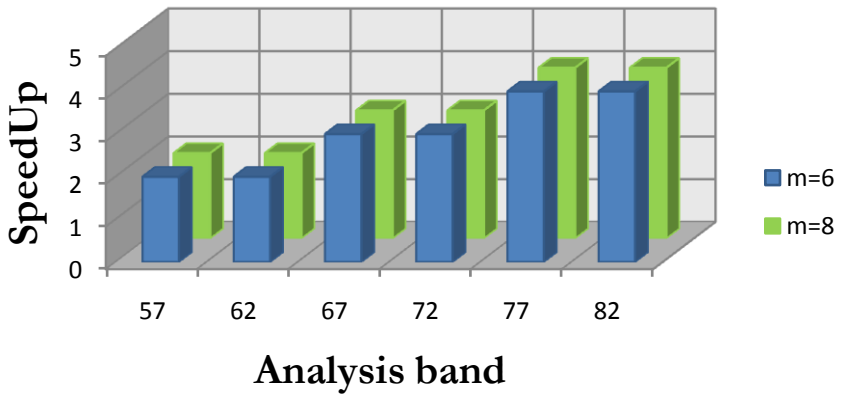

Fig. IV.13 SpeedUp versus analysis band for ULA array characterized by m=6 (blue blocks) and m=8 (green blocks) antennas.

blocks) and 8 (green blocks) antennas. It is worth highlighting that:

- the same SpeedUp is provided independently from the number of antennas involved into ULA array configurations. This result concurs with those already obtained in Section II.3.5;
- a non linear increase of SpeedUp versus analysis band is experienced, but a staircase function; that is, SU equal to 2, 3 and 4 for analysis band belongs respectively to the ranges [57 : 62] MHz, [67 : 72] MHz, and finally [77 : 82] MHz. This way, it is possible to analyze different analysis bands in the same time interval;
- SpeedUp maximum value equal to 4 is reached, when analysis band equal to 82 MHz is investigated.

IV.6 Conclusion

A new GRID architecture, capable of managing measurement instruments and their successive interaction with computational nodes, has been described. To this aim, a new component, namely Instrumentation Device, has been introduced within GRID environment, through which connectivity and interaction issues with the instruments have been overcome. Moreover, proposed architecture doesn't introduce additional elements for discovering the measurement instrumentation, but utilizes suitable scheduler features to the purpose. A WebPortal has been also implemented for providing both accessibility in simple way to the developed GRID Services and workflow management function.

On proposed GRID architecture, two GRID Services have been developed in order to take advantage form parallel calculus and reduce the processing times. Experimental results, evaluated for both GRID Services in terms of SpeedUp ratio, gives evidence of the remarkable decrease of processing time with respect to a sequential implementation.

IV.7 References

[IV.1] F. Davoli, N. Meyer, R. Pugliese, S. Zappatore, "GRID Enable Remote Instrumentation," Springer, 2008, ISBN-13: 978-0387096629.

[IV.2] B. Sotomayor, L. Childers, "*Globus Toolkit 4: Programming java services,*" Morgan-Kaufmann, 2005, ISBN-13: 978-0123694041.

[IV.3] *Globus Toolkit 4 Administration Guide*, Globus Toolkit official documentation, http://www.globus.org/toolkit/docs/4.0/, February 2004.

Chapter V

Conclusions

This Ph.D thesis has dealt with development of original GRID Services for measurements on digital wireless communication systems. The original contribution has consisted in the proposal on one hand of innovative measurement procedures, based on digital signal processing, capable of facing and overcoming the current drawbacks addressed to performance assessment of wireless digital communication systems and the others of suitable GRID architecture able to include measurement instrumentations within GRID environment, principally oriented to elaboration. Take advantage from the proposed GRID architecture, two new GRID services, rely on the proposed measurement procedures, have been developed.

Intensive experimental phase, including comparison with others solution available on the market, has shown the reliability, effectiveness, and accuracy of the methods. Additional experiments, focused principally on SpeedUp ratio evaluation, experienced from proposed GRID Services, have

evidenced the remarkable advantage of methods parallel implementation, which has allowed to abruptly decrease the processing times.

Possible future developments concern the extension of proposed method for blind power spectra separation towards signals characterized by high correlation, based on advanced signal processing techniques, such as Coherent Signals Subspace or Array Smoothed and/or development of new methods for assessing the modulation quality of new communication standards, such IEEE 802.11n standard, and finally the implementation of some of proposed algorithms on suitable and dedicated digital signal processors, or as add-on software modules on DSOs.

List of Figures

List of Tables